ON-SHELL APPROACH TO THREE-BODY SCATTERING

A Thesis Presented

by

Andris Talis Stelbovics B.Sc.(Hons.)

for the degree of Doctor of Philosophy.

Department of Mathematical Physics,

University of Adelaide.

February, 1975.

CONTENTS

ABSTRACT

Although calculations of low energy elastic neutron-deuteron scattering based on on-shell dispersion relations have met with some success, it is difficult to assess their reliability because of the number of theoretical approximations and experimental uncertainties. In this thesis a study is made of the on-shell approach in the context of the Amado model of neutron-deuteron scattering where comparison with accurate numerical solutions of the off-shell Faddeev equations is possible.

The motivation for the work is discussed in Chapter 1 and the off-shell equations for the models are introduced in Chapter 2. In Chapter 3 the on-shell amplitudes for elastic, breakup and free scattering are constructed as Fredholm series solutions, whose convergence in the limit of physical energies is determined in each case by investigating their analytic structure. As a result we are able to rigorously justify the rotation of contours method used to solve the off-shell equations.

In Chapter 4 the elastic neutron-deuteron scattering amplitudes are continued to complex energies. It is shown that they are analytic on the entire physical sheet with the exception of the real axis along which the singularities are divided into two classes; the left hand potential cuts and right hand unitarity cuts. The special class of pinch singularities between energy denominators is studied and it is found that only a single pinch singularity is possible. Contained in the first iterated term of the multiparticle scattering series it contributes only to the left hand cut.

The methods developed for the elastic amplitudes are extended in Chapter 5 to obtain the analytic structure of the breakup and free scattering amplitudes.

In Chapter 6 a rigorous dispersion relation formulated for the elastic neutron-deuteron amplitude is solved in the s-wave quartet and doublet channels using various driving terms generated by the multiple scattering solution of the Amado model equations. To take account of the breakup channel exact model inelasticities computed from the off-shell equations are used. The numerical results indicate that the quartet channel scattering is well described with the simplest driving terms, but in the doublet channel the N/D solutions approach the exact model values only slowly as the order of the inputs is increased. The effect on the solutions of various approximations to the exact inelasticities is also tested. The results show that it is important to have a good description of inelastic effects in both the quartet and doublet channels. From the calculations it appears that although on-shell techniques are capable of reproducing the main features of the exact amplitudes they cannot compete in accuracy with the complete solutions of the off-shell Faddeev equations.

Chapter 7 is devoted to a numerical study of the eigenvalue spectra of the kernels of the off-shell equations and a description of the low energy behaviour of the phase shift in the s-wave doublet in terms of the eigenvalues is presented.

This thesis contains no material which has been accepted for the award of any other degree or diploma in any University and, to the best of the candidate's knowledge and belief, the thesis contains no material previously published or written by any other person, except where due reference is made in the text of the thesis.

The author wishes to thank Dr. L.R. Dodd for his generous assistance and advice during the research and preparation of this thesis. The assistance of a Commonwealth Postgraduate Scholarship between the years 1970 to 1974 is also gratefully acknowledged.

Chapter 1

INTRODUCTION

Since the rigorous integral equation formulation of non-relativistic three-particle scattering was given by Faddeev (1) there have been many applications, particularly to the three-nucleon system (2,3,4). In general, the solution of these equations even in simplified form presents a complex numerical problem especially for positive energies where one encounters a moving logarithmic singularity in their kernels (5,6,7).

More recently there have been attempts (8,9,10,11) to apply on-shell dispersion relation techniques to non-relativistic three-body scattering. This approach has in principle several advantages over the solution of the Faddeev equations. The resulting N/D equations can be expressed in the form of non-singular linear integral equations, in contrast to the Faddeev equations which are singular for physical energies. They can be expressed entirely in real arithmetic, an advantage in numerical solution, and most importantly, their solution yields the on-shell amplitudes for all energies, whereas the off-shell Faddeev equations need to be solved explicitly for each energy. Generalization to few-particle nuclear reactions is also possible (12).

However, in applying the N/D method, several uncertainities are introduced. The input information is taken from the simplest particle exchange processes; the underlying assumption that the nearest singularities to the physical region determine the energy dependence is questionable. Inelastic channels are also only taken into account approximately. Calculations reported so far (8-10) for low energy s-wave elastic neutron-deuteron scattering

have been only moderately successful. While agreement with experiment is good in the quartet channel, in the s-wave doublet the results are less satisfactory. The amplitude is apparently sensitive to the approximations for the driving terms and to the treatment of inelastic effects arising from the breakup channel.

The work in this thesis was motivated by a desire to make a direct comparison of the on-shell approach with the solution of the off-shell Faddeev equations in the context of n-d scattering. In order to assess the reliability of the N/D method one must have a model in which the exact on-shell amplitude can be determined numerically. Secondly, in order to establish a rigorous dispersion relation, the analytic properties of the on-shell amplitudes in the model must be deduced. For this purpose we have used the well known Amado model of n-d scattering (5) in which the equations are of the Amado-Lovelace type (13,14). The equations are equivalent to the Faddeev equations with a separable form for the two-body potentials but are considerably simpler having only a single intermediate integration after partial wave analysis. Their structure is similar to a set of coupled two-particle Lipmann-Schwinger equations with non-local, energy-dependent potentials, and they can be solved numerically for physical energies in a straightforward manner by the method of rotation of contours (6,7).

The plan of the thesis is as follows. In Chapter 2 the basic equations and notation are introduced. The on-shell amplitudes for physical energies are constructed in Chapter 3 using Fredholm theory. Care is taken to prove the Fredholm series representation of the amplitudes is uniformly convergent in each case. In

addition to proving the existence of the on-shell amplitudes, we are able to rigorously justify the rotation of contours method of Hetherington and Schick (6), often used in numerical solution of the Faddeev equations.

In Chapter 4, the elastic on-shell amplitude is continued to complex energies and its analytic structure is examined. We prove that the elastic n-d amplitude in the Amado model is analytic in the entire energy plane with the exception of the real axis where the singularities consist of right hand unitarity cuts and left hand potential cuts. The positions of the class of singularities due to pinches between energy denominators are investigated. These singularities have special significance since they are present in the limiting case where the vertex function describing the nucleon-nucleon interaction is structureless. Recently Amado (15) has shown that this limit of the model can be derived from the minimal requirements of three-particle unitarity and analyticity. In the case of the n-d amplitude they are present only in the first order terms of the perturbation series expansion. These conclusions are illustrated in the context of a simple soluble one-dimensional model (16).

For completeness, the results of a similar analysis for the breakup and free particle amplitudes are given in Chapter 5. It is found that the breakup amplitude may have singularities in the complex plane due to the Born term and that the higher order terms possess an anomalous singularity. There is a further singularity found only in the first order term. Similarly the free scattering amplitude has an anomalous singularity in each order of perturbation term. In addition there is an anomalous singularity contained only in the first order terms which also have the triangle rescattering singularity. Finally, the

analytic properties of the separable potential model amplitudes are compared with those deduced by Rubin, Sugar and Tiktopoulos (17,18,19) for three-body scattering via local two-body Yukawa interactions.

Our numerical results of the comparison between the off and on-shell methods are presented in Chapter 6. First the dispersion relations for the n-d amplitudes are constructed and sufficient restrictions on the asymptotic inelasticity are determined to ensure that the resulting N/D equations are Fredholm.

Details of the method for computing approximations to the driving terms are given. The N/D equations are subsequently solved and the validity of the approximations tested. The general implications of our research for future applications of on-shell methods to three-body problems are discussed in the concluding section of Chapter 6.

The work discussed in Chapter 7 is subsidiary to the main body of the thesis. The theory developed in Chapter 3 is used to develop a numerical technique to calculate the eigenvalue spectra for the kernels of the n-d equations at physical energies. Eigenvalue trajectories are computed and the rapid variation of $k\cot\delta$ in the s-wave doublet below the three-body breakup threshold (20) is described in terms of the eigenvalues.

Chapter 2

THREE-BODY AMPLITUDES IN THE SEPARABLE MODEL

The purpose of this Chapter is to review the various models to be used and to give the off-shell equations for the amplitudes.

First let us fix our three-body notation. Consider a system of three particles with masses m_i, and momenta $\underline{k}_i$, i=1,2,3. In the barycentric system where $\Sigma\underline{k}_i = 0$ the two independent momenta may be chosen to be the momentum of one particle, $\underline{k}_\alpha$ together with the relative momentum $\underline{q}_\alpha$ of the other two, that is

$$\underline{q}_\alpha = \frac{m_\gamma \underline{k}_\beta - m_\beta \underline{k}_\gamma}{m_\beta + m_\gamma}, \quad \alpha,\beta,\gamma \text{ cyclic.} \tag{2.1}$$

Associated with this set of momenta the reduced masses μ_α, μ^α often arise and are defined by

$$\mu_\alpha = \frac{m_\beta m_\gamma}{m_\beta + m_\gamma},$$

$$\mu^\alpha = \frac{m_\alpha (m_\beta + m_\gamma)}{m_1 + m_2 + m_3}. \tag{2.2}$$

2.1. Amado-Lovelace Equations

As mentioned earlier, these equations are a variant of the Faddeev equations, and have the correct singularity structure at the three-body breakup threshold but are linear integral equations in one variable. Historically they were discovered independently by Amado (13) who derived them from a field theory model in which the Born term is generated by one particle exchange and Lovelace (14) who deduced them from the Faddeev equations under the assumption of separable two particle interactions. Suppose for simplicity that all the two-body potentials are given by a rank one

separable interaction

$$V_\alpha = -\lambda_{\alpha\ell}|\alpha_\ell><\alpha_\ell|, \tag{2.3}$$

such that

$$< \underline{k}_\alpha , \underline{q}_\alpha|\alpha_\ell> = g_{\alpha\ell}(\underline{q}_\alpha) \; <\underline{k}_\alpha|$$

where α=1 refers to the interaction between particles 2 and 3 and so on, while ℓ labels the angular momentum state. Then the AL equations for the various scattering amplitudes are as follows:*

a) Elastic and Rearrangement Scattering

$$X_{\beta\alpha}(W;\underline{k}'_\beta,\underline{k}_\alpha) = Z_{\beta\alpha}(W;\underline{k}'_\beta,\underline{k}_\alpha) + \Sigma_\gamma \int d\underline{p}_\gamma Z_{\beta\gamma}(W;\underline{k}'_\beta,\underline{p}_\gamma)\tau_\gamma(W-\frac{p_\gamma^2}{2\mu_\gamma}) \times X_{\gamma\alpha}(W;\underline{p}_\gamma,\underline{k}_\alpha) \tag{2.4}$$

$$\alpha,\beta,\gamma = 1,2,3.$$

b) Breakup Scattering

$$X_{0\alpha}(W;\underline{k}'_\alpha,\underline{q}'_\alpha;\underline{k}_\alpha) = \Sigma_\beta g_\beta(\underline{q}'_\beta)\tau_\beta(W-\frac{k'^2_\beta}{2\mu_\beta})X_{\beta\alpha}(W;\underline{k}'_\beta,\underline{k}_\alpha). \tag{2.5}$$

c) Free Scattering

$$X_{00}(W;\underline{k}',\underline{q}';\underline{k},\underline{q}) = \Sigma_\alpha \delta(\underline{k}_\alpha-\underline{k}'_\alpha) g_\alpha(\underline{q}'_\alpha)\tau_\alpha(W-\frac{k_\alpha^2}{2\mu_\alpha}) g_\alpha(\underline{q}_\alpha) + \Sigma_\alpha X_{0\alpha}(W;\underline{k}'_\alpha,\underline{q}'_\alpha;\underline{k}_\alpha)\tau_\alpha(W-\frac{k_\alpha^2}{2\mu_\alpha}) g_\alpha(\underline{q}_\alpha). \tag{2.6}$$

Here the propagators, τ_α, are derived from the t-matrices of the two-body subsystems according to

$$T_\alpha(W;\underline{q}_\alpha,\underline{q}'_\alpha) = g_\alpha(\underline{q}_\alpha)\tau_\alpha(W) g_\alpha(\underline{q}'_\alpha) \tag{2.7}$$

and are given by

$$\tau_\alpha^{-1}(W) = -\lambda_\alpha^{-1} - <\alpha|G_0(W)|\alpha> = -\lambda_\alpha^{-1} - \int d\underline{q}_\alpha \frac{g_\alpha(\underline{q}_\alpha)^2}{W-q_\alpha^2/2\mu_\alpha}. \tag{2.8}$$

If the strength of the interaction is sufficient to produce a two-body bound state with energy $-B_\alpha$, the position of the pole in the t-matrix at

$$\lambda_\alpha^{-1} = - <\alpha|G_0(-B_\alpha)|\alpha> \tag{2.9}$$

---

*Throughout the thesis the symbol W is used to denote a complex energy. While the symbol E is reserved for real energies.

fixes the strength λ_α in terms of the bound state energy. Similarly a restriction is obtained on the form factors $|\alpha>$ by the requirement of a normalised bound state wave function:

$$<\alpha|G_0^2(-B_\alpha)|\alpha> = 1. \tag{2.10}$$

The Born terms $Z_{\beta\alpha}$ are defined in terms of the form factors by

$$Z_{\beta\alpha}(W;\underline{k}'_\beta,\underline{k}_\alpha) = (1-\delta_{\beta\alpha})g_\beta(\underline{q}'_\beta)(W-\frac{k'^2_\beta}{2\mu^\beta}-\frac{q'^2_\beta}{2\mu_\beta})^{-1}g_\alpha(\underline{q}_\alpha), \tag{2.11}$$

where the $\underline{q}'_\beta$ and $\underline{q}_\alpha$ may be expressed in terms of $\underline{k}'_\beta$ and $\underline{k}'_\alpha$ via equation (2.1).

The physical on-energy shell amplitude for elastic or rearrangement scattering given by*

$$X_{\beta\alpha}(E+i0;\underline{k}'_\beta,\underline{k}_\alpha)$$

is obtained when $\underline{k}'_\beta$ and $\underline{k}_\alpha$ satisfy the on-shell conditions

$$E = -B_\alpha + \frac{k_\alpha^2}{2\mu^\alpha} = -B_\beta + \frac{k'^2_\beta}{2\mu^\beta}. \tag{2.12}$$

Similar on-shell conditions apply for on-shell breakup and free scattering. We have for breakup the requirements

$$E = -B_\alpha + \frac{k_\alpha^2}{2\mu^\alpha} = \frac{q'^2_\alpha}{2\mu_\alpha} + \frac{k'^2_\beta}{2\mu^\alpha}, \tag{2.13}$$

and for free scattering,

$$E = \frac{q_\alpha^2}{2\mu_\alpha} + \frac{k_\alpha^2}{2\mu^\alpha} = \frac{q'^2_\alpha}{2\mu_\alpha} + \frac{k'^2_\alpha}{2\mu^\alpha}. \tag{2.14}$$

It can be seen from equations (2.4), (2.5) and (2.6) that the breakup and free particle amplitudes involve apart from known form factors g_α, and propagators τ_α, the solution of the off-shell equations of the elastic and rearrangement amplitudes.

---

*E+i0 is used to denote $\lim_{\varepsilon\to 0+} X_{\beta\alpha}(E+i\varepsilon)$

Indeed, to determine the on-shell breakup amplitude only a knowledge of the half-shell elastic and rearrangement amplitudes is needed. This feature of the Amado-Lovelace equations will prove advantageous in the study of the analytic structure of the on-shell amplitudes.

2.2 Equations for Identical Particles

In this section we summarise the specific models which we shall make use of in the following chapters. In what follows our system of units is $\hbar = m = 1$.

a) System of identical spinless bosons

In this case from equation (2.4) it can be seen that there are only two distinct amplitudes, $X_{\alpha\alpha}$ the direct and $X_{\beta\alpha}$, $\beta\neq\alpha$, the exchange amplitudes. With the prescription of Goldberger and Watson (21) the correctly symmetrised amplitude obtained through asymmetrisation of the incoming and outgoing wave functions is

$$X = X_{\alpha\alpha} + 2X_{\alpha\beta}. \tag{2.15}$$

Summation of equation (2.4) over α gives the following integral equation for the symmetrised amplitude:

$$X(W;\underline{k},\underline{k}') = Z(W;\underline{k},\underline{k}') + \int d\underline{p}''\, Z(W;\underline{k},\underline{p}'')\tau(W-\tfrac{3}{4}p''^2)X(W;\underline{p}'',\underline{k}'), \tag{2.16}$$

with

$$Z(W;\underline{k},\underline{k}') = \frac{2g(\underline{k}+\tfrac{1}{2}\underline{k}')g(-\tfrac{1}{2}\underline{k}-\underline{k}')}{W-k^2-k'^2-\underline{k}.\underline{k}'}. \tag{2.17}$$

Symmetrised breakup and free scattering amplitudes can also be expressed in terms of $X(W;\underline{k},\underline{k}')$. For example the symmetrised breakup amplitude is

$$X_0(W;\underline{k}',\underline{q}';\underline{k}) = \Sigma_\alpha g(\underline{q}_\alpha)\tau(W-\tfrac{3}{4}k_\alpha'^2)X(W;\underline{k}_\alpha',\underline{k}). \qquad (2.18)$$

b) Elastic neutron-deuteron scattering

In the low energy two-body nucleon-nucleon interaction there are two dominant channels, both s-wave. They are the triplet which contains the deuteron and the singlet where a virtual state occurs. Regarding the n-d system as system of identical particles in different charge states labelled by the isotopic spin number, and since for a central two-body interaction the total spin and isotopic spin are conserved, a representation of the equations can be specified by the channel (in this case deuteron or virtual) and the spin and isotopic spin of the entire system, S, M_S, I, M_I. Labelling the triplet and singlet channels 1 and 2 respectively, the Born terms which couple all the channels are

$$Z^{IS}_{nm}(W;\underline{k},\underline{k}') = \Lambda^{IS}_{nm}\frac{g_n(\underline{k}+\tfrac{1}{2}\underline{k}')g_m(-\underline{k}'-\tfrac{1}{2}\underline{k})}{W-k'^2-k^2-\underline{k}.\underline{k}'}, \qquad (2.19)$$

where the Λ^{IS}_{nm} coefficients contain the spin and isospin dependence. In elastic neutron-deuteron scattering only states with $I=\frac{1}{2}$, where the initial state is in channel 1, containing the deuteron are needed. It is found that (14)

$$\Lambda^{\frac{1}{2}\,3/2} = \begin{pmatrix} -1 & 0 \\ 0 & 0 \end{pmatrix}, \quad \Lambda^{\frac{1}{2}\frac{1}{2}} = \begin{pmatrix} \frac{1}{2} & -\frac{3}{2} \\ -\frac{3}{2} & \frac{1}{2} \end{pmatrix}. \qquad (2.20)$$

The explicit equations are:

S = 3/2, quartet

$$X_{11}^{\frac{1}{2}\,3/2}(W;\underline{k},\underline{k}') = Z_{11}^{\frac{1}{2}\,3/2}(W;\underline{k},\underline{k}') + \int d\underline{p}\; Z_{11}^{\frac{1}{2}\,3/2}(W;\underline{k},\underline{p})\tau_1(W-\tfrac{3}{4}p^2) \times X_{11}^{\frac{1}{2}\,3/2}(W;\underline{p},\underline{k}') \tag{2.21}$$

S = ½, doublet

$$\begin{bmatrix} X_{11}^{\frac{1}{2}\frac{1}{2}}(W;\underline{k},\underline{k}') \\ X_{21}^{\frac{1}{2}\frac{1}{2}}(W;\underline{k},\underline{k}') \end{bmatrix} = \begin{bmatrix} Z_{11}^{\frac{1}{2}\frac{1}{2}}(W;\underline{k},\underline{k}') \\ Z_{21}^{\frac{1}{2}\frac{1}{2}}(W;\underline{k},\underline{k}') \end{bmatrix} + \int d\underline{p} \begin{bmatrix} Z_{11}^{\frac{1}{2}\frac{1}{2}}(W;\underline{k},\underline{p}) & Z_{12}^{\frac{1}{2}\frac{1}{2}}(W;\underline{k},\underline{p}) \\ Z_{21}^{\frac{1}{2}\frac{1}{2}}(W;\underline{k},\underline{p}) & Z_{22}^{\frac{1}{2}\frac{1}{2}}(W;\underline{k},\underline{p}) \end{bmatrix}$$

$$\times \begin{bmatrix} \tau_1(W-\frac{3}{4}p^2) & X_{11}^{\frac{1}{2}\frac{1}{2}}(W;\underline{p},\underline{k}') \\ \tau_2(W-\frac{3}{4}p^2) & X_{21}^{\frac{1}{2}\frac{1}{2}}(W;\underline{p},\underline{k}') \end{bmatrix} \tag{2.22}$$

c) Amado model

The quartet and doublet equations with the separable Yamaguchi two particle interaction

$$V(\underline{q},\underline{q}') = -\lambda(\beta^2+q^2)^{-1}(\beta^2+q'^2)^{-1} \tag{2.23}$$

were used in the pioneering calculations of the three body theory of neutron-deuteron scattering by Amado and his co-workers (5,7). Because the form factor has such a simple analytic form this proves to be a good model in which to study the properties of the on-shell amplitude. In this model the propagator calculated from equation (2.8) is *

$$\tau(W) = [-\lambda^{-1} - \pi^2/\beta(W^{\frac{1}{2}}+i\beta)^2]^{-1} \tag{2.24}$$

and the strength of the potential required to produce a bound state with energy -B is

$$\lambda = \frac{\beta}{\pi}(B^{\frac{1}{2}}+\beta)^2. \tag{2.25}$$

---

*The square root branch cut is taken along arg W=0.

The following expressions for $\tau(W)$ are also worth noting:

$$\tau(W) = \frac{-\beta}{\pi^2} \frac{(\beta+B^{\frac{1}{2}})^2 (W^{\frac{1}{2}}+i\beta)^2}{(W^{\frac{1}{2}}-iB^{\frac{1}{2}})(W^{\frac{1}{2}}+2i\beta+iB)^{\frac{1}{2}}} \tag{2.26}$$

$$\text{or } \tau(W) = \frac{S(W)}{W+B}, \tag{2.26'}$$

where

$$S(W) = \frac{-\beta}{\pi^2} \frac{(\beta+B^{\frac{1}{2}})^2 (W^{\frac{1}{2}}+i\beta)(W^{\frac{1}{2}}+iB^{\frac{1}{2}})^2}{(W^{\frac{1}{2}}+2i\beta+iB^{\frac{1}{2}})}. \tag{2.27}$$

The representation of $\tau(W)$ in equation (2.26') is often most useful but it must be remembered that the apparent pole at $W^{\frac{1}{2}} = -iB^{\frac{1}{2}}$ is cancelled by a corresponding factor in $S(W)$. We remark that in addition to the bound state at $W = -B$ on the physical sheet ($\mathrm{Im}W^{\frac{1}{2}}>0$) the propagator has a pole at $W = -(2\beta+B^{\frac{1}{2}})^2$ on the second sheet. However this pole is far away from the physical region and does not correspond to a physical particle.

As the norm of the bound state wave function is

$$N^2 = \frac{\pi^2}{\beta B^{\frac{1}{2}}} (\beta+B^{\frac{1}{2}})^{-3}, \tag{2.28}$$

normalisation of the bound state wave function to unity entails the replacements :

$$g(q) \to \frac{g(q)}{N}, \qquad \lambda \to \lambda N^2. \tag{2.29}$$

2.3 Diagrammatic Representation

The AL equations derived from Amados' point of view, in which the Born term is generated by one particle exchange lend themselves readily to a diagrammatic representation. We make

the following correspondences:

$g_\alpha(\underline{k}_\beta - \underline{k}_\gamma)$

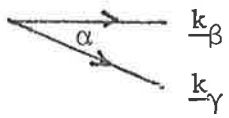

$Z_{\alpha\beta}(W;\underline{k}_\alpha,\underline{k}'_\beta)$

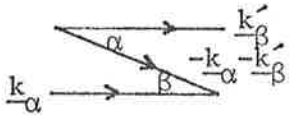

$\tau_\alpha(W - \frac{3}{4}k^2)$

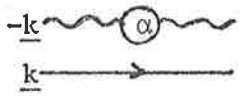

$X_{\alpha\beta}(W;\underline{k}_\alpha,\underline{k}'_\beta)$

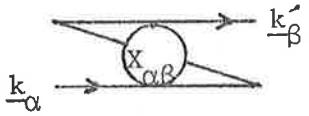

$X_{\alpha 0}(W;\underline{k}',\underline{q}';\underline{k})$

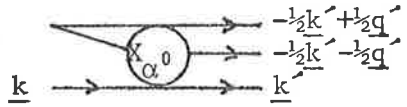

$X_{00}(W;\underline{k}',\underline{q}';\underline{k},\underline{q})$

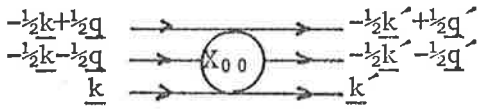

Thus the integral equation describing the elastic and rearrangement amplitudes becomes:

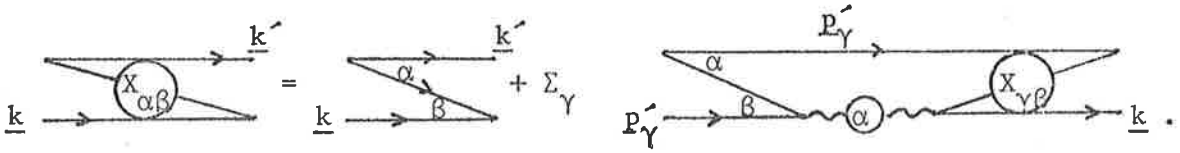

The relation between the breakup and free particle amplitude in terms of the rearrangement amplitude leads to the following equations:

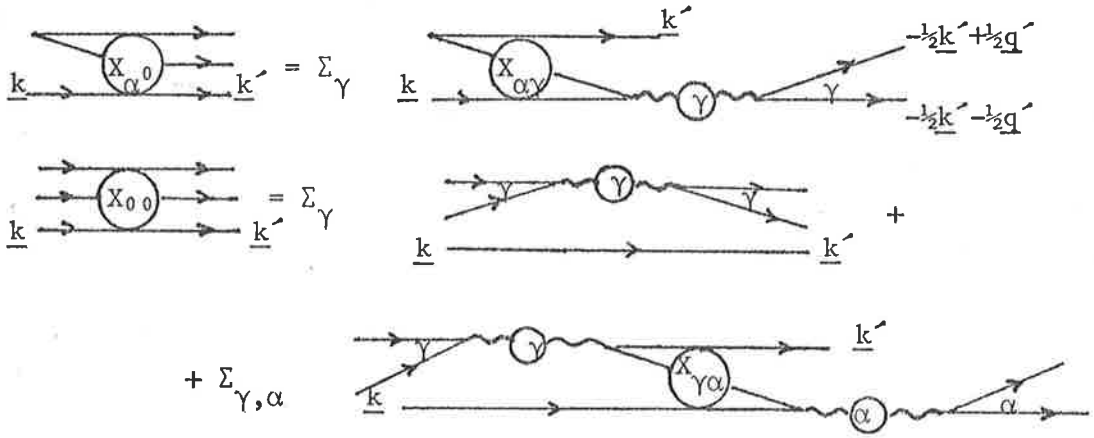

Chapter 3

CONSTRUCTION OF THE ON-SHELL AMPLITUDES

In this chapter we shall investigate the equations for rearrangement scattering and show how to construct all the on-shell three-body amplitudes for physical energies in terms of a uniformly convergent Fredholm series. For this purpose the theory of L^2 kernels (22) used so frequently in the solution of the two-body Lippmann-Schwinger equation is applied to the equations for identical particles. The results can be extended in a straight-forward way to more general cases.

The first part of the chapter is devoted to showing the existence of a Fredholm solution for complex energies W. That is, we establish there is no solution to the homogeneous equation for complex energies and then verify the AL kernel is L^2. However, in the limit of real energies in the physical scattering region, we prove the kernel is not square integrable. This means that although one may write down the physical scattering amplitudes in a formal Fredholm series, the series need not be uniformly convergent in this limit.

The same problem is encountered with the two-body Lippmann-Schwinger equation:

$$T(W) = V + VG_0(W)T(W) \tag{3.1}$$

where

$$G_0(W) = (W-H_0)^{-1}$$

is the free Greens function. The L^2 condition for $VG_0(W)$ in the momentum space representation is

$$\iint \underline{dp}\ \underline{dp'}\ \frac{|V(\underline{p},\underline{p'})|^2}{|W-p|^2} < \infty\ . \tag{3.2}$$

For local potentials this integral can be evaluated explicity (23) and does not exist in the limit $W \to E+i0$ for positive E. Thus the L^2 theory cannot be directly applied to equation (3.1) for physical energies. There are however, two ways to tackle the problem in the context of the L^2 theory. One method is to iterate the equation until an L^2 kernel is obtained. This approach was adopted by Khuri (24) who has shown the kernel of the once iterated LS equation is L^2 for local interactions. Hence the series solution of the iterated equation (which is identical to the formal solution of the original equation) is uniformly convergent. The second method which we shall utilise, is to apply a transformation to the kernel so as to make the modified kernel L^2. The original Fredholm solution which can be recovered from the solution of the modified equation is by construction uniformly convergent. A review of suitable transformations discussed in the literature has been given by Sugar and Blankenbeclar (25).

One transformation of the kernel which has received much attention is $VG_0 \to V^{\frac{1}{2}}G_0V^{\frac{1}{2}}$. For local potentials the kernel of $V^{\frac{1}{2}}$ can be constructed explicitly and $V^{\frac{1}{2}}G_0V^{\frac{1}{2}}$ has been shown to be L^2 in the scattering limit by several authors (26,27,28). However, this transformation is not suited to a discussion of the AL kernel $Z(W)\tau(W)$ where the corresponding term, $Z(W)$, is both nonlocal and energy dependent. In this case, the phase transformation used by Brown, Fivel, Lee and Sawyer (29) in studying the two-body LS equation in momentum space is more applicable. Defined by $K(\underline{p},\underline{p}') \to K(\underline{p}e^{i\theta}, \underline{p}'e^{i\theta})$ it has the effect of rotating the integration contour in equation (3.2) away from the singularity in the Greens function denominator for physical energies, and thus ensures the integral exists.

Brown, Fivel, Lee and Sawyer demonstrated that this rotation is equivalent to a similarity transformation and by formal manipulation recovered the Fredholm solution. Lovelace (30) has extended their method to three-body equations and comments on the fact that the operators which carry out the transformation are in general not square-integrable and are in certain cases unbounded.

The approach to be presented here although based on the analyticity properties of the equations, avoids the necessity of constructing the phase operators and answering questions concerning their boundedness and square-integrability. Rather, we start with the formal solution for the physical amplitude and derive the analytic properties of the perturbation series integrands, by means of which it can then be established that the series is uniformly convergent.

By use of the results for the elastic amplitude we are able to show that three-body amplitudes for breakup and free scattering may be expressed as the sum of a finite number of terms (some of which may be singular) together with a uniformly convergent series. This representation of the amplitudes will form the starting point for the subsequent investigation of their analytic structure in the complex energy plane.

3.1 Solution of the AL equation

The basic equation to be studied is equation (2.16) for the symmetrised elastic scattering amplitude:

$$X(W;\underline{k},\underline{k}') = Z(W;\underline{k},\underline{k}') + \int Z(W;\underline{k},\underline{p})\tau(W-\tfrac{3}{4}p^2)X(W;\underline{p},\underline{k}')d\underline{p}.$$

We shall first show that there is no L^2 solution to the homogeneous equation for complex energies. The proof is by contradiction.

Suppose there is a solution, call it $|\phi(W_B)>$ for some $\mathrm{Im}W_B \neq 0$. Then the functions

$$\psi^{\alpha}(W_B;\underline{k}_{\alpha},\underline{q}_{\alpha}) = (W_B - k_{\alpha}^2 - \tfrac{3}{4}q_{\alpha}^2)^{-1} g(\underline{q}_{\alpha})\tau(W_B - \tfrac{3}{4}k_{\alpha}^2)\phi(W_B,\underline{k}_{\alpha}) \tag{3.3}$$

are L^2 since the free Greens function and the propagator are bounded when $\mathrm{Im}W_B \neq 0$. The more compact operator form is

$$|\psi^{\alpha}(W_B)> = G_0(W_B)|\alpha>\tau(W_B)|\phi(W_B)>. \tag{3.4}$$

Making use of the initial assumption,

$$|\phi(W_B)> = Z(W_B)\tau(W_B)|\phi(W_B)>$$

to substitute in equation (3.4) gives, with the help of equations (2.11) and (2.15)

$$\begin{aligned} |\psi^{\alpha}(W_B)> &= \Sigma_{\beta} G_0(W_B)|\alpha>\tau(W_B)<\alpha|(1-\delta_{\alpha\beta})|\psi^{\beta}(W_B)> \\ &= \Sigma_{\beta} G_0(W_B) T_{\alpha}(1-\delta_{\alpha\beta})|\psi^{\beta}(W_B)> \\ &= G_{\alpha}(W_B) V_{\alpha} \Sigma_{\beta}(1-\delta_{\alpha\beta})|\psi^{\beta}(W_B)>. \end{aligned} \tag{3.5}$$

Multiplying equation (3.5) by the inverse of G_{α} gives

$$(W_B - H_0 - V_{\alpha})|\psi^{\alpha}(W_B)> = V_{\alpha}\Sigma_{\beta}(1-\delta_{\alpha\beta})|\psi^{\beta}(W_B)>.$$

Setting

$$|\psi(W_B)> = \Sigma_{\alpha}|\psi^{\alpha}(W_B)> \tag{3.6}$$

the above equation becomes

$$(W_B - H_0)|\psi^{\alpha}(W_B)> = V_{\alpha}|\psi(W_B)>, \tag{3.7}$$

and now summing over α, we have

$$H|\psi(W_B)> = W_B|\psi(W_B)>,$$

which is just the three-particle Schrödinger equation. But if H is Hermitian* there are no non-trivial eigenvectors

---

*Rigorous proofs of this fact have been given by Kato (31) and Faddeev (1) only for classes of local interactions.

corresponding to the complex eigenvalue W_B. Hence $|\psi(W_B)>=0$. This in turn implies from equations (3.6) and (3.4) that $|\phi(W_B)>=0$, contrary to the original assumption. Therefore there are no non-trivial solutions to the homogeneous equation for complex energies.

Now if the AL equation is Fredholm, by the Fredholm alternative there must exist a solution to the inhomogeneous equation. In the L^2 theory the equation is Fredholm provided its kernel is L^2 and the Born term $Z(W;\underline{k},\underline{k}')$ is an L^2 function of $\underline{k}$ for each $\underline{k}'$, W. The L^2 condition for the kernel requires

$$||K(W)||^2 = 4\int d\underline{k}\, d\underline{k}' \frac{|g(\underline{k}+\tfrac{1}{2}\underline{k}')g(-\underline{k}'-\tfrac{1}{2}\underline{k})\tau(W-\frac{3}{4}k^2)|^2}{|W-\frac{3}{4}k'^2-(\underline{k}+\tfrac{1}{2}\underline{k}')^2|^2} < \infty. \qquad (3.8)$$

For complex energies the energy denominator and the propagator are bounded. Therefore K will be L^2 provided the form factors $g(\underline{k}+\tfrac{1}{2}\underline{k}'), g(-\underline{k}'-\tfrac{1}{2}\underline{k})$ decrease sufficiently rapidly as $k, k' \to \infty$. That this is so in the case of Yamaguchi form factors can be checked by power counting. The condition that $Z(W;\underline{k},\underline{k}')$ be an L^2 function of $\underline{k}$,

$$\int d\underline{k}\,|Z(W;\underline{k},\underline{k}')|^2 < \infty \qquad (3.9)$$

is also satisfied for complex energies. Thus the conditions necessary for Smithies form (22) of the Fredholm solution are satisfied. The solution is

$$X(W;\underline{k},\underline{k}') = Z(W;\underline{k},\underline{k}') + \int d\underline{p}\, R(W;\underline{k},\underline{p})Z(W;\underline{p},\underline{k}') \qquad (3.10)$$

where $X(W;\underline{k},\underline{k}')$ is an L^2 function of $\underline{k}$. The resolvent is an L^2 kernel and satisfies the operator equation

$$R(W) = K(W) + K(W)R(W)$$

whose solution is given by the ratio of two Fredholm series:

$$R(W;\underline{k},\underline{k}') = \frac{N(W;\underline{k},\underline{k}')}{D(W)} \qquad (3.11)$$

with

$$D(W) = \Sigma_n D_n(W), \tag{3.12}$$

$$N(W;\underline{k},\underline{k}') = \Sigma_n N_n(W;\underline{k},\underline{k}'). \tag{3.13}$$

The series for $D(W)$ is absolutely convergent. $N(W;\underline{k},\underline{k}')$ is an L^2 kernel and its series is uniformly absolutely convergent in $\underline{k}$ and $\underline{k}'$. In the Smithies representation where

$$\sigma_n(W) = \int d\underline{k}\, K^n(W;\underline{k},\underline{k}),\ n \geq 2, \tag{3.14}$$

D_n and N_n are given by the formulae

$$D_0(W) = 1,\ N_0(W) = K,$$

$$D_n(W) = \frac{(-1)^n}{n!} \begin{vmatrix} 0 & n-1 & 0 & \cdots & 0 & 0 & 0 \\ \sigma_2 & 0 & n-2 & \cdots & 0 & 0 & 0 \\ \sigma_3 & \sigma_2 & 0 & \cdots & 0 & 0 & 0 \\ \cdots & \cdots & \cdots & \cdots & \cdots & \cdots & \cdots \\ \sigma_{n-1} & \sigma_{n-2} & \sigma_{n-3} & \cdots & \sigma_2 & 0 & 1 \\ \sigma_n & \sigma_{n-1} & \sigma_{n-2} & \cdots & \sigma_3 & \sigma_2 & 0 \end{vmatrix}, \tag{3.15}$$

$$N_n(W) = \frac{(-1)^n}{n!} \begin{vmatrix} K & n & 0 & 0 & \cdots & 0 & 0 & 0 \\ K^2 & 0 & n-1 & 0 & \cdots & 0 & 0 & 0 \\ K^3 & \sigma_2 & 0 & n-2 & \cdots & 0 & 0 & 0 \\ \cdots & \cdots & \cdots & \cdots & \cdots & \cdots & \cdots & \cdots \\ K^n & \sigma_{n-1} & \sigma_{n-2} & \sigma_{n-3} & \cdots & \sigma_2 & 0 & 1 \\ K^{n+1} & \sigma_n & \sigma_{n-1} & \sigma_{n-2} & \cdots & \sigma_3 & \sigma_2 & 0 \end{vmatrix}. \tag{3.16}$$

We have seen that the AL equation has a unique L^2 solution for complex energies. Now consider the solution in the limit $\varepsilon \to 0$ when

$$W = E + i\varepsilon,\ \varepsilon > 0,\ E > -B$$

which is needed in order to construct any of the physical three-particle scattering amplitudes. In this limit the kernel of the AL equation is no longer L^2.

To prove this we show $\varepsilon||K(E+i\varepsilon)||^2$ does not vanish in the limit $\varepsilon\to 0$ for $E > -B$:

$$\lim_{\varepsilon\to 0} \varepsilon||K(E+i\varepsilon)||^2 = \lim_{\varepsilon\to 0} \varepsilon\int d\underline{k}\, d\underline{k}'$$

$$\times \frac{4\left|g(\underline{k}+\tfrac{1}{2}\underline{k}')g(-\underline{k}'-\tfrac{1}{2}\underline{k})S(E+i\varepsilon-\frac{3}{4}k^2)\right|^2}{(\varepsilon^2+[E-(\underline{k}+\tfrac{1}{2}\underline{k}')^2-\frac{3}{4}k'^2]^2)(\varepsilon^2+[E-\frac{3}{4}k^2+B]^2)}$$

$$> \lim_{\varepsilon\to 0} \varepsilon\int d\underline{k}\, d\underline{k}' \frac{4\left|g(\underline{k}+\tfrac{1}{2}\underline{k}')g(-\underline{k}'-\tfrac{1}{2}\underline{k})S(E+i\varepsilon-\frac{3}{4}k^2)\right|^2}{(\eta+[E-(\underline{k}+\tfrac{1}{2}\underline{k}')^2-\frac{3}{4}k'^2]^2)(\varepsilon^2+[E-\frac{3}{4}k^2+B]^2)}$$

Here η is an arbitrary finite positive number. Now making use of the fact that

$$S(E+i0-\tfrac{3}{4}k_B^2) = \langle g|G_0^2(-B)|g\rangle = 1,$$

the inequality reduces to

$$\int d\underline{k}\, d\underline{k}' \frac{4\left|g(\underline{k}+\tfrac{1}{2}\underline{k}')g(-\underline{k}'-\tfrac{1}{2}\underline{k})\right|^2\pi\,\delta(E-\frac{3}{4}k^2+B)}{(\eta+[E-(\underline{k}+\tfrac{1}{2}\underline{k}')^2-\frac{3}{4}k'^2]^2)}$$

$$= \frac{2\pi}{3} k_B \int d\hat{k}\, d\underline{k}' \frac{\left|g(\underline{k}_B+\tfrac{1}{2}\underline{k}')g(-\underline{k}-\tfrac{1}{2}\underline{k}_B)\right|^2}{(\eta+[E-(\underline{k}_B+\tfrac{1}{2}\underline{k}')^2-\frac{3}{4}k'^2]^2)}. \qquad (3.17)$$

The vector $\underline{k}_B$ is defined as follows:

$$\underline{k}_B = \hat{n}\, k_B,\quad k_B = (\tfrac{4}{3}(E+B))^{\frac{1}{2}}.$$

Since the integrand of equation (3.17) is positive definite the integral cannot vanish.

Hence

$$\lim_{\varepsilon\to 0} \varepsilon||K(E+i\varepsilon)||^2 > 0 \quad \text{and} \quad ||K(E+i0)||$$

does not exist.

The same type of argument suffices to show that the inhomogeneous term $Z(W)$ is not an L^2 function in the limit $\varepsilon \to 0$ with one exception. We have for $E>0$,

$$\lim_{\varepsilon\to 0} \varepsilon \int d\underline{k} \frac{4\left|g(\underline{k}+\tfrac{1}{2}\underline{k}')g(-\underline{k}'-\tfrac{1}{2}\underline{k})\right|^2}{\varepsilon^2+(E-(\underline{k}+\tfrac{1}{2}\underline{k}')^2-\frac{3}{4}k'^2)^2}$$

$$= \tfrac{1}{2}(E-\tfrac{3}{4}k'^2)^{\frac{1}{2}} \int d\hat{x} \left|g(\underline{x})g(-\tfrac{1}{2}\underline{x}-\tfrac{3}{4}\underline{k}')\right|^2$$

where $\underline{x} = \hat{x}(E-\frac{3}{4}k'^2)^{\frac{1}{2}}$.

The right hand side is equal to zero only when $k' = (\frac{4}{3}E)^{\frac{1}{2}}$.

Thus the L^2 theory tells one nothing about the convergence of the Fredholm series for the on-shell elastic amplitude. In the remainder of this chapter, an approach based on the analyticity properties of the perturbation series of the AL equation will be developed by means of which we shall be able to prove all the three-body scattering amplitudes may be represented as the sum of a finite number of terms in the perturbation series and a uniformly convergent Fredholm series.

3.2 Singularity Structure of a General Perturbation Series Term

First let us introduce some notation. The n^{th} order term of the perturbation series of the AL equation is given by

$$T_n(W) = K^n(W)Z(W). \tag{3.18}$$

In momentum space

$$T_n(W;\underline{k},\underline{k}') = \int d\underline{p}_1 \,..\, d\underline{p}_n \; Z(W;\underline{k},\underline{p}_1)\tau(W-\tfrac{3}{4}p_1^2)Z(W;\underline{p}_1,\underline{p}_2) \;...\; \times$$

$$\times \;...\; Z(W;\underline{p}_{n-1},\underline{p}_n)\tau(W-\tfrac{3}{4}p_n^2)Z(W;\underline{p}_n,\underline{k}'). \tag{3.19}$$

Basically what we intend to do in this section is to analyse the singularity structure of the integrand of (3.19). Our aim is to prove the integration contours $\underline{p}_1, \ldots, \underline{p}_n$ can be rotated away from the energy dependent singularities as they approach the integration contours without changing the value of integral. For definiteness the Amado model is used. Rather than treating the problem as one involving a contour deformation in the complex space C^{3n} we shall adopt a much simpler approach which only requires complex analysis in one variable.

We begin our analysis by simplifying the unwieldy momentum integrations. From equations (2.17) and (2.23) it can be seen that the integrand of T_n depends only on the magnitudes of the momenta, p_i, and on the cosines, u_i, of the angles between them where

$$u_1 = \hat{k}\cdot\hat{p} \ ,$$

$$u_{i+1} = \hat{p}_i\cdot\hat{p}_{i+1}, \quad i=1, \ldots, n-1 \tag{3.20}$$

and

$$u_{n+1} = \hat{k}'\cdot\hat{p}_n.$$

To discuss the integrand, rather than using the cartesian coordinates of $\underline{p}_i = (p_{i1},p_{i2},p_{i3})$ we shall use the system of coordinates P, θ_i, $i=1,\ldots, 3n-1$ defined by

$$p_{ij} = P\cos\theta_{3i+j-4} \prod_{k=3i+j-3}^{3n-1} \sin\theta_k, \quad i=1,\ldots,n, j=1,2,3,$$

$$P > 0, \ \theta_0 \equiv 0, \ 0 < \theta_1 \leq 2\pi, \ 0 \leq \theta_k \leq \pi \ k = 2, \ldots, 3n-1. \tag{3.21}$$

This system, just the generalisation of the spherical polar coordinates in R^3 has the advantage that only the P variable ranges over the semi-infinite interval $[0,\infty)$. It follows from (3.21) that $p_i^2 = \Sigma_j\, p_{ij}^2 \leq \Sigma_{ij} p_{ij}^2 = P^2$.

Therefore we may set

$$p_i = z_i P, \quad 0 \leq z_i \leq 1, \quad i=1, \ldots, n. \tag{3.22}$$

The z_i are independent of the u_i, but both are functions of $\theta_1, \ldots, \theta_{3n-1}$. In this coordinate system, the integral for T_n takes the form

$$T_n(W;\underline{k},\underline{k}') = \int_0^\infty dP\, P^{3n-1} \int_{\Omega_{3n}} d\hat{P}\, I_n(W;k,k',P;z_1,..,z_n;u_1,..,u_{n+1}).$$

As the angle itegrations contained in $d\hat{P}$ are carried out, the z_i range over the interval $[0,1]$ and the u_i over $[-1,1]$.

We are now in a position to determine the singularities of the integrand as function of the P variable. There are pole singularities due to the vanishing of the denominators of Z and τ, and a square root branch point in the argument of τ. Only the denominators of the two terms of type $Z(W;\underline{k},\underline{p}')$ contain the external momenta, the remainder of the terms being of the type $Z(W;\underline{p}_i,\underline{p}_j)$ or $\tau(W-\frac{3}{4}p_i^2)$.

Consider first the denominators independent of W. From equations (2.17) and (2.23) the form factor denominators in $Z(W;\underline{k};\underline{p}')$ vanish when

$$\beta^2 + k^2 + \tfrac{1}{4}P^2 z_1^2 + kPu_1 z_1 = 0, \tag{3.23}$$

or

$$\beta^2 + \tfrac{1}{4}k^2 + P^2 z_1^2 + kPu_1 z_1 = 0. \tag{3.24}$$

We denote the solutions of equations (3.23) and (3.24) by $S_{1\,\pm}(u_1,z_1)$ and $S_{2\,\pm}(u_1,z_1)$ respectively, the + and - subscripts referring to the two possible solutions for each u_1, z_1. As u_1 and z_1 take on all values in their range, $S_{1\,\pm}$, $S_{2\,\pm}$ trace out families of curves which occupy the shaded regions indicated in figure 3.1.

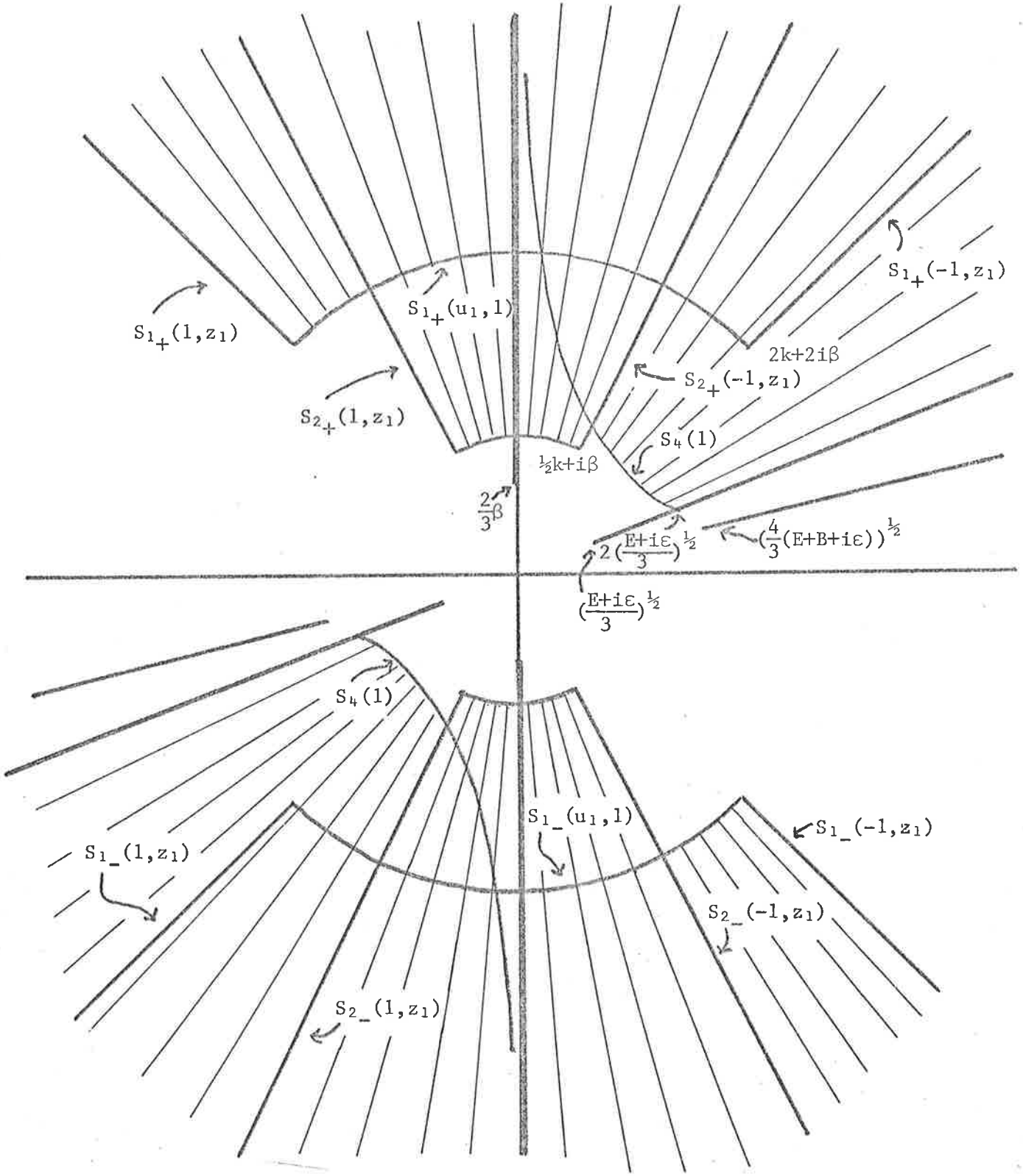

Figure 3.1

Singularity structure of integrand of T_n excluding the Green function in $Z(W;\underline{k},\underline{p}')$. Shaded area represents regions in which integrand is singular.

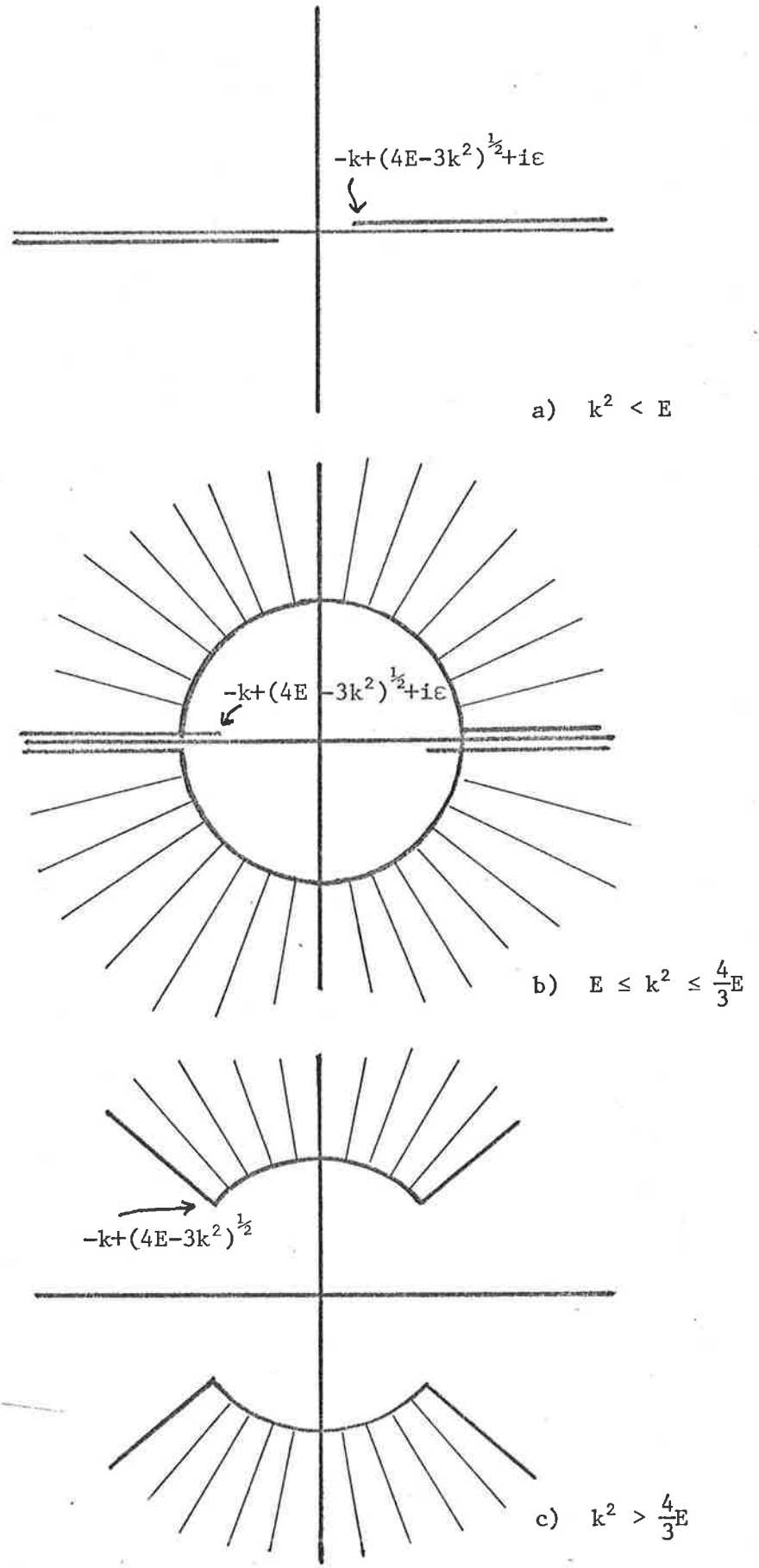

Figure 3.2

Singularity structure of Greens function in $Z(E+i\varepsilon; \underline{k}, \underline{p}')$ in the limit $\varepsilon \to 0$ for positive E.

The form factor denominators in the terms $Z(W;\underline{p}_i,\underline{p}_{i+1})$ vanish when either

$$\beta^2 + P^2 z_i^2 + \tfrac{1}{4}P^2 z_{i+1}^2 + P^2 z_i z_{i+1} u_{i+1} = 0, \tag{3.25}$$

or

$$\beta^2 + \tfrac{1}{4}P^2 z_i^2 + P^2 z_{i+1}^2 + P^2 z_i z_{i+1} u_{i+1} = 0. \tag{3.26}$$

The solutions of these equations, $S_3 \pm (z_i, z_{i+1}, u_{i+1})$, $S_3 \pm (z_{i+1}, z_i, u_{i+1})$ lie on the imaginary P axis for $|\mathrm{Im}P| \geq \frac{2}{3}\beta$ and are represented in figure 3.1 by the heavy lines.

Turning to the energy dependent denominators, the condition that the energy dependent denominators of the $Z(W;\underline{p}_i,\underline{p}_{i+1})$ type terms vanish, is

$$W - P^2 z_i^2 - P^2 z_{i+1}^2 - P^2 z_i z_{i+1} u_{i+1} = 0 \tag{3.27}$$

and for the denominators of the propagators,*

$$W + B - \frac{3}{4} P^2 z_i^2 = 0. \tag{3.28}$$

The loci of solutions of equations (3.27) and (3.28) for varying z_i, u_i, are the lines

$$\mathrm{arg}P = \pm \tfrac{1}{2}\,\mathrm{arg}W, \qquad |P| \geq \left|\frac{1}{3} W\right|^{\frac{1}{2}} \tag{3.29}$$

and

$$\mathrm{arg}P = \pm \tfrac{1}{2}\,\mathrm{arg}(W+B), \qquad |P| \geq \left|\frac{4}{3}(W+B)\right|^{\frac{1}{2}}. \tag{3.30}$$

They are shown in figure 3.1 for an energy $W=E+i\varepsilon$, $E > 0$.

The branch cut of the square root branch point in the propagator is taken along $\mathrm{arg}(W - \frac{3}{4}P^2 z_i^2) = 0$, whose locus

$$\frac{3}{2}\,\mathrm{Im}P\,\mathrm{Re}P = \frac{\mathrm{Im}W}{z_i^2}, \quad (\mathrm{Im}P)^2 \geq \frac{-\mathrm{Re}W + |W|}{\frac{3}{2}z_i^2}, \tag{3.31}$$

is that portion of the hyperbola shown in the figure as $S_4\,(z_i)$.

---

*In the Amado model, the propagator (see equation (2.26)) also has a pole on the second W sheet. But it does not enter the present discussion since we are interested only in the amplitudes on the physical sheet.

Finally, there remains to discuss the singularities arising from the Greens function term in $Z(W;\underline{k},\underline{p}')$. The condition its denominator vanishes,

$$W-k^2-P^2z_1^2 - kPu_1z_1 = 0, \tag{3.32}$$

leads in the limit $\varepsilon\to 0$ to the solutions

$$P = \frac{-u_1k \pm (k^2(u_1^2-4)+4E)^{\frac{1}{2}}}{2z_1} \tag{3.33}$$

which may be real or complex depending on k. The different cases are shown in fig. 3.2. When $k^2 < E$ the solutions are real. For $E \le k^2 \le \frac{4}{3}E$ they may be either real or complex depending on the value of u_1, and are complex for $k^2 > \frac{4}{3}E$.

This completes the discussion of the singularities of the integrand of T_n. We remark that our results are unchanged if the single rank 1 separable Yamaguchi interaction is replaced by a sum of separable interactions so long as the singularities of their form factors lie along the imaginary axis.

3.3 The Fredholm Solution of the Three-body Scattering Amplitudes for Physical Energies

We have seen in the first section that the convergence of the Fredholm series could not be justified for the scattering amplitudes in the limit of physical energies. With the results of the last section we shall now show that it is possible to express the formal Fredholm series as series for an L^2 kernel along a rotated contour which is uniformly convergent in the momenta $\underline{k}$ and $\underline{k}'$. Because the proof of this assertion depends implicitly on the magnitude of the incoming and outgoing momenta we consider the proof for each of the three-body amplitudes in turn:

a) Elastic amplitude

The formal solution for the elastic amplitude is

$$X(E+i0;\underline{k}_B,\underline{k}_B') = Z(E;\underline{k}_B,\underline{k}_B') + \lim_{\varepsilon\to 0} \frac{\Sigma_n}{D(E+i\varepsilon)} \int d\underline{p}_1 \times$$

$$\times N_n(E+i\varepsilon;\underline{k}_B,\underline{p}_1) Z(E+i\varepsilon,\underline{p}_1,\underline{k}_B')$$

with

$$k_B = k_B' = \left(\frac{4}{3}(E+B)\right)^{\frac{1}{2}}.$$

An alternative form for the solution may be deduced using the analyticity properties of perturbation series terms T_n. To see how this may be achieved note firstly, that each term $N_n Z$ is a combination of T_1, T_2, ..., T_n and σ_2, ..., σ_n. For $\underline{k}_B$, $\underline{k}_B'$, the results of the last section (summarised in figs. 3.1 and 3.2a) imply the integrands of the T_i are singularity free in the sector of the P plane

$$-\theta_m < \arg P < 0$$

where

$$\theta_m = \text{minimum } \{\text{atan } \frac{\beta}{k_B} , \text{ atan } \frac{2B^{\frac{1}{2}}}{k_B}\}.$$

In our work we shall always assume $\beta > 4B^{\frac{1}{2}}$ so that

$$\theta_m = \text{atan } \frac{2B^{\frac{1}{2}}}{k_B}. \qquad (3.34)$$

Thus the integration contour in the P plane can be rotated through a negative angle without crossing any singularity in the integrand and therefore the T_i are unchanged under this rotation. In terms of the $\underline{p}_i$ the rotation is from equation (3.21) formally equivalent to the transformation $\underline{p}_i \to \underline{p}_i e^{i\theta}$. That is, the perturbation term is unchanged if the integration over $\underline{p}_1$, ..., $\underline{p}_n$ is replaced by the contours obtained by a simultaneous rotation of the $\underline{p}_i$ through an angle θ,

provided $-\theta_m < \theta < 0$. If we define the operator A_θ associated with each operator A by

$$A_\theta(E;\underline{p},\underline{p}') = e^{3i\theta}A(E;\underline{p}e^{i\theta},\underline{p}'e^{i\theta}), \tag{3.35}$$

this invariance under a simultaneous rotation of contours may be expressed as

$$\begin{aligned} T_n(E+i0;\underline{k}_B,\underline{k}_B') &= \lim_{\varepsilon\to 0} \int d\underline{p}_n K^n(E+i\varepsilon;\underline{k}_B,\underline{p}_n)Z(E+i\varepsilon;\underline{p}_n,\underline{k}_B') \\ &= \int d\underline{p}_1 d\underline{p}_n e^{3i\theta}K(E;\underline{k}_B,\underline{p}_1 e^{i\theta})K_\theta^{n-1}(E;\underline{p}_1,\underline{p}_n) \times \\ &\quad \times Z(E;\underline{p}_n e^{i\theta},\underline{k}_B'), \quad -\theta_m < \theta < 0. \end{aligned} \tag{3.36}$$

In a similar way an alternative expression for $\sigma_n(E+i\varepsilon)$ can be found. If the integrals in its definition (equation (3.14)) are written in the generalised spherical polar coordinates the integrand only has terms of the type $Z(E+i\varepsilon,\underline{p}_i,\underline{p}_{i+1})$, $\tau(E+i\varepsilon-\frac{3}{4}p_i^2)$ which as we have seen for $E > 0$ have no singularities in the fourth quadrant of the P plane, enabling a rotation of the contour to be performed. Thus

$$\begin{aligned} \sigma_n(E+i0) &= \lim_{\varepsilon\to 0} \int d\underline{p}\, K^n(E+i\varepsilon;\underline{p},\underline{p}) \\ &= \int d\underline{p}\, K_\theta^n(E;\underline{p},\underline{p}), \quad -\pi/2 < \theta < 0. \end{aligned} \tag{3.37}$$

Defining $\sigma_{\theta n}(E)$ by

$$\sigma_{\theta n}(E) = \int d\underline{p}\, K_\theta^n(E;\underline{p},\underline{p})$$

we have

$$\sigma_n(E+i0) = \sigma_{\theta n}(E), \quad -\pi/2 < \theta < 0. \tag{3.37'}$$

Since $D(E+i0)$ is just a combination of the σ_i,

$$D(E+i0) = D_\theta(E) = \Sigma_n D_{\theta n}(E), \quad -\pi/2 < \theta < 0 \tag{3.38}$$

where D_θ is the Fredholm determinant of the kernel K_θ,

the elastic amplitude can now be written in the form

$$X(E+i0;\underline{k}_B,\underline{k}_B') = Z(E;\underline{k}_B,\underline{k}_B') + \int d\underline{p}_1 e^{3i\theta} K(E;\underline{k}_B,\underline{p}_1 e^{i\theta}) \times$$

$$\times Z(E;\underline{p}_1 e^{i\theta},\underline{k}_B') + \int d\underline{p}_1 d\underline{p}_2 e^{3i\theta} K(E;\underline{k}_B,\underline{p}_1 e^{i\theta}) \times$$

$$\times R_\theta(E;\underline{p}_1,\underline{p}_2) Z(E;\underline{p}_2 e^{i\theta},\underline{k}_B'), \quad -\theta_m < \theta < 0, \qquad (3.39)$$

where

$$R_\theta(E;\underline{p}_1,\underline{p}_2) \equiv \frac{\Sigma_n N_{\theta n}(E;\underline{p}_1,\underline{p}_2)}{\Sigma_n D_{\theta n}(E)} . \qquad (3.40)$$

But $R_\theta(E)$ is the resolvent of the operator $K_\theta(E)$. Moreover, since $||K_\theta(W)||^2 < \infty$ unless $\arg W = 2\theta$ or $\arg(W+B) = 2\theta$, $R_\theta(E)$ is an L^2 operator. Also

$\int d\underline{p}_1 |K(E;\underline{k}_B,\underline{p}_1 e^{i\theta})|^2$, $\int d\underline{p}_2 |Z(E;\underline{p}_2 e^{i\theta},\underline{k}_B')|^2 < \infty$

for $-\theta_m < \theta < 0$, so that $K(E;\underline{k}_B,\underline{p}_1 e^{i\theta})$, $Z(E;\underline{p}_2 e^{i\theta},\underline{k}_B)$ are L^2 functions of $\underline{p}_1$ and $\underline{p}_2$. Therefore, by the Fredholm theory of L^2 kernels equation (3.39) is uniformly convergent in $\underline{k}_B$ and $\underline{k}_B'$. Furthermore, because

$$|\underline{k}_B| = |\underline{k}_B'| = (\tfrac{4}{3}(E+B))^{\frac{1}{2}}$$

it is uniformly convergent with respect to E as well.

b) Breakup amplitude

Since the breakup amplitude is given by

$$X_0(E+i0;\underline{k}',\underline{q}';\underline{k}_B) = \Sigma_i g(\underline{q}_i')\tau(E-\tfrac{3}{4}k_i^2)X(E+i0;\underline{k}_i',\underline{k}_B)$$

one need only prove the Fredholm series solution of $X(E+i0;\underline{k}_F,\underline{k}_B)$ is convergent* Because $k_F < (\frac{4}{3}E)^{\frac{1}{2}}$, the proof must be modified since the free Greens function in $Z(W;\underline{k}_F,\underline{p})$ may have singularities along the positive axis which prevent a rotation of contours (see fig. 3.2b). To overcome this difficulty we make the following change

---

*In future to distinguish the free particle momentum from $\underline{k}_B$ it will be denoted by $\underline{k}_F$.

of variables in the integrands:

$$\underline{p}_1 \to \underline{q}_1 = \underline{p}_1 + \tfrac{1}{2}\underline{k}_F$$

$$\underline{p}_i \to \underline{q}_i = \underline{p}_i, \quad i=2,\ldots,n-1. \tag{3.41}$$

Then

$$T_1(E+i0;\underline{k}_F,\underline{k}_B) = \lim_{\varepsilon\to 0} \int d\underline{q}_1 K(E+i\varepsilon;\underline{k}_F,\underline{q}_1-\tfrac{1}{2}\underline{k}_F) \times$$

$$\times Z(E+i\varepsilon;\underline{q}_1-\tfrac{1}{2}\underline{k}_F,\underline{k}_B),$$

$$T_n(E+i0;\underline{k}_F,\underline{k}_B) = \lim_{\varepsilon\to 0} \int d\underline{q}_1\ldots d\underline{q}_n K(E+i\varepsilon;\underline{k}_F,\underline{q}_1-\tfrac{1}{2}\underline{k}_F) \times$$

$$\times K(E+i\varepsilon;\underline{q}_1-\tfrac{1}{2}\underline{k}_F,\underline{q}_2)\ldots Z(E+i\varepsilon;\underline{q}_n,\underline{k}_B). \tag{3.42}$$

Now one can analyse the integrands of these terms as was done in the last section. First consider the denominators peculiar to T_1. Contained in $Z(E+i\varepsilon;\underline{q}_1-\tfrac{1}{2}\underline{k}_F,\underline{k}_B)$ they give possible singularities of T_1 in the regions determined by the following equations:

$$q_1^2 + q_1 t_1 |\underline{k}_B-\underline{k}_F| + \beta^2 + \tfrac{1}{4}(\underline{k}_B-\underline{k}_F)^2 = 0,$$

$$\tfrac{1}{4}q_1^2 + q_1 t_2 |\underline{k}_B-\tfrac{1}{4}\underline{k}_F| + \beta^2 + (\underline{k}_B-\tfrac{1}{4}\underline{k}_F)^2 = 0,$$

$$q_1^2 + q_1 t_1 |\underline{k}_B-\underline{k}_F| + B + \tfrac{1}{4}(\underline{k}_B-\underline{k}_F)^2 = 0; \tag{3.43}$$

t_1 and t_2 are defined by

$$t_1 = \hat{q}_1 \cdot \widehat{(\underline{k}_B-\underline{k}_F)}$$

$$t_2 = \hat{q}_1 \cdot \widehat{(\underline{k}_B-\tfrac{1}{4}\underline{k}_F)}.$$

It is straightforward to check that there are no solutions of equations (3.43) in the sector of the q_1 plane

$$-\text{atan}\,\frac{2B^{\frac{1}{2}}}{|\underline{k}_B-\underline{k}_F|} < \arg q_1 < \text{atan}\,\frac{2B^{\frac{1}{2}}}{|\underline{k}_B-\underline{k}_F|}.$$

And since $|\underline{k}_B-\underline{k}_F| < 2\underline{k}_B$ one can see there are no singularities in the region $|\arg q_1| < \psi_m$ where $\psi_m = \text{atan}\,\frac{B^{\frac{1}{2}}}{k_B} < \theta_m$.

The remaining terms in T_1 are also present in T_n. The only modified denominators introduced by the transformation (3.41) occur in the terms $Z(E+i\varepsilon;\underline{k}_F,\underline{q}_1-\frac{1}{2}\underline{k}_F)$, $\tau(E+i\varepsilon-\frac{3}{4}(\underline{q}_1-\frac{1}{2}\underline{k}_F)^2)$ and $Z(E+i\varepsilon;\underline{q}_1-\frac{1}{2}\underline{k}_F,\underline{q}_2)$. Proceeding as in section 2 we transform the integrations $\underline{q}_1\ldots\underline{q}_n$ in the general n^{th} order perturbation series term to the system of generalised spherical polars:

$$T_n(E+i0;\underline{k}_F,\underline{k}_B) = \lim_{\varepsilon\to 0} \int dQ\, Q^{3n-1} \int_{\Omega_{3n}} d\hat{Q} I_n(E+i\varepsilon;k_F,k_B;Q;$$

$$;z_1,..,z_n;u_1,..,u_n;\alpha_1,\alpha_2,\alpha_3)$$

where

$$u_1 = \hat{k}_B\cdot\hat{q}_1,\ u_i = \hat{q}_{i-1}\cdot\hat{q}_i,\ i=2,\ldots,n.$$

$$\alpha_1 = \hat{k}_F\cdot\widehat{(\underline{q}_1+\tfrac{1}{2}\underline{q}_2)}$$

$$\alpha_2 = \hat{k}_F\cdot\widehat{(\tfrac{1}{2}\underline{q}_1+\underline{q}_2)}$$

$$\alpha_3 = \hat{k}_F\cdot\hat{q}_1$$

$$Q^2 = \Sigma_{i=1}^n \underline{q}_i^2,\ q_i = z_i Q.$$

The modified form factor denominators one must consider in $Z(E+i\varepsilon;\underline{k}_F,\underline{q}_1-\frac{1}{2}\underline{k}_F)$ are

$$\beta^2 + \frac{9}{16}k_F^2 + \tfrac{1}{4}Q^2z_1^2 + \frac{3}{4}\alpha_1 z_1 Q k_F, \tag{3.44}$$

and

$$\beta^2 + z_i^2Q^2,$$

while those present in $Z(E+i\varepsilon;\underline{q}_1-\frac{1}{2}\underline{k}_F,\underline{q}_2)$ are

$$\beta^2 + \frac{9}{4}\omega_1^2Q^2 + \tfrac{1}{4}k_F^2 - \frac{3}{2}\omega_1\alpha_1 Q k_F,$$

$$\beta^2 + \frac{1}{16}k_F^2 + \frac{9}{4}\omega_2^2Q^2 - \frac{3}{4}\omega_2\alpha_2 Q k_F. \tag{3.45}$$

ω_1 and ω_2 are given by

$$\omega_1 = \frac{2}{3}(z_1^2 + \tfrac{1}{4}z_2^2 + z_1 z_2 u)^{\frac{1}{2}},$$

$$\omega_2 = \frac{2}{3}(z_2^2 + \tfrac{1}{4}z_1^2 + z_1 z_2 u)^{\frac{1}{2}}.$$

One can verify in a straightforward way that these denominators cannot vanish for any complex Q in the sector $|\arg Q| < \operatorname{atan} \frac{4\beta}{3k_F}$. The regions in which the denominators can vanish are shown in fig. 3.3.

This leaves only the energy denominators to consider. The condition that the modified Greens functions vanish gives the equations

$$E+i\varepsilon - \frac{3}{4}k_F^2 - z_1^2 Q^2 = 0, \tag{3.46}$$

$$E+i\varepsilon - \tfrac{1}{4}k_F^2 - Q^2(z_1^2+z_2^2+z_1 z_2 u_1) + \frac{3}{2}\alpha_1\omega_1 Q k_F = 0, \tag{3.47}$$

while for the propagator denominator one has

$$E+i\varepsilon - \frac{3}{16}k_F^2 + B - \frac{3}{4}z_1^2 Q^2 + \frac{3}{4}z_1 u_1 Q k_F = 0. \tag{3.48}$$

Using the fact that $k_F^2 < \frac{4}{3}E$ it is not difficult to show that in the limit $i\varepsilon \to 0$ the solutions of these equations are confined to the third and first quadrants of the Q plane lying a distance ε away from the real axis. The positions of the remaining singularities were determined earlier in connection with the elastic amplitude and are summarised in figs. 3.1 and 3.2(c). It is apparent that the effect of the transformation (3.41) has been to remove the troublesome singularities in $Z(E+i\varepsilon;\underline{k}_F,\underline{q}_1)$ yet preserve the sector $-\psi_m < \arg Q < 0$ in the Q plane free of singularities. Therefore the contours of rotation of the perturbation series terms may be rotated through a negative angle without changing the integrals and we have the alternative expression for the half off-shell

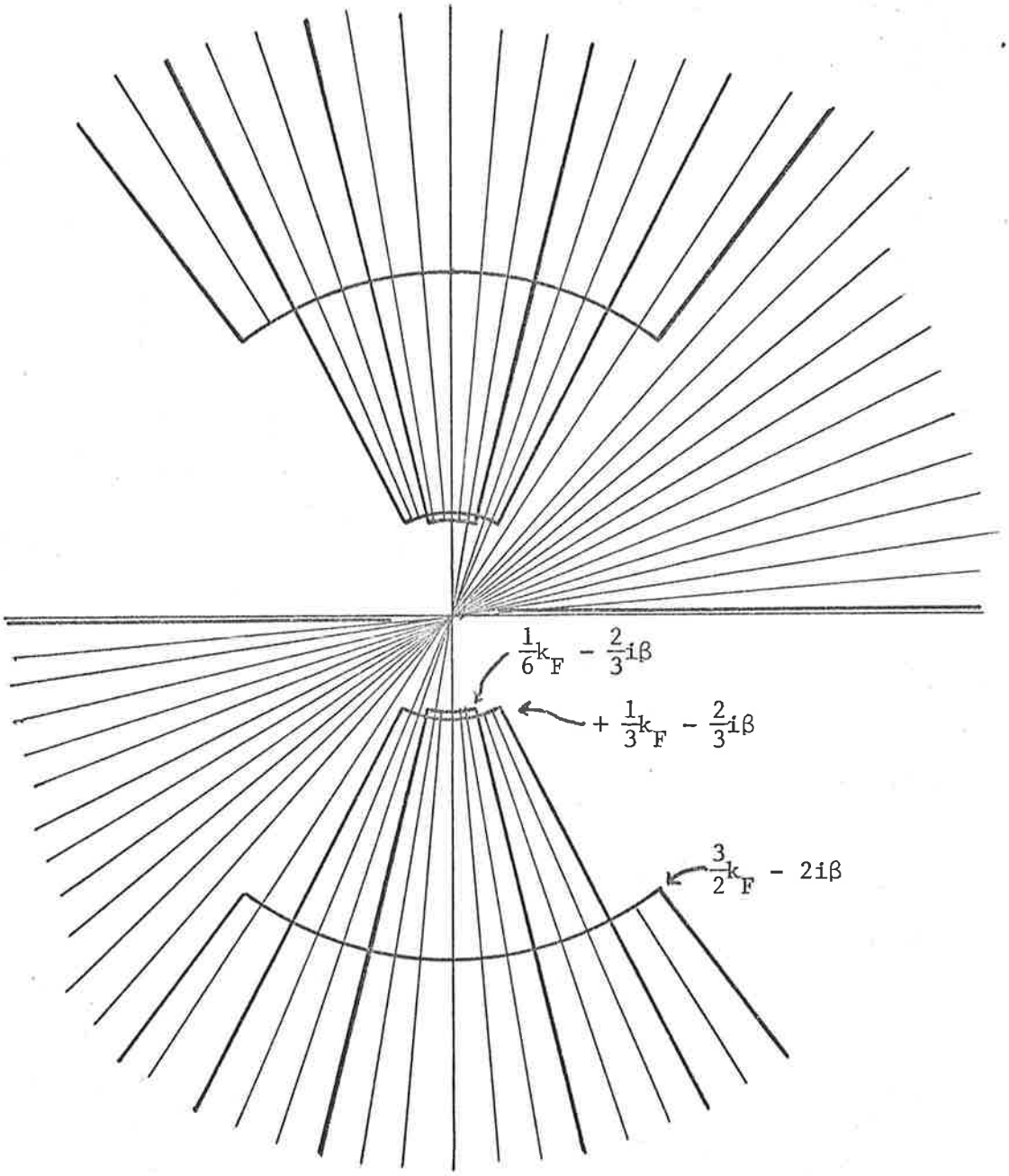

Figure 3.3

Singularities of $Z(E+i\varepsilon;\underline{k}_F,\underline{q}_1-\frac{1}{2}\underline{k}_F)$, $\tau(E+i\varepsilon-\frac{3}{4}(\underline{q}_1-\frac{1}{2}\underline{k}_F)^2)$, $Z(E+i\varepsilon;\underline{q}_1-\frac{1}{2}\underline{k}_F,\underline{q}_2)$ in Q plane in limit $\varepsilon\to 0$.

elastic amplitude:

$$X(E+i0;\underline{k}_F,\underline{k}_B) = Z(E;\underline{k}_F,\underline{k}_B) + \int d\underline{q}_1 e^{3i\theta} K(E;\underline{k}_F,\underline{q}_1 e^{i\theta}-\tfrac{1}{2}\underline{k}_F) \times$$

$$\times Z(E;\underline{q}_1 e^{i\theta}-\tfrac{1}{2}\underline{k}_F,\underline{k}_B) + \int d\underline{q}_1 d\underline{q}_2 e^{6i\theta} \times$$

$$\times K(E;\underline{k}_F,\underline{q}_1 e^{i\theta}-\tfrac{1}{2}\underline{k}_F) K(E;\underline{q}_1 e^{i\theta}-\tfrac{1}{2}\underline{k}_F,\underline{q}_2 e^{i\theta}) \times$$

$$\times Z(E;\underline{q}_2 e^{i\theta},\underline{k}_B) + \int d\underline{q}_1 d\underline{q}_2 d\underline{q}_3 e^{6i\theta} \times$$

$$\times K(E;\underline{k}_F,\underline{q}_1 e^{i\theta}-\tfrac{1}{2}\underline{k}_F) K(E;\underline{q}_1 e^{i\theta}-\tfrac{1}{2}\underline{k}_F,\underline{q}_2 e^{i\theta}) \times$$

$$\times R_\theta(E;\underline{q}_2,\underline{q}_3) Z(E;\underline{q}_3 e^{i\theta};\underline{k}_B), \quad -\psi_m < \theta < 0. \qquad (3.49)$$

Now, since there are no singularities in the terms $K(E+i0;\underline{k}_F,\underline{q}_1-\tfrac{1}{2}\underline{k}_F), K(E+i0;\underline{q}_1-\tfrac{1}{2}\underline{k}_F,\underline{q}_2)$ in the sector $-\psi_m < \arg Q < 0$,

$$\int d\underline{q}_2 \left| \int d\underline{q}_1 K(E;\underline{k}_F,\underline{q}_1 e^{i\theta}-\tfrac{1}{2}\underline{k}_F) e^{6i\theta} K(E;\underline{q}_1 e^{i\theta}-\tfrac{1}{2}\underline{k}_F,\underline{q}_2 e^{i\theta}) \right|^2$$

$$\leq \int d\underline{q}_1 d\underline{q}_2 \left| K(E;\underline{k}_F,\underline{q}_1 e^{i\theta}-\tfrac{1}{2}\underline{k}_F) K(E;\underline{q}_1 e^{i\theta}-\tfrac{1}{2}\underline{k}_F,\underline{q}_2 e^{i\theta}) \right|^2 < \infty. \qquad (3.50)$$

That is, the term premultiplying the kernel R_θ, regarded as a function of $\underline{q}_2$ is an L^2 function. We have already noted $Z(E;\underline{q}_3 e^{i\theta},\underline{k}_B)$ is an L^2 function of $\underline{q}_3$ and also that R_θ is an L^2 kernel. Therefore the Fredholm series solution is uniformly convergent in $\underline{k}_F$, $\underline{k}_B$ and as $k_F^2 < \frac{4}{3}E$ also with respect to energy. Of the remaining terms in the expansion of $X(E+i0;\underline{k}_F,\underline{k}_B)$, neither T_1 nor T_2 is singular because the same rotation can be performed. Finally, $Z(E+i0;\underline{k}_F,\underline{k}_B)$ clearly cannot have singularities from the form factor denominators when $\underline{k}_F$ and $\underline{k}_B$ are real, which leaves the energy denominator

$$E - \tfrac{3}{4}k_B^2 - (\underline{k}_F+\tfrac{1}{2}\underline{k}_B)^2$$

to consider. But it is obvious this denominator will never vanish for real $\underline{k}_F$, $\underline{k}_B$ because $E - \frac{3}{4}k_B^2 = -B$. To conclude

our proof for the breakup amplitude we note that $\tau(E - \frac{3}{4}k_F^2)$ cannot be singular because $E > \frac{3}{4}k_F^2$. Thus we have the result that the breakup amplitude for real positive energy and momenta can be represented in the form of a uniformly convergent Fredholm series.

c) Free particle amplitude

We have

$$X_{00}(E+i0;\underline{k}_F',q',\underline{k}_F,q) = \Sigma_i \delta(\underline{k}_{F_i} - \underline{k}_{F_i}')\tau(E - \tfrac{3}{4}k_{F_i}^2)g(q_i')g(q_i)$$

$$+ \Sigma_{ij} g(q_i')\tau(E - \tfrac{3}{4}k_{F_i}'^2)X(E+i0;\underline{k}_{F_i}',\underline{k}_{F_j})\tau(E - \tfrac{3}{4}k_{F_j}^2)g(q_i).$$

The singularities encountered in the integrands of the perturbation terms of the off-shell amplitude $X(E+i0;\underline{k}_F,\underline{k}_F')$ have already been discussed in relation to the breakup amplitude. The fact that both k_F, $k_F' < (\frac{4}{3}E)^{\frac{1}{2}}$ means that the transformation (3.41) must be applied to both ends of each perturbation term. This leads to the following expression for the off-shell amplitude:

$$X(E+i0;\underline{k}_F',\underline{k}_F) = Z(E+i0;\underline{k}_F',\underline{k}_F) + T_1(E+i0;\underline{k}_F',\underline{k}_F) + T_2(E+i0;\underline{k}_F',\underline{k}_F)$$

$$+ \int dq_1 dq_2 dq_3 e^{9i\theta} K(E;\underline{k}_F', q_1 e^{i\theta} - \tfrac{1}{2}\underline{k}_F') K(E; q_1 e^{i\theta} - \tfrac{1}{2}\underline{k}_F', q_2 e^{i\theta}) \times$$

$$\times K(E; q_2 e^{i\theta}, q_3 e^{i\theta} - \tfrac{1}{2}\underline{k}_F) Z(E; q_3 e^{i\theta} - \tfrac{1}{2}\underline{k}_F, \underline{k}_F) + \int dq_1 dq_2 dq_3 dq_4 e^{9i\theta} \times$$

$$\times K(E;\underline{k}_F', q_1 e^{i\theta} - \tfrac{1}{2}\underline{k}_F') K(E; q_1 e^{i\theta} - \tfrac{1}{2}\underline{k}_F', q_2 e^{i\theta}) R_\theta(E; q_2, q_3) \times$$

$$\times K(E; q_3 e^{i\theta}, q_4 e^{i\theta} - \tfrac{1}{2}\underline{k}_F) Z(E; q_4 e^{i\theta} - \tfrac{1}{2}\underline{k}_F, \underline{k}_F), \quad -\psi_m < \theta < 0. \qquad (3.51)$$

Since R_θ is L^2 and the functions of q_2 and q_3 on either side are L^2 functions in these momenta (see equation (3.50)) the Fredholm series term is once again uniformly convergent.

Similarly one can show without difficulty that the rotation of coordinates can be carried out for T_2 and so this term is not singular either. However, in the case of T_1 the coordinate transformation (3.41) does not remove the singularities from the vicinity of the integration path. In fact this term contains the well known triangle rescattering singularity which we shall discuss in more detail in Chapter 5. The Born term $Z(E+i0;\underline{k}_F,\underline{k}_F')$ will also give rise to a pole singularity for suitable combinations of $\underline{k}_F$, $\underline{k}_F'$. Hence the free scattering amplitude can be expressed in the form of a sum of three singular terms; the term with momentum conservation δ functions, the Born term and T_1 the term containing the rescattering singularity together with a uniformly convergent Fredholm series.

3.4 Rotation of Contours Method

The method we have used to construct the scattering amplitude makes it easy to prove the validity of the rotation of contours method. This is a technique originally suggested by Hetherington and Schick (6) to solve the rearrangement scattering equations above the breakup threshold and has been used extensively in the literature. The idea is to deform the contour of integration of the AL equation away from the momentum dependent singularities in the kernel which are close to the integration contour at positive energies. The validity of such a contour deformation was assumed in the early calculations. It was left to Brayshaw (32) who studied the analyticity of the half off-shell amplitude in the complex momentum plane to justify the correctness of the method. Using his results the analytic

continuation $X(E;\underline{p}e^{i\theta},\underline{k}_B')$ can be shown to satisfy the question

$$X(E;\underline{p}e^{i\theta},\underline{k}_B') = Z(E;\underline{p}e^{i\theta},\underline{k}_B') + \int d\underline{p}'e^{3i\theta}K(E;\underline{p}e^{i\theta},\underline{p}'e^{i\theta}) \times$$

$$\times X(E;\underline{p}'e^{i\theta},\underline{k}_B'). \tag{3.52}$$

Since this equation has an L^2 kernel and $Z(E;\underline{p}e^{i\theta},\underline{k}_B')$ is an L^2 function of $\underline{p}$ it may be easily solved numerically by quadratures. The required amplitude can then be determined by substituting back in the original equation:

$$X(E+i0;\underline{k}_B,\underline{k}_B') = Z(E;\underline{k}_B,\underline{k}_B') + \int d\underline{p}\ K(E;\underline{k}_B,\underline{p}e^{i\theta})X(E;\underline{p}e^{i\theta},\underline{k}_B'). \tag{3.53}$$

However, by means of the Fredholm solution it is possible to prove the method *without* a knowledge of the analytic properties of the half off-shell amplitude. For let us define $X_\theta(E;\underline{p},\underline{k}_B')$ to be the kernel which satisfies the equation

$$X_\theta(E;\underline{p},\underline{k}_B') = Z(E;\underline{p}e^{i\theta};\underline{k}_B') + \int d\underline{p}\ \ K_\theta(E;\underline{p},\underline{p}')X_\theta(E;\underline{p}',\underline{k}_B'),$$

$$-\theta_m < \theta < 0. \tag{3.54}$$

Since we assume no knowledge of the analytic properties in the p variable we cannot make the identification

$$X_\theta(E;\underline{p},\underline{k}_B') = X(E;\underline{p}e^{i\theta},\underline{k}_B').$$

But because equation (3.54) is Fredholm when $\theta > -\theta_m$ it has the solution

$$X_\theta(E;\underline{p},\underline{k}_B') = Z(E;\underline{p}e^{i\theta},\underline{k}_B') + \int d\underline{p}'R_\theta(E;\underline{p},\underline{p}')Z(E;\underline{p}'e^{i\theta},\underline{k}_B'), \tag{3.55}$$

which combined with the Fredholm solution for the on-shell amplitude (equation (3.39)) gives

$$X(E+i0;\underline{k}_B,\underline{k}_B') = Z(E;\underline{k}_B,\underline{k}_B') + \int d\underline{p}e^{3i\theta}K(E;\underline{k}_B,\underline{p}e^{i\theta})X_\theta(E;\underline{p},\underline{k}_B'),$$

$$-\theta_m < \theta < 0. \tag{3.56}$$

Chapter 4

ANALYTICITY IN ENERGY OF THE ON-SHELL ELASTIC AMPLITUDE

In this chapter, we undertake a study of the analyticity in energy of the on-shell elastic amplitude in the Amado Model. Analyticity properties of the breakup and free particle amplitudes will be discussed in the following Chapter.

Such a program has been carried out by Rubin, Sugar and Tiktopoulos* (17,18,19) for amplitudes derived from the Faddeev equations with local Yukawa two-body potential interactions. However, as we have emphasised in Chapter 2, in the separable model the breakup and free scattering amplitudes are given in terms of the AL equations for elastic and rearrangement scattering. This is in contrast to the amplitudes derived from the Faddeev equations, which can be constructed only after the equations for the transition operators have been solved. Because of this simplification, the analytic structure of the separable model three-body amplitudes can be uncovered more easily than those based on the full Faddeev equations. In addition, because these amplitudes differ from those studied by RST only in the type of two-particle interaction, it follows that they should have the same singularities resulting from pinches between energy denominators in the integrals.

In the first section, the analytic properties of the elastic amplitude are determined for a system of three identical bosons, in the Amado model. The analysis utilises much of the

---

*Future references to these authors are indicated by the abbreviation RST.

theory developed in the latter part of Chapter 3. The results are then extended to the amplitudes for elastic neutron-deuteron scattering.

The classes of singularities arising from pinches between the energy denominators are investigated in the third section. Application of the results to the Skorniakov - Ter - Martirosian equation (33) and to a soluble three-body model (16) is discussed.

4.1 Analytic Continuation of On-Shell Elastic Amplitudes

a) System of identical spinless bosons

Our starting point is the series solution for the physical scattering amplitude. This series has been shown to be uniformly convergent with respect to the energy and momentum variables. Now if the energy is continued into a region of the complex plane in each term of the series, the sum which we denote by $X(W;\underline{k}_B,\underline{k}_B')$ where $k_B^2 = k_B'^2 = \frac{4}{3}(W+B)$ will define an analytic continuation of the physical amplitude subject to the following restrictions:

1) the energy dependent singularities in the integrands of the series terms do not cross any integration contours;

2) the series for all such energies is uniformly convergent.

That is, the continuation of the on-shell amplitude to complex energies is

$$X(W;\underline{k}_B,\underline{k}_B') = Z(W;\underline{k}_B,\underline{k}_B') + \int d\underline{p}\; K(W;\underline{k}_B,\underline{p})Z(W;\underline{p},\underline{k}_B') + \frac{\sum_{n=0}^{\infty}}{D(W)} \int d\underline{p}\, d\underline{p}'\; K(W;\underline{k}_B,\underline{p})N_n(W;\underline{p},\underline{p}')Z(W;\underline{p}',\underline{k}_B'), \qquad (4.1)$$

when there is a region in the W plane for which

$$\int d\underline{p}\,|K(W;\underline{k}_B\underline{p})|^2,\ \int d\underline{p}\,|Z(W;\underline{k}_B,\underline{p})|^2 < \infty, \tag{4.2}$$

$$||K(W)|| < \infty, \tag{4.3}$$

and at the same time the first condition is satisfied.

As the first step in the construction of a continuation we shall therefore find a region in which (4.2) and (4.3) hold. The norms of equation (4.2) will certainly exist in the region where the denominators

$$\beta^2 + (\underline{p} + \tfrac{1}{2}\underline{k}_B)^2 \tag{4.4}$$

$$\beta^2 + (\tfrac{1}{2}\underline{p} + \underline{k}_B)^2 \tag{4.5}$$

$$B + (\underline{p} + \tfrac{1}{2}\underline{k}_B)^2 \tag{4.6}$$

$$W + B - \frac{3}{4}p^2, \tag{4.7}$$

and

$$W + (2\beta + B^{\frac{1}{2}})^2 - \frac{3}{4}p^2, \tag{4.8}$$

do not vanish. In fact as discussed in Chapter 2 the vanishing of denominator (4.7) may give rise to a singularity only when Im $W^{\frac{1}{2}} > 0$. Similarly denominator (4.8) may cause a singularity in the integrand only for Im $W^{\frac{1}{2}} < 0$. For the present we restrict the discussion to Im $W^{\frac{1}{2}} > 0$. Then denominator (4.8) cannot vanish and need not be considered further.

For the purposes of the following analysis we shall work in the variable k_B rather than W because all the denominators are simple quadratic functions in k_B. The region in the k_B plane which corresponds to Im $W^{\frac{1}{2}} > 0$ is shown in fig. 4.1 over:

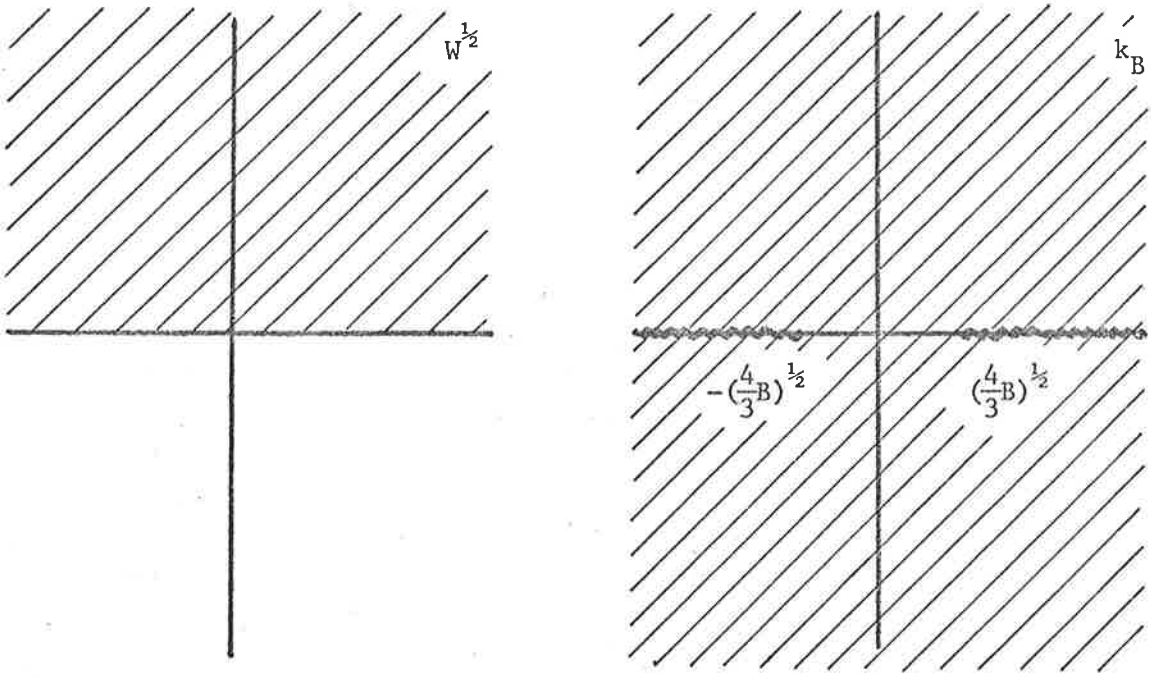

Figure 4.1

Mapping of Im $W^{\frac{1}{2}} > 0$ into the first sheet of the k_B plane.

The first three denominators are of the type

$$N^2 + (\underline{X} + M\underline{k}_B)^2. \tag{4.9}$$

Setting $k_B = R + iI$, $\hat{n} = \underline{k}_B/k_B$ the condition that this denominator vanish, namely

$$N^2 + (\underline{X} + M\hat{n}(R+iI))^2 = 0 \tag{4.10}$$

gives, upon collection of real and imaginary parts the equations

$$N^2 + (\underline{X}+M\hat{n}R)^2 - M^2I^2 = 0, \tag{4.11}$$

$$(\underline{X} + M\hat{n}R)\cdot\hat{n}I = 0. \tag{4.12}$$

It is obvious that there are no solutions whenever $I^2M^2 < N^2$. Consequently, the denominators of equations (4.4), (4.5) and (4.6) do not vanish when

$(\text{Im } k_B)^2 \leq$ minimum of $\{4B, \beta^2\}$.

And since we shall assume that the bound state wave number $B^{\frac{1}{2}}$, is much smaller than the inverse range parameter β, there can be no solution if $|\text{Im } k_B| < 2B^{\frac{1}{2}}$.

The denominator (4.7) may be written as $\frac{3}{4}(k_B^2 - p^2)$ and it vanishes along the line $\text{Im } k_B = 0$. Thus the norms in equation (4.2) exist provided k_B is restricted to the region

$$0 < \text{Im } k_B < 2B^{\frac{1}{2}}, \quad \text{Im } W^{\frac{1}{2}} > 0. \tag{4.13}$$

$||K(W)||$ has already been examined and exists unless $\text{Im } k_B = 0$. Hence the series for $X(W, \underline{k}_B, \underline{k}_B')$ (excluding the Born term) is uniformly convergent for k_B in the region of equation (4.13). The proof of analyticity of the amplitude follows immediately; the integrands of the perturbation series terms are analytic in the region (4.13) and therefore so are the integrals. Finally the singularities of the Born term, $Z(W; \underline{k}_B, \underline{k}_B')$ are poles at

$$k_B = \frac{\pm i\beta}{(\frac{5}{4} + Z)^{\frac{1}{2}}} \quad \text{or} \quad \frac{\pm iB^{\frac{1}{2}}}{(\frac{5}{4} + Z)^{\frac{1}{2}}}, \quad Z = \hat{n} \cdot \hat{n}'. \tag{4.14}$$

Combining regions (4.13) and (4.14) we conclude that $X(W; \underline{k}_B, \underline{k}_B')$ defines an analytic continuation of the physical elastic scattering amplitude in the region of the complex energy plane

$$0 < \text{Im } k_B < (\tfrac{4}{3}B)^{\frac{1}{2}}, \quad \text{Im } W^{\frac{1}{2}} > 0. \tag{4.15}$$

For future reference this region is denoted by d_0.

We shall now show how to extend the domain of analyticity beyond d_0. For this purpose, we define the amplitude $X_\theta(W; \underline{k}_B, \underline{k}_B')$:

$$X_\theta(W;\underline{k}_B,\underline{k}_B') = Z(W;\underline{k}_B,\underline{k}_B') + \int d\underline{p}\, K(W;\underline{k}_B,\underline{p}e^{i\theta})Z(W;\underline{p}e^{i\theta},\underline{k}_B')e^{3i\theta}$$

$$+ \frac{\Sigma_n}{D(W)} \int d\underline{p}_1 d\underline{p}_2 e^{3i\theta} K(W;\underline{k}_B,\underline{p}_1 e^{i\theta}) N_{\theta n}(W;\underline{p}_1,\underline{p}_2) \times$$

$$\times Z(W;\underline{p}_2 e^{i\theta},\underline{k}_B'). \qquad (4.16)$$

This amplitude is an analytic continuation of the amplitude $X(W;\underline{k}_B,\underline{k}_B')$. To prove this assertion we shall first deduce a region of analyticity for X_θ. Arguing as before it is clear that the series of equation (4.16) will be uniformly convergent when

$$\int d\underline{p}|K(W;\underline{k}_B,\underline{p}e^{i\theta})|^2,\ \int d\underline{p}|Z(W;\underline{k}_B,\underline{p}e^{i\theta})|^2 < \infty \qquad (4.17)$$

and $||K_\theta(W)||$ exists. This will be the case provided none of the following denominators vanish:

a) in $K(W;k_B,\underline{p}e^{i\theta})$

$$\beta^2 + (\underline{p}e^{i\theta} + \tfrac{1}{2}\underline{k}_B)^2, \qquad (4.18)$$

$$\beta^2 + (\tfrac{1}{2}\underline{p}e^{i\theta} + \underline{k}_B)^2,$$

$$B + (\underline{p}e^{i\theta} + \tfrac{1}{2}\underline{k}_B)^2,$$

$$W + B - \frac{3}{4}p^2 e^{2i\theta} \qquad (4.19)$$

and

b) in $K(W;\underline{p}_1 e^{i\theta},\underline{p}_2 e^{i\theta})$ (where there are only two energy dependent denominators),

$$W - \frac{3}{4}p_1^2 e^{2i\theta} - (\underline{p}_2 e^{i\theta} + \tfrac{1}{2}\underline{p}_1 e^{i\theta})^2 \text{ and} \qquad (4.20)$$

$$W + B - \frac{3}{4}p^2 e^{2i\theta}$$

again. The task of determining a region where the denominators do not vanish is simplified by setting

$$k_B e^{-i\theta} = R + iI.$$

The denominators in equation (4.18) are the same type. The condition that they vanish is described by an equation of the form

$$N^2 e^{-2i\theta} + (\underline{X} + M\hat{n}(R+iI))^2 = 0. \qquad (4.21)$$

Separating into real and imaginary parts gives the following equations:

$$N^2\cos 2\theta + (MR + \underline{X}\cdot\hat{n})^2 - X^2 - M^2I^2 = 0, \tag{4.22}$$

$$N^2\sin 2\theta = I(MR + \underline{X}\cdot\hat{n}). \tag{4.23}$$

With substitution of the second equation into the first, it is easy to see that there are no solutions if $I^2M^2 < N^2\cos^2\theta$. Hence the denominators of equation (4.18) will not vanish when

$$|\text{Im } k_B e^{-i\theta}| < 2B^{\frac{1}{2}} \cos\theta.$$

It is also clear that denominator (4.19) does not vanish if $\arg (k_B e^{-i\theta}) \neq 0$. Thus the two function norms exist when k_B belongs to the region

$$0 < \text{Im } k_B e^{-i\theta} < 2B^{\frac{1}{2}} \cos\theta. \tag{4.24}$$

Next, consider the denominator in equation (4.20). It vanishes when

$$\arg We^{-2i\theta} = 0. \tag{4.25}$$

The corresponding curve in the k_B plane is determined from the equations

$$-\frac{4}{3}B\cos 2\theta + R^2 - I^2 = X^2, \tag{4.26}$$

and

$$\frac{4}{3}B\sin 2\theta + 2IR = 0, \tag{4.27}$$

whose solution is the set of points on the rectangular hyperbola of equation (4.27) such that

$$|\text{Im } k_B e^{-i\theta}| \leq (\tfrac{4}{3}B)^{\frac{1}{2}} |\sin\theta|.$$

We denote this set by ℓ_θ. Finally, because the singularities of the Born term are in the region $|\text{Im } k_B e^{-i\theta}| \geq (\frac{4}{3}B)^{\frac{1}{2}}$ it can be concluded the amplitude X_θ is represented by a uniformly convergent series in the

region d_θ:

$$0 < \text{Im } k_B e^{-i\theta} < (\tfrac{4}{3}B)^{\frac{1}{2}}\cos\theta, \quad \text{Im } k_B e^{-i\theta} \notin \ell_\theta, \quad \text{Im } W^{\frac{1}{2}} e^{-i\theta} > 0. \tag{4.28}$$

It follows trivially that X_θ is analytic in d_θ. For, the energy denominators in the integrands of the perturbation terms are analytic functions of energy which do not vanish in this region. The square root branch point in τ has its branch cut along $\arg (We^{-2i\theta}) = 0$ which is the region ℓ_θ. Hence all the integrands are analytic and therefore X_θ when $k_B \in d_\theta$.

The regions of analyticity of the two amplitudes are shown in fig. 4.2. There are two points to be noted. The first is that there is always a region of overlap of d_0 and d_θ. Second, the endpoints of ℓ_θ are fixed independently of the angle θ.

Now it is easy to prove $X_\theta(W;\underline{k}_B,\underline{k}_B')$ is the analytic continuation of $X(W;\underline{k}_B,\underline{k}_B)$ from d_0 to d_θ since it is evident from the figure that the portion of the imaginary axis, $0 < \text{Im } k_B < (\frac{4}{3}B)^{\frac{1}{2}}$ is always in the region of overlap, $d_0 \cap d_\theta$. Therefore, by the fundamental theorem of analytic continuation* it is necessary only to show X and X_θ are identical along this line. By equations (4.16), (4.1) this is equivalent to showing (since N_n is a combination of perturbation series terms) that

$$\int d\underline{p}_1 d\underline{p}_n \; K(E;\underline{k}_B,\underline{p}_1) K^{n-1}(E;\underline{p}_1,\underline{p}_n) Z(E;\underline{p}_n,\underline{k}_B')$$

$$= \int d\underline{p}_1 d\underline{p}_n e^{3i\theta} K(E;\underline{k}_B,\underline{p}_1 e^{i\theta}) K_\theta^{n-1}(E;\underline{p}_1,\underline{p}_n) Z(E;\underline{p}_n e^{i\theta},\underline{k}_B') \tag{4.29}$$

---

*Let f be analytic in G, g analytic in G'. If $G \cap G' \neq \phi$ and $f(Z) = g(Z)$ for every $Z \in G \cap G'$, then there is exactly one analytic function h in $G \cup G'$ such that $h(Z) = f(Z)$ for every $Z \in G$ and $h(Z) = g(Z)$ for every $Z \in G'$. The function g is called the analytic continuation of f to G'.

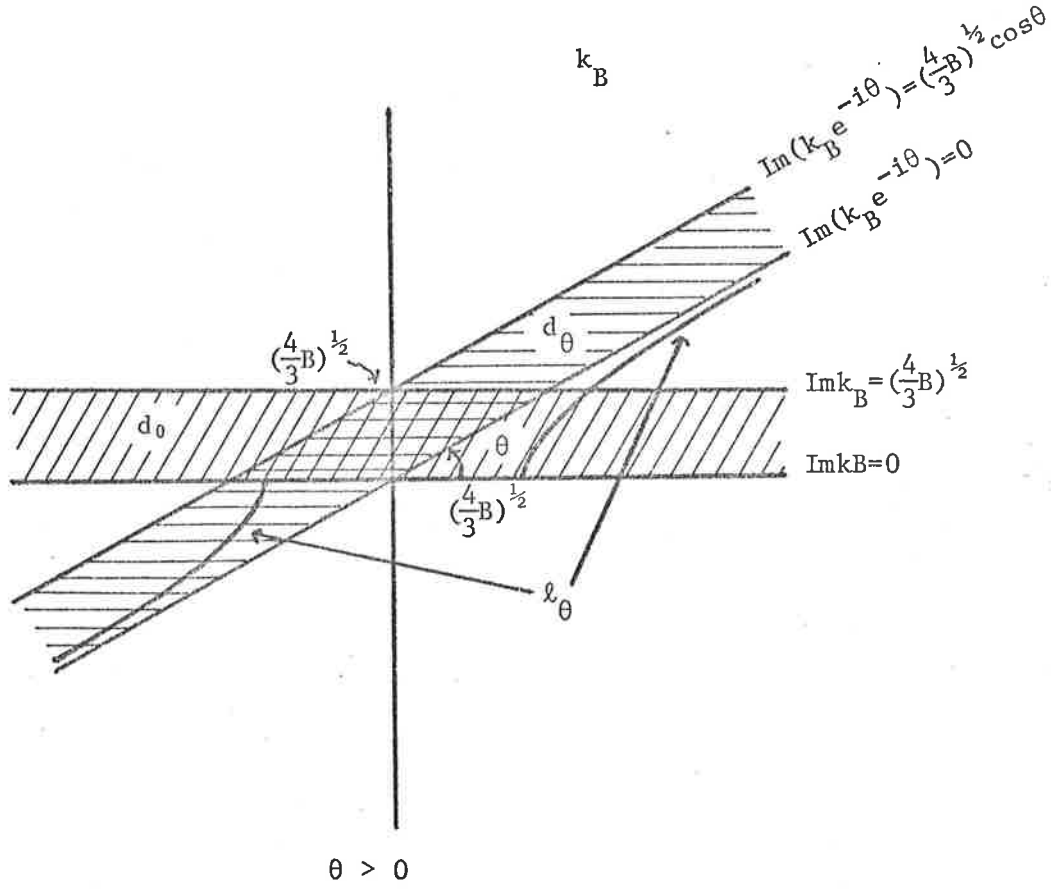

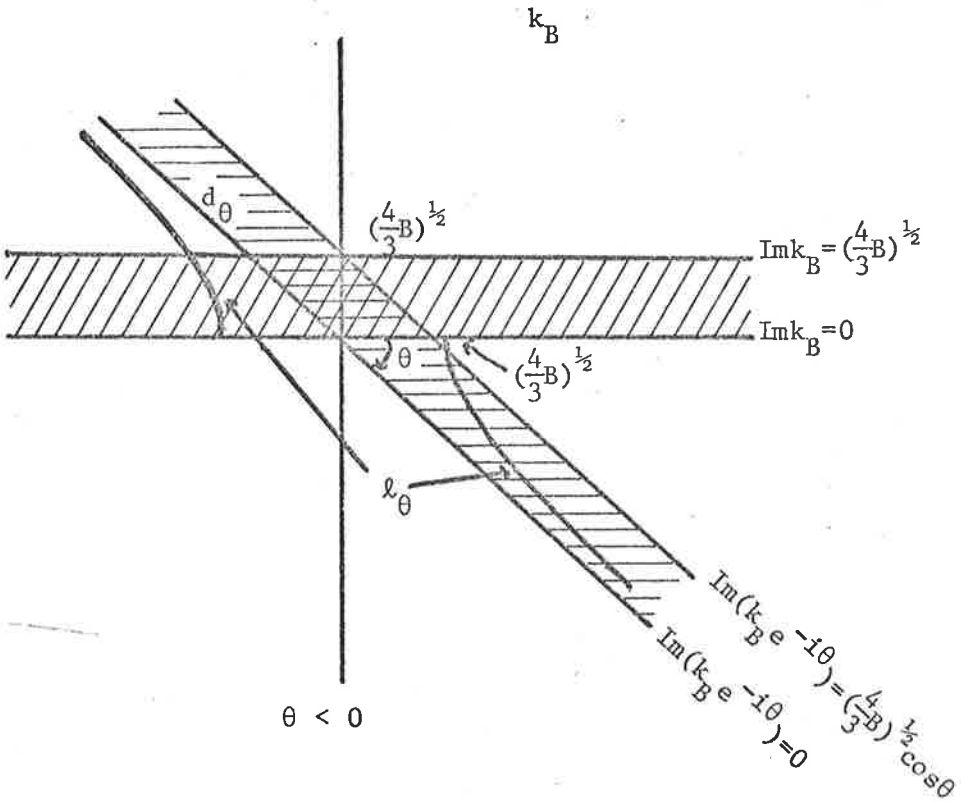

Figure 4.2

/// Region of analyticity of X

≡ Region of analyticity of X_Ω

when $-2B < E < -B$. To prove equation (4.29) one can write T_n as an integral over $\underline{p}_1, \ldots, \underline{p}_n$ and then proceed as in Chapter 3 to examine the positions of the singularities of the integrand in the P variable. Their positions are given by solution of equations (3.23) to (3.32) inclusively. An examination of these equations for negative E and imaginary k_B reveals that *all* the singularities lie along the imaginary axis in the P plane. Consequently the integral is unchanged by a rotation of the P integration contour through the range $|\theta| < \pi/2$. This completes the proof.

As θ is varied continuously from $-\pi/2$ through to $+\pi/2$ analytic continuation of $X(W;k_B,k_B')$ is established in the region $\cup_{|\theta|<\pi/2} d_\theta$. Returning to fig. 4.2 it can be seen that this region is the entire k_B plane with the exception of points along

1) the imaginary axis with Im $k_B > (\frac{4}{3}B)^{\frac{1}{2}}$, Im $k_B \leq 0$.

2) $k_B = (\frac{4}{3}B)^{\frac{1}{2}}, -(\frac{4}{3}B)^{\frac{1}{2}}$.

We shall leave discussion of the singularities to the next section. Thus in the first sheet (Im $W^{\frac{1}{2}} > 0$) of the W plane the on-shell amplitude has no singularities for complex energies. Along the real axis it has singularities arising from pinches between denominators when $E \leq -2B$ and the right hand unitarity cuts.

b) Neutron-deuteron elastic amplitudes

Extension of the results in the spinless boson case to the quartet channel amplitude of the Amado model follows straight away. The quartet channel amplitude (equation (2.21)) satisfies the same type of equation apart from isospin and

spin coefficients in the Born term. Thus it has the same analytic structure, except for the positions and strengths of the potential singularities.

In the doublet channel there is mixing between singlet and triplet channels, resulting in a coupled integral equation. In this case one can define $||K_D||^2 = \Sigma_{i,j=1}^{2} ||K_{ij}(W)||^2$, with $K_{ij} = Z_{ij}^{\frac{1}{2}\frac{1}{2}} \tau_j$.

The triplet propagator τ_1, has a deuteron bound pole on the first sheet but the antibound state pole in the singlet is on the second energy sheet. Hence the norms which include τ_1, i.e. K_{11} and K_{21} exist in the same region as in the spinless model. Obviously K_{12} and K_{22} must also be defined here on the physical sheet. The Fredholm solution for the doublet amplitude takes the form

$$X_{11}^{\frac{1}{2}\frac{1}{2}} = Z_{11}^{\frac{1}{2}\frac{1}{2}} + \Sigma_{j=1}^{2} Z_{1j}^{\frac{1}{2}\frac{1}{2}} Z_{j1}^{\frac{1}{2}\frac{1}{2}} + \Sigma_{i,j=1}^{2} Z_{1j}^{\frac{1}{2}\frac{1}{2}} R_{ji} Z_{il}^{\frac{1}{2}\frac{1}{2}} \tag{4.30}$$

where the R_{ij} are defined by

$$(1-K_D)^{-1} = \begin{bmatrix} 1-K_{11} & -K_{12} \\ -K_{21} & 1-K_{22} \end{bmatrix}^{-1} = \begin{bmatrix} R_{11} & R_{12} \\ R_{21} & R_{22} \end{bmatrix} = R(W). \tag{4.31}$$

$R(W)$ is an L^2 kernel whenever K_D is and therefore so are the R_{ij}. The rest of the argument is the same as before. A region of analyticity for $X_{11}^{\frac{1}{2}\frac{1}{2}}$ can be found by looking at a general term in the perturbation series:

$$K_{1i_1} K_{i_1 i_2} \cdots K_{i_{n-1} i_n} Z_{i_n 1}$$

with $i_k = 1$ or 2, $k = 1, \ldots, n$. Because of the coupling in the intermediate states, there are 2^{n-1} different n^{th}

order terms. Taking into account the two different range parameters β_1, β_2 of the singlet and triplet channels does not alter the previous argument. However, it does lead to a much more complicated singularity structure along the left hand potential cut in the physical sheet for $X_{11}^{\frac{1}{2}\frac{1}{2}}$.

4.2 Position of Singularities

We now direct our attention to finding the position of the singularities along the left hand cut on the physical sheet. In general, singularities result when the integration contours in perturbation terms are trapped between a pinch of two or more singularities in their integrands. Rules for locating the singularities were first developed in connection with the similar problem of finding the analytic structure of Feynman graphs in field theory. They are sometimes called the Landau rules and a brief resume is given in Appendix A*.

The denominators of the integrand may be split into the following classes:

1) Greens function in $Z(W;\underline{P}_i,\underline{P}_j)$

2) Greens function in $Z(W;\underline{k}_B,\underline{P}_i)$

3) Bound state denominators in $\tau(W - \frac{3}{4}p_i^2)$

4) Form factors in $Z(W;\underline{P}_i,\underline{P}_j)$

5) Form factors in $Z(W;k_B,\underline{P}_i)$.

Clearly there are many possibilities for pinch singularities. Apart from form factor denominators which give different singularities with different potentials, the remaining denominators are always present irrespective of the type of potential. We concentrate therefore on the singularities due to pinches between denominators of type 1), 2) and 3).

---

*For a comprehensive discussion of the rules and their application see (34).

The result of such an analysis may be stated as follows:

There is only *one* singularity in the bound state amplitude due to pinches of Green functions and propagators. It occurs in $T_1(W;\underline{k}_B,\underline{k}_B')$ and is the result of a pinch between the Greens functions in $Z(W;\underline{p}_1,\underline{k}_B)$ and $Z(W;\underline{k}_B',\underline{p}_1)$.

To prove this we apply the Landau rules to each perturbation term. Thus to determine the singularities of

$$T_1(W;\underline{k}_B,\underline{k}_B') = \int d\underline{p}_1\ K(W;\underline{k}_B,\underline{p}_1)Z(W;\underline{p}_1,\underline{k}_B')$$

due to the pinches between energy denominators we write the Feynmanised denominator as

$$D_2 = \alpha_1(W - \tfrac{3}{4}k_B^2 - (\underline{p}_1+\tfrac{1}{2}\underline{k}_B)^2) + \alpha_2(p_1^2-k_B^2) + \alpha_3(W-\tfrac{3}{4}k_B'^2 - \times$$

$$\times\ (\underline{p}_1+\tfrac{1}{2}\underline{k}_B')^2).$$

Applying the condition $\frac{\partial D_2}{\partial \underline{p}_1} = 0$ which is necessary for a singularity, results in the equation

$$\underline{p}_1(2\alpha_1+2\alpha_2+2\alpha_3) + \tfrac{1}{2}\underline{k}_B(2\alpha_1) + \tfrac{1}{2}\underline{k}_B'(2\alpha_3) = 0$$

where $\alpha_i \geq 0$. The subsidiary equations are

$$\alpha_1 = 0 \quad \text{or} \quad (\underline{p}_1+\tfrac{1}{2}\underline{k}_B)^2 = -B,$$

$$\alpha_2 = 0 \quad \text{or} \quad p_1^2 = k_B^2,$$

$$\alpha_3 = 0 \quad \text{or} \quad (\underline{p}_1+\tfrac{1}{2}\underline{k}_B')^2 = -B.$$

Since it is known the singularities lie on the imaginary axis we can set $\underline{k}_B = i\underline{K}_B$ where $\underline{K}_B$ is real. Then the singularities in the integrand of T_1 regarded as functions of p_1 are all on the imaginary p_1 axis. Thus by rotating the $\underline{p}_1$ contour through $\pi/2$ and letting $\underline{p}_1 = i\underline{q}_1$ the Landau equations can be written in terms of vectors in R^3. We have

$$2\underline{q}_1(\alpha_1+\alpha_2+\alpha_3) + \tfrac{1}{2}\underline{K}_B(2\alpha_1) + \tfrac{1}{2}\underline{K}_B'(2\alpha_3) = 0, \qquad (4.32)$$

and

$$\alpha_1 = 0 \quad \text{or} \quad (\underline{q}_1+\tfrac{1}{2}\underline{K}_B)^2 = B, \tag{4.33}$$

$$\alpha_2 = 0 \quad \text{or} \quad q_1^2 = K_B^2 \tag{4.34}$$

$$\alpha_3 = 0 \quad \text{or} \quad (\underline{q}_1+\tfrac{1}{2}\underline{K}_B')^2 = B. \tag{4.35}$$

Equation (4.32) is most clearly represented by the construction of a vector diagram (the Landau diagram). It constrains $\underline{q}_1$, $\underline{K}_B$ and K_B' to lie in a plane and $\underline{q}_1$ to be inside the triangle formed by $-\frac{1}{2}\underline{K}_B$ and $-\frac{1}{2}\underline{K}_B'$, which is denoted by $\Delta(-\frac{1}{2}\underline{K}_B, -\frac{1}{2}\underline{K}_B')$. The Landau diagram for the case α_1, α_2, $\alpha_3 > 0$ is shown in fig. 4.3.

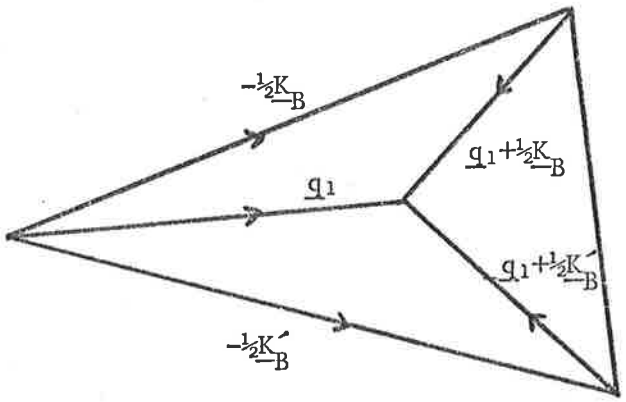

Figure 4.3

Landau Diagram for T_1. α_1, α_2, $\alpha_3 > 0$.

One can see there are no singularities in this case. For, if $\alpha_2 > 0$, $q_1 = K_B$ which is impossible since $\underline{q}_1$ is inside the triangle. Thus the equations are inconsistent, and there is no singularity due to a simultaneous pinch of three energy denominators in T_1. In fact all diagrams with $\alpha_2 > 0$ can be eliminated for this reason. In the remaining case $\alpha_2 = 0$, α_1, $\alpha_3 > 0$ the endpoint of $\underline{q}_1$is along $\frac{1}{2}(\underline{K}_B-\underline{K}_B')$ as in fig. 4.4.

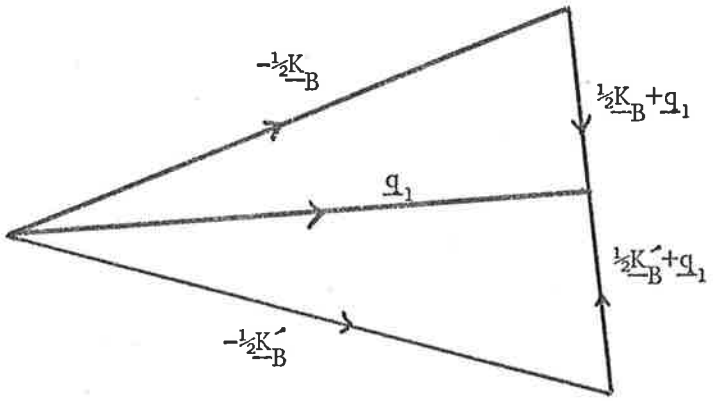

Figure 4.4

$\alpha_2 = 0,\ \alpha_1, \alpha_3 > 0$

The other constraints imply

$$\tfrac{1}{2}|\underline{K}_B - \underline{K}'_B| = 2B^{\frac{1}{2}},$$

so a singularity can occur when

$$K_B^2 = \frac{8B}{1-z}, \qquad z = \hat{k}_B \cdot \hat{k}'_B \ . \tag{4.36}$$

In order to prove there are no singularities arising from energy denominator pinches in *all* higher order terms in the perturbation series consider T_n. Its Feynmanised denominator is (setting $\underline{p}_i = i\underline{q}_i$, $\underline{k}_B = i\underline{K}_B$).

$$D_n = \alpha_1(-B+(\tfrac{1}{2}\underline{K}_B+\underline{q}_1)^2) + \alpha_2(-B-\tfrac{3}{4}K_B^2-(\underline{q}_2+\tfrac{1}{2}\underline{q}_1)^2) + \ldots$$

$$+ \ldots \alpha_j(-B-\tfrac{3}{4}K_B^2 + (\underline{q}_{j-1}+\tfrac{1}{2}\underline{q}_j)^2 + \tfrac{3}{4}q_j^2) + \ldots + \alpha_n(-B+(\tfrac{1}{2}\underline{K}_B+\underline{q}_{n-1})^2)$$

$$+ \alpha_{n+1}(q_1^2-K_B^2) + \ldots + \alpha_{n+j}(q_j^2-K_B^2) + \ldots + \alpha_{2n-1}(q_{n-1}^2-K_B^2). \tag{4.37}$$

The conditions $\dfrac{\partial D_n}{\partial \underline{q}_i} = 0$ yield the equations

$$\underline{q}_1 = \frac{2\alpha_1}{2\alpha_1+2\alpha_2+2\alpha_{n+1}}(-\tfrac{1}{2}\underline{K}_B) + \frac{\alpha_2}{2\alpha_1+2\alpha_2+2\alpha_{n+1}}(-\underline{q}_2),$$

$$\underline{q}_j = \frac{\alpha_j}{2\alpha_j+2\alpha_{j+1}+2\alpha_{n+j}}(-\underline{q}_{j-1}) + \frac{\alpha_{j+1}}{2\alpha_j+2\alpha_{j+1}+2\alpha_{n+j}}(-\underline{q}_{j+1}),\ j=2,..,n-2,$$

$$\underline{q}_{n-1} = \frac{\alpha_{n-1}}{2\alpha_{n-1}+2\alpha_n+2\alpha_{2n-1}}(-\underline{q}_{n-2}) + \frac{2\alpha_n}{2\alpha_{n-1}+2\alpha_n+2\alpha_{2n-1}}(-\tfrac{1}{2}\underline{K}_B'). \quad (4.38)$$

The remaining conditions for a singularity are

$$\alpha_1 = 0 \quad \text{or} \quad (\underline{q}_1+\tfrac{1}{2}\underline{K}_B)^2 = B, \quad (4.39)$$

$$\alpha_j = 0 \quad \text{or} \quad q_{j-1}^2+(\underline{q}_{j-1}+\underline{q}_j)^2+q_j^2 = 2(B+\tfrac{3}{4}K_B^2),\ j=2,..,n-2 \quad (4.40)$$

$$\alpha_n = 0 \quad \text{or} \quad (\underline{q}_{n-1}+\tfrac{1}{2}\underline{K}_B')^2 = B, \quad (4.41)$$

$$\alpha_{n+j} = 0 \text{ or } q_j^2 = K_B^2,\ j=1,..,n-1. \quad (4.42)$$

Equations (4.38) constrain each $(-1)^{j+1}\underline{q}_j$ to the inside of $\Delta(-\frac{1}{2}\underline{K}_B,(-1)^{n+1}\frac{1}{2}\underline{K}_B')$. Furthermore each $\underline{q}_j$ is in the interior of the triangle formed from the vectors adjacent to it. That is $\underline{q}_1$ lies inside $\Delta(-\frac{1}{2}\underline{K}_B,-\underline{q}_2)$, $\underline{q}_j$ inside $\Delta(-\underline{q}_{j-1},-\underline{q}_{j+1})$ and $\underline{q}_{n-1}$ in $\Delta(-\underline{q}_{n-2},-\frac{1}{2}\underline{K}_B)$. The resulting diagram is shown in fig. 4.5.

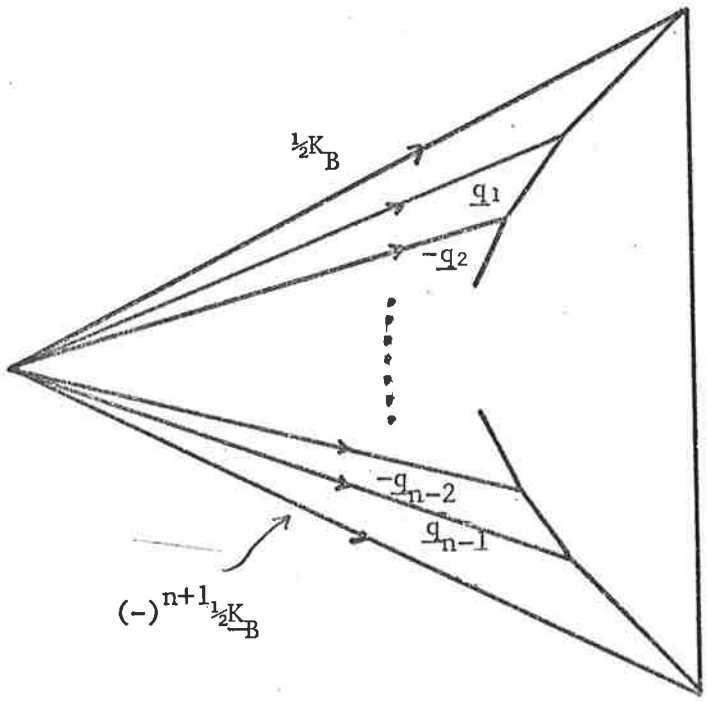

Figure 4.5

Landau diagram of n^{th} order term, $\alpha_j > 0$, $j=1,\ldots,n-1$.

Consider the diagrams with $\alpha_j > 0$, $j=1,\ldots,n-1$. Then each $q_j < K_B$ from fig. 4.5. Therefore $\alpha_{n+j} = 0$ for $j=1,\ldots,n-1$ otherwise $q_j = K_B$. However, the diagram with all $\alpha_j > 0$ and $\alpha_{n+j} = 0$ is inconsistent. This follows from the fact that $q_j < \frac{1}{2}K_B$ and therefore $q_j^2 + (q_{j-1}+q_j)^2 + q_j^2 \leq \frac{3}{2}K_B^2$. But this is inconsistent with equation (4.40).

Now we are left with the class of diagrams in which one or more of the α_j's $= 0$. Suppose $\alpha_1 = 0$, $\alpha_j > 0$, $j=2,\ldots,n$. Then from equation (4.38) it can be seen that $\underline{q}_1||\underline{q}_2||..||\underline{q}_{n-1}||\underline{K}_B'$. It is easy to show then that $\frac{1}{2}K_B \geq q_1 \geq 2q_2 \geq 4q_3 .. \geq 2^{n-1}q_n$. That is $q_j < \frac{1}{2}K_B$ and so we must have $\alpha_{n+j} = 0$, $j=1,\ldots,n-1$. But $\alpha_j > 0$, $j=2,\ldots,n$ is also inconsistent with equation (4.40). Thus there are no diagrams with $\alpha_1 = 0$ which lead to a singularity.

Say $\alpha_j = 0$ and all the other α's > 0. Then by equation (4.38) $\underline{q}_j||\underline{q}_{j+1}||\ldots||\underline{K}_B'$ and $\underline{K}_B||\underline{q}_1||\underline{q}_2\ldots||\underline{q}_{j-1}$. Hence $q_j < \frac{1}{2}q_{j+1} \ldots <$ $< (\frac{1}{2})^{n-j+1}K_B$ and $q_{j-1} < \frac{1}{2}q_{j-2} \ldots < (\frac{1}{2})^j K_B$. But then these conditions are not consistent with equations (4.40) or (4.42). It is not hard to see that the same type of reasoning applies if more than one of the $\alpha_j = 0$. In other words there are no solutions to the Landau equations for T_n, $n \geq 2$.

Thus the only singularities on the physical sheet of the on-shell elastic amplitude due to energy denominators are poles in $Z(W;k_B,k_B')$ at

$$W = -B\,\frac{z+2}{\frac{5}{4}+z}\,, \tag{4.43}$$

and the pinch singularity in T_1 at

$$W = -\,B(\frac{7-z}{1-z}). \tag{4.44}$$

Presumably if the amplitude is continued through the branch cut in $\tau(W-\frac{3}{4}p^2)$ onto the sheet where the other denominator equation (4.8) can vanish a different set of pinch singularities may be possible. However, the pole on the second sheet is far away from the physical sheet, and we shall not consider it further.

4.3 Equations with Zero Range Forces

The class of singularities found in the last section provide the complete singularity structure of the left hand cut in the case of zero range two body interactions. This can be seen from the Amado model by taking the limit $\beta\to\infty$ (since β is on inverse range). The Born term in this limit is (equations (2.17), (2.23), (2.28), (2.29)),

$$Z_{TMR}(W;\underline{p},\underline{p}') = \frac{B^{\frac{1}{2}}}{\pi^2}\frac{1}{W-p^2-p'^2-\underline{p}\cdot\underline{p}'}$$

and for the propagator we have

$$\tau_{TMR}(W-\tfrac{3}{4}p^2) = \tfrac{1}{2}\frac{1}{(B^{\frac{1}{2}}+i(W-\frac{3}{4}p^2)^{\frac{1}{2}})B^{\frac{1}{2}}} .$$

The resulting integral equation

$$X_{TMR}(W;\underline{p},\underline{p}') = \frac{2B^{\frac{1}{2}}}{\pi^2}\frac{1}{W-(\underline{p}+\frac{1}{2}\underline{p}')^2-\frac{3}{4}p'^2}+\frac{1}{\pi^2}\int d\underline{p}''\ \times$$

$$\times\frac{X_{TMR}(W;\underline{p}'',\underline{p}')}{(W-(\underline{p}+\frac{1}{2}\underline{p}'')^2-\frac{3}{4}p''^2)(B^{\frac{1}{2}}+i(W-\frac{3}{4}p''^2)^{\frac{1}{2}})}\ ; \qquad (4.45)$$

the Skorniakov - Ter - Martirosian* equation (33) was formulated in the 1950's preceding the work of Faddeev. Although it incorporates the effect of the three body threshold, it has the drawback that it has a three-body bound state of infinite

---

*These authors derived the equation in coordinate space. It has been given in momentum space by Faddeev (35). See also ref.(36).

energy. This consequence of the assumption of the zero range interaction had already been noted by Thomas (37) back in 1931.

The on-shell amplitude of this equation, by the results of the last section has only two singularities along the left hand cut, which are contained in the first two terms of the multiple scattering series.

Interestingly enough Amado (15) has recently rederived equation (4.45) purely by implementing the constraints of two-body unitarity on a three-body final state, suggesting that this amplitude is the simplest form of three-body bound-state scattering amplitude compatible with the general constraints of quantum mechanics.

The analogue of the STM equation in one dimension is also interesting. The equation is

$$X(W;p,p') = \frac{\lambda^3}{2\pi}\frac{1}{W-\frac{3}{4}p'^2-(p+\frac{1}{2}p')^2} - \frac{\lambda}{\pi}\int_{-\infty}^{\infty} \times$$

$$\times \frac{X(W;p'',p')(W-\frac{3}{4}p''^2)^{\frac{1}{2}}dp''}{(W-\frac{3}{4}p''^2-(p+\frac{1}{2}p'')^2)(2(W-\frac{3}{4}p''^2)^{\frac{1}{2}}-i\lambda)}, \qquad (4.46)$$

where λ is the strength of the two-body interaction in coordinate space, i.e. $V(r,r') = -\lambda\delta(r)\delta(r')$. Dodd (16) has shown that the half-off-shell amplitude* can be expressed in closed form:

$$X(W;p,k_B) = \frac{-\lambda^3}{2\pi^2}\frac{(2(W-\frac{3}{4}p^2)^{\frac{1}{2}}-i\lambda)p(3k_B+i\lambda)}{(p-k_B)((p+\frac{1}{2}k_B)^2+\lambda^2/4)(k_B-i\lambda)}, \quad \text{Im } k_B > 0. \qquad (4.47)$$

In this model the relation between the two-body bound state energy and λ is

$$B = \lambda^2/4.$$

---

*In ref.(16) the two body bound state has been normalised to $(-2\pi\lambda^{-3})^{\frac{1}{2}}$.

In contrast to the STM equation it has been shown (37) that there is a three-body bound state at $W = -4B$. There are only two possible on-shell amplitudes, one in the forward direction and the backscattering one. Taking the limit $P \to k_B$ in equation (4.47) the forward scattering amplitude is found to be

$$X(W;k_B,k_B) = \frac{-6\lambda k_B^2}{\pi(3k_B-i\lambda)(k_B-i\lambda)} \quad , \text{ Im } k_B > 0. \tag{4.48}$$

The pole at $k_B = i\lambda$ is associated with the three body bound state and is not present in the perturbation terms.

This leaves only the singularity at $k_B = \frac{i\lambda}{3}$. It checks with the results of the last section according to which the Born term has a pole at $k_B = \frac{i\lambda}{3}$ when $z=1$.

If the limit $p \to -k_B$ is taken in equation (4.47) one finds that the backscattering amplitude reduces to

$$X(W;-k_B,k_B) = 0, \quad \text{Im } k_B > 0. \tag{4.49}$$

At first sight this seems unreasonable because there is a singularity predicted in $Z(W;-k_B,k_B)$ and $T_1(W;-k_B,k_B)$ at $k_B = i\lambda$. However, a calculation reveals that the residues of Z and T_1 at this pole are equal in magnitude and opposite in sign.

Thus this model demonstrates the point, that the amplitude need not have all the singularities of its perturbation series terms. In addition the amplitude can have poles due to the vanishing of the Fredholm denominator which are not present in the perturbation series.

4.4 Discussion

In summary it has been shown that the analytic properties of the elastic amplitude for a system of three bosons is

similar in most respects to the two-body amplitudes based on the Lippmann - Schwinger equation. There are no singularities in the complex energy plane and for real energies there are the usual left hand "potential" cuts and right hand unitary cuts. However, there is a difference in that the three-body on-shell amplitude has apart from the square root branch point at the two-body threshold a logarithmic branch point at W=0, the three-body threshold. The existence of these branch points at $k_B=0$ and $k_B=(\frac{4}{3}B)^{\frac{1}{2}}$ follows from our analysis. Their exact nature has been discussed by Graves-Morris (38).

We should also mention that the left hand cut has quite a complicated singularity structure. This is due to the fact that there are singularities arising from pinches of the various form factor denominators between themselves, pinches between form factor denominators and energy denominators and of course the pinches between energy denominators which we studied in detail. One unusual aspect of the singularities in the Amado model has been observed by Greben (39). With the Yamaguchi form factor the leading singularities of the higher order perturbation terms move to the left as the order is increased but accumulate at a finite point. In the three spinless boson case this accumulation point is at $-B - 3\beta^2$. One can also derive this result by considering the on-shell analogues of the singularities listed by Brayshaw (32) (especially the appendix).

Because the inverse range parameters, β_i are usually much larger than that associated with the two-body bound state, the nearest singularities to the physical region are those due the energy denominator pinches. As we have seen apart from the Born term there is only one pinch singularity and this occurs in T_1.

The question of whether these nearest singularities provide a good approximation to the discontinuity across the left hand cut in dispersion type equations is taken up in Chapter 6.

In connection with dispersion relations it should be mentioned that the analyticity properties of the partial wave amplitudes are essentially the same as for the full fixed angle on-shell amplitudes. This is because regions in which the fixed angle amplitude is analytic will under integration with a Legendre polynomial give an analytic result. The analyticity properties of the neutron-deuteron amplitudes are used in Chapter 6 to construct a rigorous partial wave dispersion relation which is then applied to an investigation of numerical on-shell approaches to the solution of the neutron-deuteron amplitudes.

Chapter 5

ANALYTICITY OF BREAKUP AND FREE SCATTERING AMPLITUDES

The advantage of studying the analytic properties in the complex energy plane of the three-body breakup and free scattering amplitudes in the separable model is apparent. Referring to equations (2.5) and (2.6) we see essentially one only need determine the analytic properties of the half-on and off-shell rearrangement amplitudes, or in the case of identical bosons the symmetrised elastic amplitude. The analytic continuation of the momenta $\underline{k}_R$, $\underline{k}_F$ describing the free particle state* may be defined in the following way. The on-shell condition $E = k_R^2 + \frac{3}{4}k_F^2$ for physical energies enables one to write

$$\underline{k}_R = E^{\frac{1}{2}}\underline{n}_R, \quad \underline{k}_F = E^{\frac{1}{2}}\underline{n}_F \text{ with } n_R \leq 1, \; n_F \leq (\tfrac{4}{3})^{\frac{1}{2}}.$$

In order to continue the momenta to complex energies we therefore define

$$\underline{k}_R = k\underline{n}_R, \quad \underline{k}_F = k\underline{n}_F \text{ where } k = W^{\frac{1}{2}}.$$

The discussion in this chapter is limited to systems of identical spinless bosons. Nevertheless, we shall find the breakup and free particle amplitudes have quite a rich analytic structure through the occurrence of several types of anomalous singularities along the real negative axis in the range $-\frac{4}{3}B < E < -B$. With the exception of the Born term in the breakup amplitude which can under certain conditions have pole singularities at complex energies the remaining singularities lie along the real axis and consist of left hand potential cuts, the right hand unitarity and anomalous cuts and in the case of the free particle

---

*To emphasise the continuation of the momenta to complex energies, we use $\underline{k}_R$ rather than $\underline{q}$ to label the relative momentum.

amplitude rescattering cuts. With the rescattering cuts defined to run along the negative real axis and the Born term in the lower half-plane suitably defined, both the amplitudes are Hermitian analytic on the physical sheet.

The results we obtain are in accord with those of Rubin, Sugar and Tiktopoulos for amplitudes based on the Faddeev equations with Yukawa potential interactions. This is not surprising because the analytic structure of their amplitudes should only differ in the location and strength of potential cuts. We conclude the chapter by showing directly the manner in which their analysis reduces to a study of the Amado model when the Yukawa interaction is replaced by the separable Yamaguchi potential.

5.1 Breakup Amplitude

Remembering the breakup amplitude is

$$X_0(E+i0;\underline{k}_R,\underline{k}_F;\underline{k}_B) = \Sigma_i\, g(\underline{k}_{R_i})\tau(k^2_{R_i})X(E+i0;\underline{k}_{F_i};\underline{k}_B)$$

the problem reduces to one of finding the analytic structure of $X(W;\underline{k}_F,\underline{k}_B)$. Our approach is very similar to the one used in the case of the elastic on-shell amplitude. That is we shall determine a region of analyticity of $X(W;\underline{k}_F,\underline{k}_B)$ by studying the analyticity of the perturbation series terms in its Fredholm expansion. Then we seek to extend this region by defining new amplitudes $X_\theta(W;\underline{k}_F,\underline{k}_B)$ which are identical to $X(W;\underline{k}_F,\underline{k}_B)$ in the region of overlap. This proves to be a more complicated procedure than for the elastic amplitude for two reasons. First, the Greens function denominator in $Z(W;\underline{k}_F,\underline{p})$ can always vanish for some real $\underline{p}$ when $n_F > 1$ and second there is a non-linear

relationship between k and k_B; that is $k = (-B + \frac{3}{4}k_B^2)^{\frac{1}{2}}$.

We begin by considering the Fredholm solution of $X(E+i0;k_F,k_B)$ in the form

$$X(E+i0;\underline{k}_F,\underline{k}_B) = Z(E;\underline{k}_F,\underline{k}_B) + T_1(E+i0;\underline{k}_F,\underline{k}_B) + X_R(E+i0;\underline{k}_F,\underline{k}_B)$$

where it is known from the work in Chapter 3 that X_R is the sum of a uniformly convergent series. Because of the Greens function denominator in $Z(W;\underline{k}_F,\underline{p})$ one cannot obtain a region in the W plane where the denominators of the perturbation series terms do not vanish. If one tries the substitution $\underline{p}_1 \to \underline{p}_1 - \frac{1}{2}\underline{k}_F$ a region in which the modified denominators do not vanish exists. However, problems are then encountered in attempts to analytically continue the region to all parts of the energy plane. To overcome this difficulty we employ a device used by RST. The trick is to combine the denominator of the propagator $\tau(E+i\varepsilon-\frac{3}{4}q_1^2)$ and the free Greens function in $Z(E+i\varepsilon,\underline{k}_F,\underline{q}_1)$ by means of Feynmans identity. That is, we write

$$(\tfrac{4}{3}(W+B)-q^2)^{-1}(W-\tfrac{3}{4}k_F^2-(q_1+\tfrac{1}{2}k_F)^2)^{-1}$$

$$= \int_0^1 dx\,((\tfrac{4}{3}x(W+B)-xq^2+(1-x)(W-\tfrac{3}{4}k_F^2-(q_1+\tfrac{1}{2}k_F)^2)^{-2}. \qquad (5.1)$$

After a little rearrangement the denominator becomes

$$-(q_1+\frac{(1-x)}{2}k_F)^2 + k^2(1+\tfrac{1}{3}x + (x-1)n_F^2 + \frac{(x-1)^2}{4}n_F^2) + \tfrac{4}{3}xB,$$

which with the transformation $q_1 \to q_1 - \frac{(1-x)}{2}k_F$ reduces to

$$-q_1^2 + k^2(1 + \tfrac{1}{3}x + (x-1)n_F^2 + \frac{(x-1)^2}{4}n_F^2) + \tfrac{4}{3}xB. \qquad (5.1')$$

Thus the perturbation series terms $T_n(E+i0;\underline{k}_F,\underline{k}_B)$ in the Fredholm series are now given by the following integrals:

$$T_1(E+i0;\underline{k}_F,\underline{k}_B) = \lim_{\varepsilon\to 0}\int_0^1 dx \int d\underline{q}_1 K(E+i\varepsilon;\underline{k}_F,\underline{q}_1-\frac{(1-x)}{2}\underline{k}_F) \times$$

$$\times\, Z(E+i\varepsilon;\underline{q}_1-\frac{(1-x)}{2}\underline{k}_F,\underline{k}_B),$$

$$T_n(E+i0;\underline{k}_F,\underline{k}_B) = \lim_{\varepsilon\to 0}\int_0^1 dx \int d\underline{q}_1 \ldots d\underline{q}_n K(E+i\varepsilon;\underline{k}_F,\underline{q}_1-\frac{(1-x)}{2}\underline{k}_F) \times$$

$$\times K(E+i\varepsilon;\underline{q}_1-\frac{(1-x)}{2}\underline{k}_F,\underline{q}_2)\ldots Z(E+i\varepsilon;\underline{q}_n,\underline{k}_B), \qquad (5.2)$$

$$n \geq 2,$$

where it is to be understood that the Greens function and propagator denominator have been combined according to equations (5.1) and (5.1'). With the denominators of the perturbation terms in this form one can then proceed to find a region of analyticity for $X(W;\underline{k}_F,\underline{k}_B)$. Because T_1 has some denominators which are not in the Fredholm series of X_R it is convenient to study the analytic structure of X_R and T_1 separately.

a) Analyticity of $X_R(W;\underline{k}_F,\underline{k}_B)$

Since the analytic continuation of $X_R(W;\underline{k}_F,\underline{k}_B)$ inevitably leads to consideration of $X_{R\theta}(W;\underline{k}_F,\underline{k}_B)$ defined from $X_R(W;\underline{k}_F,\underline{k}_B)$ by the simultaneous rotation of contours $\underline{q}_i \to \underline{q}_i e^{i\theta}$, the argument is simplified somewhat by noting that with $\theta=0$, $X_{R\theta} \equiv X_R$. New denominators one encounters on applying the rotation of contours to the integrals in equation (5.2) are as follows:

$$\beta^2 + (\underline{k}_F + \tfrac{1}{4}(x-1)\underline{k}_F + \tfrac{1}{2}\underline{q}_1 e^{i\theta})^2, \qquad (5.3)$$

$$\beta^2 + (\tfrac{1}{2}\underline{k}_F + \tfrac{1}{2}(x-1)\underline{k}_F + \underline{q}_1 e^{i\theta})^2, \qquad (5.4)$$

$$\beta^2 + (\underline{q}_2 e^{i\theta} + \tfrac{1}{4}(x-1)\underline{k}_F + \tfrac{1}{2}\underline{q}_1 e^{i\theta}), \qquad (5.5)$$

$$\beta^2 + (\tfrac{1}{2}\underline{q}_2 e^{i\theta} + \tfrac{1}{2}(x-1)\underline{k}_F + \underline{q}_1 e^{i\theta}), \qquad (5.6)$$

$$W - \frac{3}{4}q_2^2 e^{2i\theta} - (\tfrac{1}{2}\underline{q}_2 e^{i\theta} + \underline{q}_1 e^{i\theta} - \frac{(1-x)}{2}\underline{k}_F)^2, \qquad (5.7)$$

and of course the combined denominator of equation (5.1'). The remaining denominators in each perturbation term have

been studied in Chapter 4. They are non-vanishing in the region

$$0 < \text{Im } k_B e^{-i\theta} < 2B^{\frac{1}{2}}\cos\theta. \tag{5.8}$$

One can similarly show (see appendix B) that the denominators of equations (5.3) and (5.7) cannot vanish in the region

$$0 < \text{Im } k e^{-i\theta} < (\tfrac{4}{3})^{\frac{1}{2}}\beta\cos\theta, \tag{5.9}$$

while for the combined denominator (5.1') the effect of the rotation of q_1 is to restrict the possible vanishing points to the region bounded by the rectangular hyperbolae

$$\begin{aligned} 2\text{Im } k e^{-i\theta}\ \text{Re} k e^{-i\theta} &= V\sin 2\theta, \\ 2\text{Im } k e^{-i\theta}\ \text{Re} k e^{-i\theta} &= B^{\frac{1}{2}}\sin 2\theta, \end{aligned} \tag{5.10}$$

and

$$\text{Re} k > 0.$$

Here V is defined as follows:

$$\begin{aligned} V &= B^{\frac{1}{2}}, \quad 0 \le n_F \le 1 \\ &= \frac{\frac{4}{3} x_m B^{\frac{1}{2}}}{1 + \frac{1}{3}x_m + (x_m - 1 + \frac{(x_m-1)^2}{4})n_F^2}, \quad 1 < n_F < (\tfrac{4}{3})^{\frac{1}{2}}, \end{aligned} \tag{5.11}$$

where

$$x_m = (\frac{2}{n_F})^2 - 3.$$

Consequently V lies in the range $B^{\frac{1}{2}} \le V < (\frac{4}{3}B)^{\frac{1}{2}}$.

To investigate the nature of the region in equation (5.8) in the k plane we have computed it numerically for $\theta=\pi/4$ (see fig. 5.1). The mapping of the k_B plane into the k plane depends on whether the k_B trajectory crosses the left hand cut or not. For example, consider trajectory (6) on the first sheet of k_B. As k_B approaches the cut from below the corresponding k values approach the real axis. When k_B

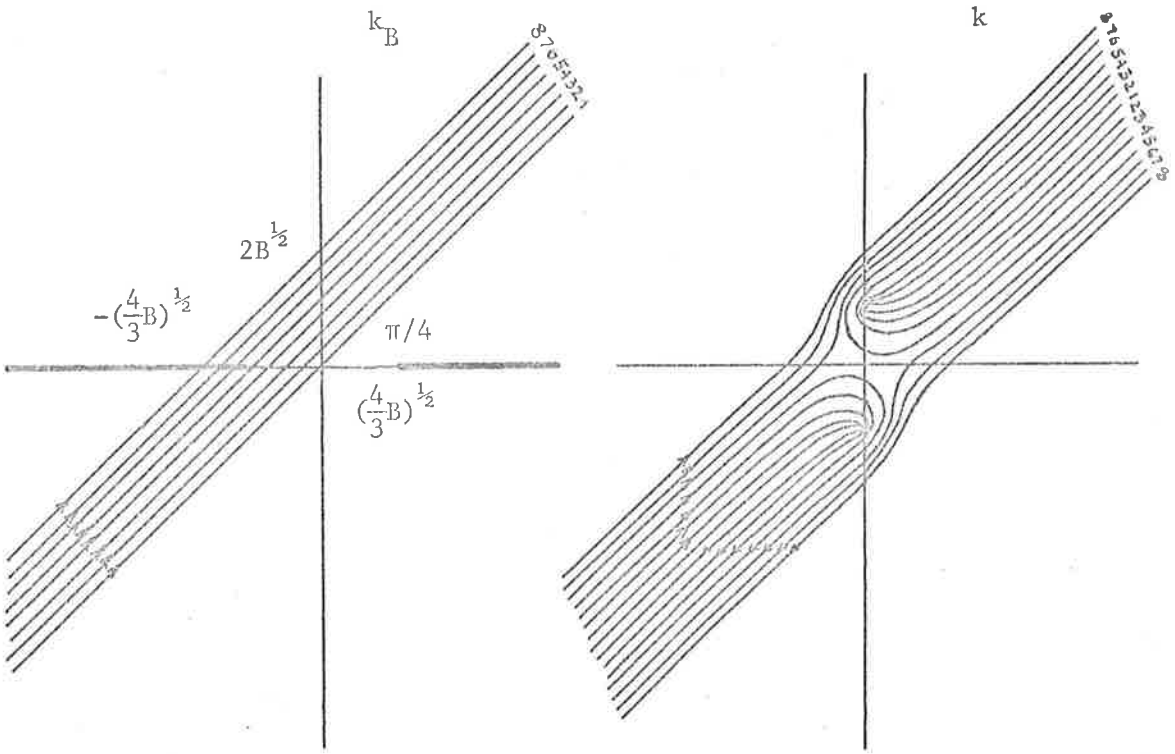

Figure 5.1

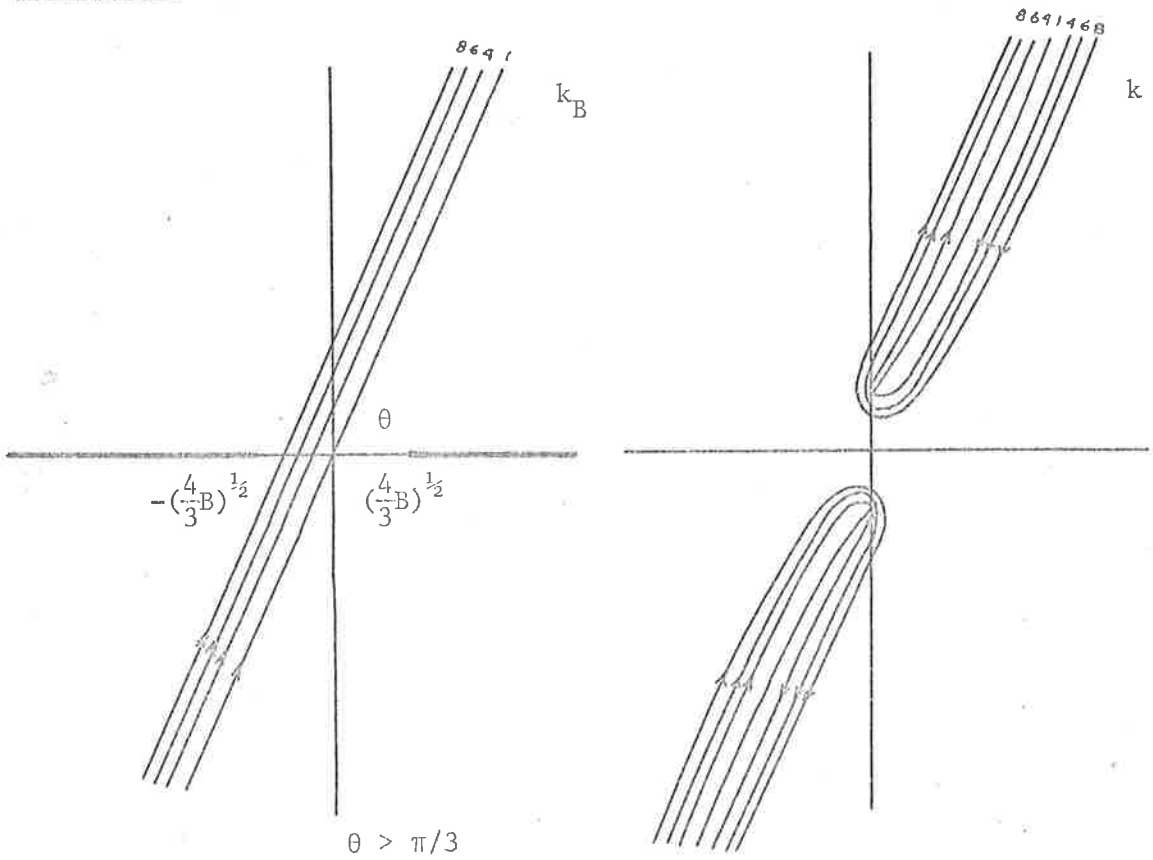

Figure 5.2

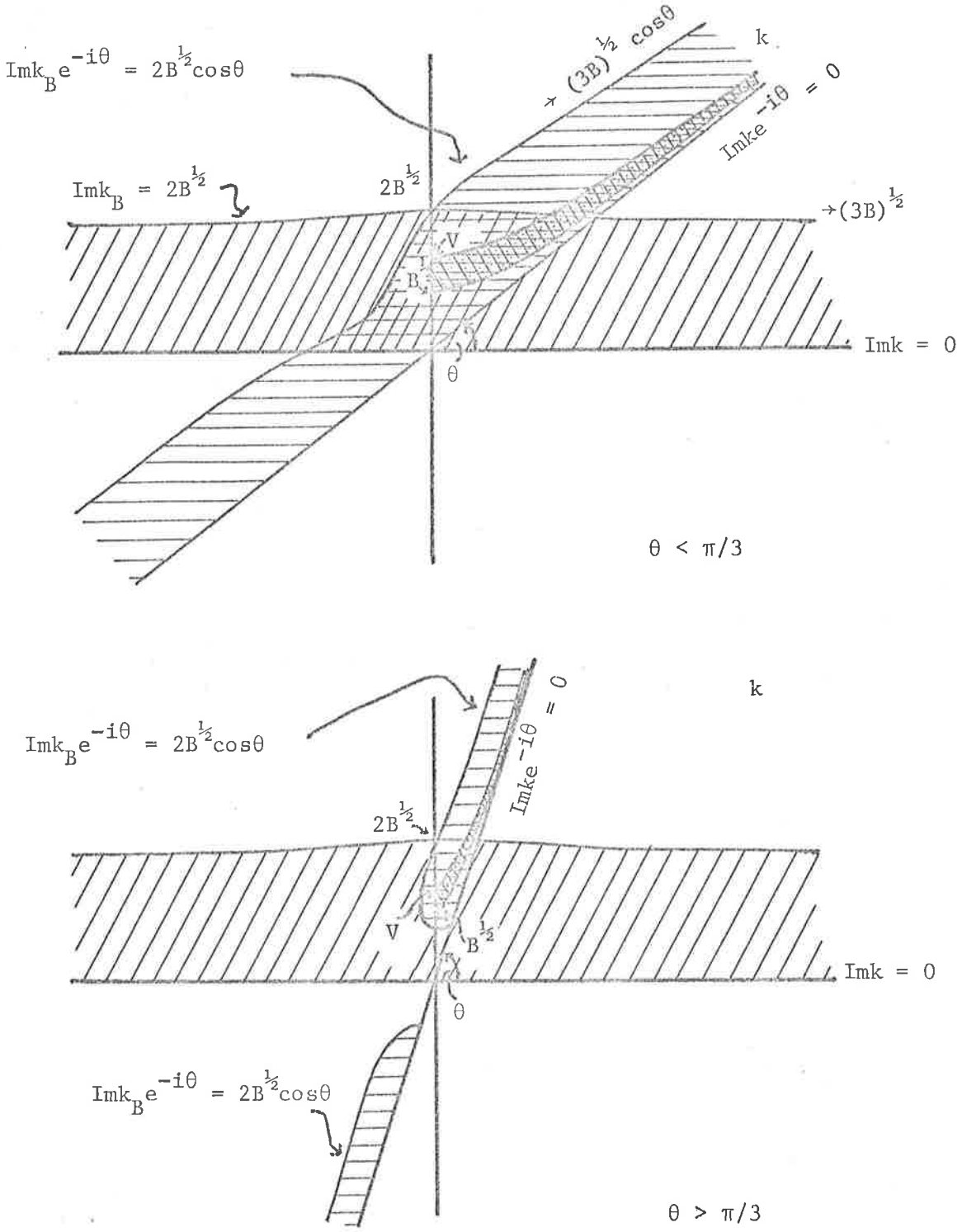

Figure 5.3

//// Region of analyticity of X_R

Region of analyticity of $X_{R\theta}$

Region of singularities of combined Green function and propagator denominators.

crosses the cut there is a discontinuity in the k trajectory, while if k_B is continued through the cut on to the second sheet, the k values map continuously into the lower half plane. Therefore, if one takes into account the two sheeted nature of the mapping, the strip region in the k_B plane is mapped into the interior of the simply connected region bounded by $\text{Im } k_B e^{-i\theta} = 2B^{\frac{1}{2}}\cos\theta$ excluding the points along $\text{Im } k_B e^{-i\theta} = 0$, which are segments of a rectangular hyperbola in the k plane.

However, when $\theta > \pi/3$, the strip is rotated sufficiently so that no part of it passes through the branch cut. In this case the strip is mapped into the two distinct regions of fig. 5.2 corresponding to the two different sheets of k_B.

The domains of analyticity of X_R and $X_{R\theta}$ are shown in fig. 5.3 in the two cases. One can see that so long as $|\theta| < \pi/2$, the portion of the imaginary axis $(\frac{4}{3}B)^{\frac{1}{2}} < \text{Im } k < 2B^{\frac{1}{2}}$ is common to X_R and $X_{R\theta}$. Now, if one converts the integrals in the perturbation terms to the generalised spherical polar coordinates and studies the positions of the singularities of the integrands in the Q plane, for k in this strip all the singularities lie on the imaginary Q axis. Thus the simultaneous rotation of coordinates can be rigorously performed and $X_R = X_{R\theta}$ along this strip. But this is sufficient to ensure $X_{R\theta}$ provides an analytic continuation of X_R. From fig. 5.3 it can be seen that as θ is rotated through $-\pi/2$ to $+\pi/2$, the analytic continuation covers the entire upper half k plane with the exception of the

following parts of the imaginary axis :

$$B^{\frac{1}{2}} < \text{Im } k < (\tfrac{4}{3}B)^{\frac{1}{2}}, \quad \text{Im } k > 2B^{\frac{1}{2}} \text{ and } k = 0.$$

It will become clear when the class of pinch singularities from the energy denominators is found that they lie in the region $B^{\frac{1}{2}} < \text{Im } k < (\frac{4}{3}B)^{\frac{1}{2}}$ while the point $k = 0$ is the logarithmic branch point due to the breakup threshold.

When the domain of analyticity of $X_{R\theta}$ consists of a single strip, that is when $|\theta| < \pi/3$ we can also extend the analyticity of X_R to the lower half k plane with the exception of the sector $-2\pi/3 < \arg k < -\pi/3$.

b) Analyticity of $T_1(W;\underline{k}_F,\underline{k}_B)$

Apart from the denominators we have investigated in connection with $X_{R\theta}$, $T_{1\theta}$ has new denominators from the $Z(W;\underline{q}_1 e^{i\theta} - \frac{(1-x)}{2}\underline{k}_F,\underline{k}_B)$ term:

$$\beta^2 + (\underline{k}_B + \tfrac{1}{4}(x-1)\underline{k}_F + \tfrac{1}{2}\underline{q}_1 e^{i\theta})^2, \tag{5.12}$$

$$\beta^2 + (\tfrac{1}{2}\underline{k}_B + \frac{(x-1)}{2}\underline{k}_F + \underline{q}_1 e^{i\theta})^2,$$

and

$$B + (\tfrac{1}{2}\underline{k}_B + \frac{(x-1)}{2}\underline{k}_F + \underline{q}_1 e^{i\theta})^2.$$

It is shown in appendix B that the denominators of equation (5.12) do not vanish in the region:

$$0 < |\text{Im } k_B e^{-i\theta}| + (\tfrac{4}{3})^{\frac{1}{2}} \text{ Im } k e^{-i\theta} < 2B^{\frac{1}{2}} \cos\theta \tag{5.13}$$

$$\text{Im } k e^{-i\theta} > 0.$$

The features of this mapping into the k plane are discussed in appendix C. The domain of analyticity of $T_{1\theta}$ is shown in fig. 5.4 for $\theta = \pi/4$. It consists of the regions bounded by the lines

$$\text{Im } k_B e^{-i\theta} + (\tfrac{4}{3})^{\frac{1}{2}} \text{ Im } k e^{-i\theta} = 2B^{\frac{1}{2}} \cos\theta$$

and

$\text{Im}\ \ ke^{-i\theta} = 0,$

excluding the region of equation (5.10).

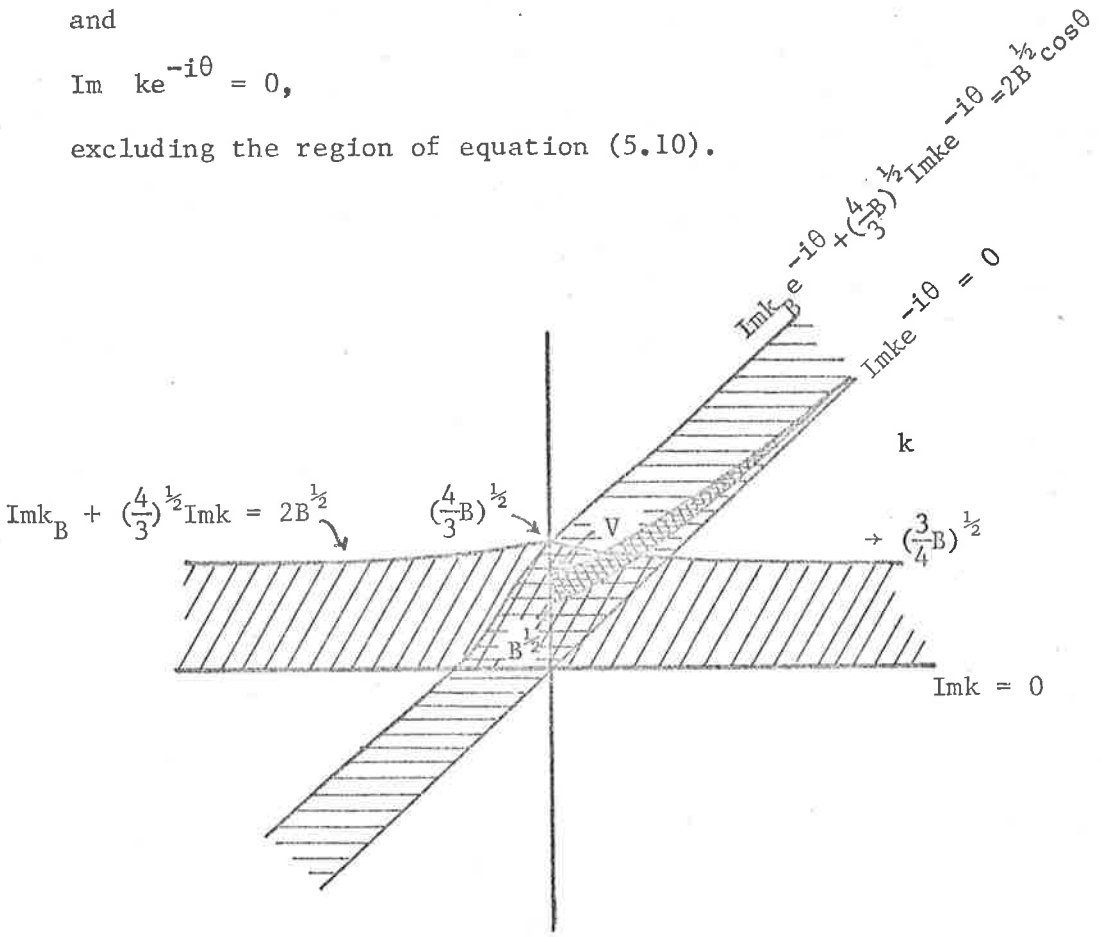

Figure 5.4

Region of analyticity of T_1, $T_{1\theta}$, $\theta = \pi/4$.

When $|\theta| > \pi/3$ the domain of analyticity of $T_{1\theta}$ splits in two distinct regions, in much the same way as happened with $X_{R\theta}$. However, the domain of analyticity of $T_{1\theta}$ overlaps with that of T_1 in the upper half k plane along the imaginary axis in the region

$V < \text{Im } k < (\frac{4}{3}B)^{\frac{1}{2}}$.

One can prove that $T_1 = T_{1\theta}$ for k in this region by studying the singularities in the Q plane when $|\theta| < \pi/2$.

Thus T_{1_θ} is an analytic continuation of T_1, and as θ is varied from $-\pi/2$ to $+\pi/2$, the domain of analyticity can be extended to the entire upper half k plane except for possible singularities along the portion of the imaginary axis,

$$\text{Im } k > \left(\tfrac{4}{3}B\right)^{\frac{1}{2}}$$

$$B^{\frac{1}{2}} < \text{Im } k < V \leq \left(\tfrac{4}{3}B\right)^{\frac{1}{2}}.$$

To complete the discussion of the analytic properties of $X(W;\underline{k}_F,\underline{k}_B)$ there is still the Born $Z(W;\underline{k}_F,\underline{k}_B)$ term to consider. It will have pole singularities at

$$k^2 = \frac{\frac{4}{3}Bn_F^2z^2 - 2(\beta^2+\frac{4}{3}B)(\frac{4}{3}+\frac{1}{4}n_F^2) - \frac{4}{3}n_Fz(Bn_F^2z^2+(3\beta^2+4B)(\beta^2-\frac{1}{4}Bn_F^2))^{\frac{1}{2}}}{2((\frac{4}{3}-\frac{1}{4}n_F^2)+\frac{4}{3}n_F^2(1-z^2))}, \quad (5.14)$$

$$k^2 = \frac{\frac{4}{3}Bn_F^2z^2 - 2(\beta^2+\frac{1}{3}B)(\frac{1}{3}+n_F^2) - \frac{4}{3}n_Fz[Bn_F^2z^2+3(\beta^2+\frac{1}{3}B)(\beta^2-n_F^2B)]^{\frac{1}{2}}}{2((\frac{1}{3}+n_F^2)^2 - \frac{4}{3}n_F^2z^2)},$$

or

$$k^2 = \frac{-\frac{4}{3}B(\frac{2}{3}+n_F^2(2-z^2)+n_Fz(n_F^2z^2+4-4n_F^2)^{\frac{1}{2}})}{2((\frac{1}{3}+n_F^2)^2-\frac{4}{3}n_F^2z^2))}, \quad Z = \hat{k}_B\cdot\hat{n}_F.$$

When $1 < n_F^2 < \frac{4}{3}$ the singularities of the energy denominator may occur at complex energies, depending on the value of z.

The breakup amplitude in the separable model also contains pole singularities in the terms $g(\underline{k}_B)$ and $\tau(k_R^2)$ which lie along the real axis for $E < -B$.

Recapitulating, we have seen that the singularities of the breakup amplitude, excluding the Born term, lie on the real energy axis. To ensure that the amplitude is Hermitian analytic, i.e. $X_0(W^*) = X_0^*(W)$ it is therefore

necessary to define the analytic continuation of $Z(W)$ to the lower half of the physical sheet by $Z(W^*) = Z^*(W)$. The remaining terms are Hermitian analytic because they each possess a portion of the real axis free of singularities, and one can therefore apply the Schwartz reflection principle.

5.2 Free Particle Amplitude

In contrast to the breakup amplitude where the appearance of k_B and k simultaneously in the denominators complicates the study, the analytic properties of the free scattering amplitude given by

$$X_{00}(E+i0;\underline{k}_F',\underline{k}_R',\underline{k}_F,\underline{k}_R) = \Sigma_i \delta(\underline{k}_{F_i} - \underline{k}_{F_i}')g(\underline{k}_{R_i}')\tau(k_{R_i}^2)g(\underline{k}_{R_i}) + \Sigma_{ij}\, g(\underline{k}_{R_i}')\tau(k_{R_i}'^2)X(E+i0;\underline{k}_{F_i}',\underline{k}_{F_j})\tau(k_{R_j}^2)g(\underline{k}_{R_j})$$

are more easily found. To continue $X(E+i0;\underline{k}_F',\underline{k}_F)$ one can use the Fredholm solution as given by equation (3.51) with $\theta = 0$:

$$X(E+i0;\underline{k}_F',\underline{k}_F) = Z(E+i0;\underline{k}_F',\underline{k}_F) + T_1(E+i0;\underline{k}_F',\underline{k}_F) + T_2(E+i0;\underline{k}_F',\underline{k}_F) + X_{RF}(E+i0;\underline{k}_F',\underline{k}_F).$$

Different types of denominators can occur in three classes of perturbation terms:

$$T_1(E+i0;\underline{k}_F',\underline{k}_F) = \lim_{\varepsilon\to 0} \int d\underline{q}_1 K(E+i\varepsilon;\underline{k}_F',\underline{q}_1 - \tfrac{1}{2}\underline{k}_F')Z(E+i\varepsilon;\underline{q}_1 - \tfrac{1}{2}\underline{k}_F',\underline{k}_F) \quad (5.15)$$

$$T_2(E+i0;\underline{k}_F',\underline{k}_F) = \lim_{\varepsilon\to 0} \int d\underline{q}_1 d\underline{q}_2 K(E+i\varepsilon;\underline{k}_F',\underline{q}_1 - \tfrac{1}{2}\underline{k}_F')K(E+i\varepsilon;\underline{q}_1 - \tfrac{1}{2}\underline{k}_F',\underline{q}_2 - \tfrac{1}{2}\underline{k}_F) \times Z(E+i\varepsilon;\underline{q}_2 - \tfrac{1}{2}\underline{k}_F,\underline{k}_F), \quad (5.16)$$

and $T_n(E+i0;\underline{k}_F',\underline{k}_F)$, $n \geq 3$. As with the breakup amplitude it is more convenient to deduce the analyticity of $X(E+i0;\underline{k}_F',\underline{k}_F)$ by studying the parts T_1, T_2 and X_{RF} one at a time.

a) Analyticity of $X_{RF}(W;\underline{k}_F',\underline{k}_F)$

$X_{RF\theta}$ only has the perturbation terms of order $n \geq 3$. The denominators in these terms which have not been discussed before are the energy denominators in $Z(W;\underline{k}_F,\underline{q}_1 e^{i\theta}-\frac{1}{2}\underline{k}_F)$ and $\tau(W-\frac{3}{4}(\underline{q}_1 e^{i\theta}-\frac{1}{2}\underline{k}_F)^2)$:

$$k^2 - q_1^2 e^{2i\theta}, \tag{5.17}$$

$$W+B - \frac{3}{4}(\underline{q}_1 e^{i\theta} - \frac{1}{2}\underline{k}_F)^2. \tag{5.18}$$

Obviously, the first one cannot vanish for complex $ke^{-i\theta}$ while the region in which denominator (5.18) vanishes is shown in appendix B to be

$$0 < \text{Im } ke^{-i\theta} < (\tfrac{4}{3}B)^{\frac{1}{2}} \cos\theta.$$

Together with the other denominators we therefore see that $X_{RF\theta}$ must be analytic in the strip

$$(\tfrac{4}{3}B)^{\frac{1}{2}} \cos\theta < \text{Im } ke^{-i\theta} < (\tfrac{4}{3}\beta^2)^{\frac{1}{2}} \cos\theta. \tag{5.19}$$

This region is shown in fig. 5.5 over. By varying θ from $-\pi/2$ to $+\pi/2$, the whole k plane is covered with the exception of the imaginary axis. In the upper half plane there are no singularities along the imaginary axis for $(\frac{4}{3}B)^{\frac{1}{2}} < \text{Im } k < (\frac{4}{3}\beta^2)^{\frac{1}{2}}$ and this strip of analyticity is always in the region of overlap of X_{RF} and $X_{RF\theta}$. As in previous cases, for k in this strip, the singularities of the integrands of X_{RF}, regarded as functions of Q lie on the imaginary axis. Thus $X_{RF} = X_{RF\theta}$ here, and the $X_{RF\theta}$ define analytic continuations of X_{RF}.

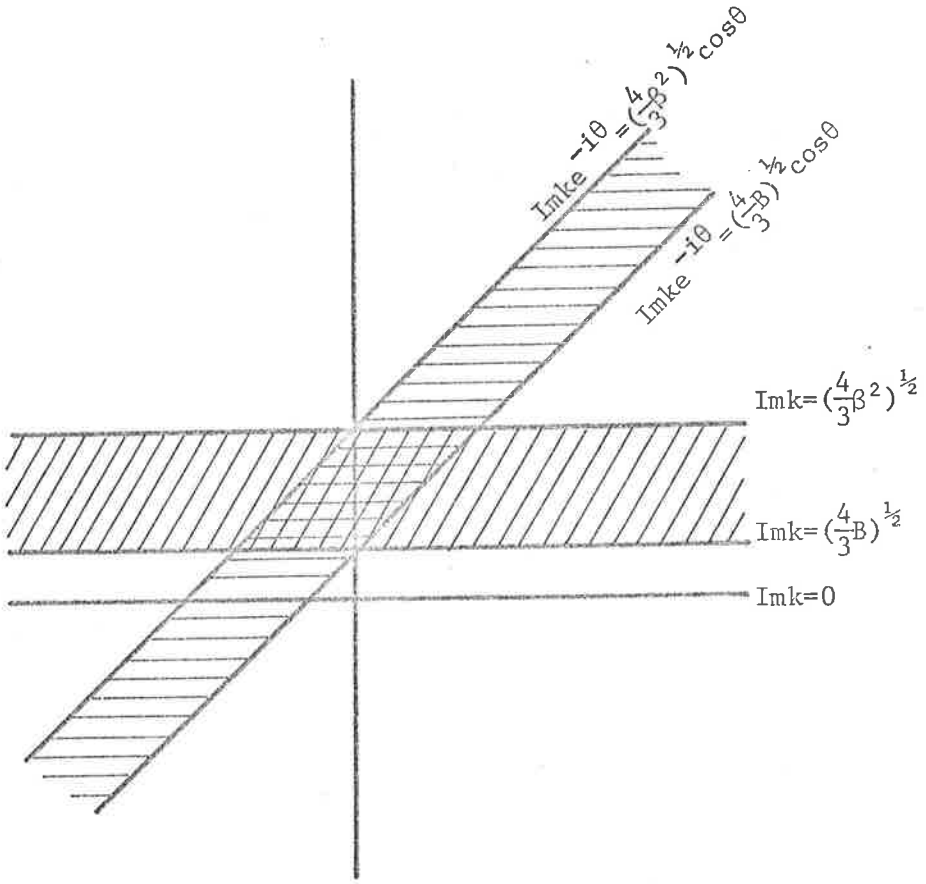

Figure 5.5

Region of analyticity of X_{RF}, $X_{RF\theta}$, T_2, T_{2_θ}.

b) Analyticity of $T_2(W;\underline{k}_F',\underline{k}_F)$

The only new denominators which occur in the integrand of $T_{2_\theta}(W;\underline{k}_F,\underline{k}_F')$ are contained in $K(W;\underline{q}_1 e^{-i\theta}-\frac{1}{2}\underline{k}_F', \underline{q}_2 e^{i\theta}-\frac{1}{2}\underline{k}_F)$. They are

$$\beta^2 + ((\underline{q}_1+\tfrac{1}{2}\underline{q})e^{i\theta}-\tfrac{1}{2}(\underline{k}_F'+\tfrac{1}{2}\underline{k}_F))^2,$$

$$\beta^2 + ([\underline{q}_1+\tfrac{1}{2}\underline{q}_1]e^{i\theta}-\tfrac{1}{2}(\underline{k}_F+\tfrac{1}{2}\underline{k}_F'))^2,$$

and

$$W - (\underline{q}_1 e^{i\theta}-\tfrac{1}{2}\underline{k}_F')^2-(\underline{q}_2 e^{i\theta}-\tfrac{1}{2}\underline{k}_F)^2-(\underline{q}_1 e^{i\theta}-\tfrac{1}{2}\underline{k}_F')\cdot(\underline{q}_2 e^{i\theta}-\tfrac{1}{2}\underline{k}_F). \qquad (5.20)$$

From appendix B one has the result that these denominators do not vanish in the strip of equation (5.19). Thus T_{2_θ} is analytic in the same region as $X_{RF\theta}$ and one may prove straightforwardly that the T_{2_θ} are analytic continuations of T_2, so that T_2 has the same analytic form as X_{RF}.

c) Analyticity of $T_1(W;\underline{k}_F',\underline{k}_F)$ and $Z(W;\underline{k}_F',\underline{k}_F)$

Unlike all the higher order perturbation terms where one can find a region where all the denominators cannot vanish under the transformation $\underline{q}_1 \to \underline{q}_1 - \frac{1}{2}\underline{k}_F$ no such region exists for T_1. The problem here is that the modified Greens function in the denominator $Z(W;\underline{q}_1-\frac{1}{2}\underline{k}_F',\underline{k}_F)$ may still vanish anywhere in the complex plane. To see this we write the equation

$$W - \frac{3}{4}k_F^2 - (\underline{q}_1+\tfrac{1}{2}(\underline{k}_F-\underline{k}_F')^2) = 0 \qquad (5.21)$$

in the terms of real and imaginary parts :

$$(n_R^2-n_D^2)((\mathrm{Re}k - \frac{\underline{q}_1\cdot\underline{n}_D}{(n_R^2-n_D^2)})^2 - \mathrm{Im}k^2)) - \frac{(\underline{q}_1\cdot\underline{n}_D)^2}{n_R^2-n_D^2} - q_1^2 = 0,$$

$$\mathrm{Im}k\ (\mathrm{Re}k(n_R^2-n_D^2) - \underline{q}_1\cdot\underline{n}_D) = 0. \qquad (5.22)$$

Here $\underline{n}_D = \frac{1}{2}(\underline{n}_F-\underline{n}_F')$. When $n_R^2-n_D^2 > 0$ equations (5.22) have no solution if Im $k \neq 0$. But if $n_R^2-n_D^2 < 0$ they always have a solution. Of course the fact that the denominator may vanish does not imply T_1 has a singularity. For a singularity to occur it is necessary that both Green function denominators vanish simultaneously, pinching the contour between them. Using the Landau rules one has the conditions

$$(\alpha_1+\alpha_2)\underline{p}_1 = -\tfrac{1}{2}\alpha_1\underline{k}_F-\tfrac{1}{2}\alpha_2\underline{k}_F', \qquad (5.23)$$

$$(\underline{p}_1+\tfrac{1}{2}\underline{k}_F)^2 = \tfrac{1}{4}k_R^2,$$

and

$$(\underline{p}_1+\tfrac{1}{2}\underline{k}_F')^2 = \tfrac{1}{4}k_R'^2.$$

From the Landau diagram (fig. 5.6) it can be seen the rules are satisfied if

$$|\underline{k}_F - \underline{k}'_F| = k_R + k'_R$$

or equivalently

$$2n_D = n_R + n'_R. \qquad (5.24)$$

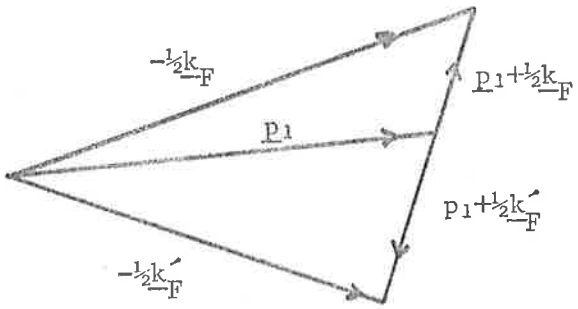

Figure 5.6

Landau diagram for rescattering singularity in T_1

This singularity is the wellknown triangle rescattering singularity due to a rescattering of the three particles on the energy shell (fig. 5.7).

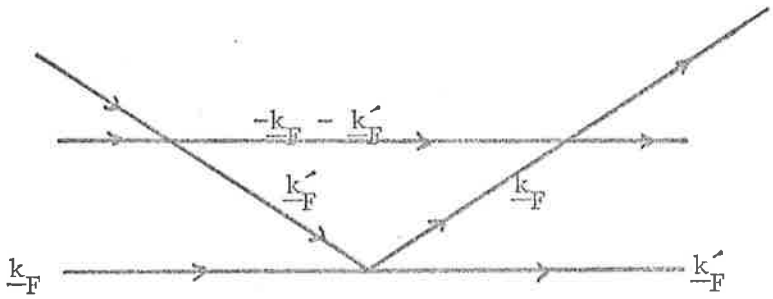

Figure 5.7

If $2n_D < n_R + n'_R$ one can readily show T_1 is analytic in the upper half k plane with the exception of part of the

imaginary axis. When $2n_D > n_R+n_R'$ analyticity of T_1 can be established in the first quadrant. However, RST (17) have shown that if one continues into the second quadrant, complex singularities are encountered. Therefore, T_1 is not in general a Hermitian analytic function. To overcome this difficulty one may *define* the analytic continuation to the second quadrant by

$$T_1(-k^*) = T_1(k^*),$$

and because T_1 is not in general a real function of k on the imaginary axis we introduce a branch cut running along its entire length.

Similarly, in the case of the Born term $Z(W;\underline{k}_F',\underline{k}_F)$ the Greens function denominator

$$k^2 - \frac{3}{4}k_F^2 - (\underline{k}_F'+\tfrac{1}{2}\underline{k}_F) \tag{5.25}$$

gives rise to a pole singularity when

$$n_F^2 + n_F'^2 + (\underline{n}_F+\underline{n}_F')^2 = 2, \tag{5.26}$$

and a pole of order 2 at k = 0. Because the position of the singularity given by equation (5.26) is independent of k, $Z(W;\underline{k}_F',\underline{k}_F)$ is not a real function of k on the imaginary axis. Thus in order to make it Hermitian analytic in the upper half k plane one must again introduce a rescattering cut along the length of the imaginary axis.

In summary, the off-shell amplitude $X(W;\underline{k}_F,\underline{k}_F')$ is Hermitian analytic on the physical energy sheet and all its singularities lie along the real axis. The portion of the amplitude excluding the Born term and first order perturbation term have right hand cuts along the positive axis which do not overlap with the left hand potential cuts. The Born term and first order perturbation term

are defined to be Hermitian analytic by introducing a rescattering cut to run along the entire negative axis in addition to the other cuts.

Having determined the analyticity of $X(W;\underline{k}_F,\underline{k}_F')$ there remains to consider the kinematic singularities of the δ functions in the lowest order terms to complete the discussion of the analytic properties of the free scattering amplitude. Because

$\delta(\underline{k}_F-\underline{k}_F') = k^{-3}\delta(\underline{n}_F-\underline{n}_F')$

the δ function terms are not real analytic. So for these terms, one also must take a cut running the length of the imaginary axis and *define* $f(\underline{k}) = \delta(\underline{k}_F-\underline{k}_F')$ in the left hand plane by $f(-\underline{k}^*) = f(\underline{k})^*$. With this definition the free scattering amplitude is now a Hermitian analytic function on the physical sheet.

5.3 Position of Singularities

To determine the singularities due to pinches between energy denominators in the breakup and free scattering amplitudes, one can use the Landau equations derived for the bound state scattering amplitude provided $\underline{k}_B$ and $\underline{k}_B'$ are replaced by $\underline{k}_F$ and $\underline{k}_F'$ where necessary. In addition to the definitions of Chapter 4 we define $k = iK$ when k is pure imaginary. We shall see that the effect of altering the constraints in the equations is to permit several new types of pinch singularities to appear. We shall consider the new singularities of the breakup and free amplitudes in turn.

a) Breakup amplitude

The conditions for a singularity in $T_1(W;\underline{k}_B,\underline{k}_F)$ are from equations (4.32) to (4.35)

$$\underline{q}_1(2\alpha_1+2\alpha_2+2\alpha_3) + \tfrac{1}{2}\underline{K}_B(2\alpha_1) + \tfrac{1}{2}\underline{K}_F\ (2\alpha_3) = 0 \qquad (5.27)$$

and

$$\alpha_1 = 0 \text{ or } (\underline{q}_1+\tfrac{1}{2}\underline{K}_B)^2 = B$$

$$\alpha_2 = 0 \text{ or } q_1^2 = K_B^2$$

$$\alpha_3 = 0 \text{ or } (\underline{q}_1+\tfrac{1}{2}\underline{K}_F)^2 = \underline{K}_R^2 \qquad (5.28)$$

where

$$\underline{K}_F = -i\underline{k}_F = K\underline{n}_F$$

$$\underline{K}_R = K\underline{n}_R.$$

The four possible Landau diagrams are shown below in fig. 5.8.

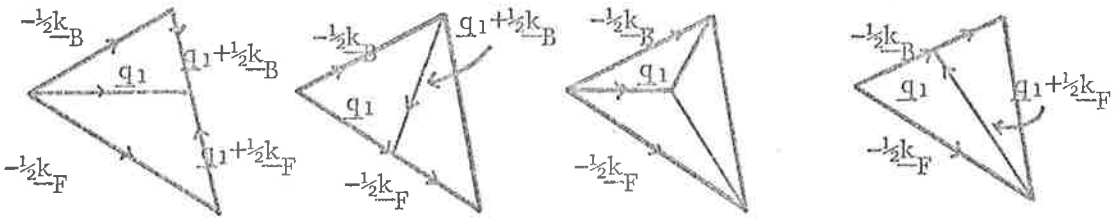

$\alpha_1>0,\alpha_2=0,\alpha_3>0$ (a) $\alpha_1=0,\alpha_2>0,\alpha_3>0$ (b) $\alpha_1>0,\alpha_2>0,\alpha_3>0$ (c) $\alpha_1>0,\alpha_2>0,\alpha_3=0$ (d)

Figure 5.8

Diagram (a) of fig. 5.8 corresponds to the pinch of the two Greens function denominators. From equation (5.28) one finds a pinch occurs when

$$\tfrac{1}{2}|\underline{K}_B-\underline{K}_F| = B^{\frac{1}{2}} + K_R, \qquad (5.29)$$

which yields a quartic equation in K. However, in the case $z=-1\ (z=\hat{k}_B\cdot\hat{k}_F)$ the equation can be easily solved to give

$$K = \frac{2B^{\frac{1}{2}}(2n_R-n_F)+2B^{\frac{1}{2}}(\frac{16}{9} - \frac{1}{3}(2n_R-n_F)^2)^{\frac{1}{2}}}{\frac{4}{3} - (2n_R-n_F)^2}, \qquad (5.30)$$

with the restrictions

$$(\tfrac{1}{3})^{\frac{1}{2}} < n_F < (\tfrac{4}{3})^{\frac{1}{2}},$$

which follows from $K_B > 0$. Now one can deduce from

equation (5.29) that K(-1) is the minimum of K(z) in the range [-1,1]. When $n_F = (\frac{1}{3})^{\frac{1}{2}}$, $K(-1) = \infty$, so the branch point enters the physical sheet at ∞ and as n_F increases to $(\frac{4}{3})^{\frac{1}{2}}$ moves down the imaginary axis to $(\frac{4}{3}B)^{\frac{1}{2}}$.

The second diagram of fig. 5.8 represents the pinch of the free Greens function with the propagator pole, the condition for which is

$$\tfrac{1}{2}K_F = K_B + K_R. \tag{5.31}$$

It has the solution

$$K = \left[\frac{B}{1 - \frac{3}{16}(2n_R - n_F)^2}\right]^{\frac{1}{2}} \tag{5.32}$$

with

$$1 < n_F < (\tfrac{4}{3})^{\frac{1}{2}}.$$

When $n_F < 1$ the branch point is not on the physical sheet. It enters through the two body threshold at $n_F = 1$ rising to $K = (\frac{4}{3}B)^{\frac{1}{2}}$ as n_F increases to $(\frac{4}{3})^{\frac{1}{2}}$.

The simultaneous pinch of three energy denominators represented by the Landau diagram (c) of fig. 5.8 does not yield a singularity because it is incompatible with the constraints of equation (5.28). The first two constraints clearly restrict K^2 to the range $\frac{4}{3}B \leq K^2 \leq 3B$. But since q_1 lies inside $\Delta(-\frac{1}{2}K_B, -\frac{1}{2}K_F)$, $q_1 = K_B < \frac{1}{2}K_F$ which requires $K^2 < \frac{4}{3}B$ and the diagram is not geometrically feasible.

Similarly one can reject the last diagram on account of the subsidiary condition $q_1 = K_B$.

The Landau diagrams of the perturbation terms of order $n \geq 2$ are all of the form given in fig. 5.9. with the subsidiary conditions

$$\alpha_1 = 0 \text{ or } (\underline{q}_1+\tfrac{1}{2}\underline{K}_B)^2 = B$$

$$\alpha_j = 0 \text{ or } q_{j-1}^2+(\underline{q}_{j-1}+\underline{q}_j)^2+q_j^2 = 2K^2,\ j=2,\ldots,n-2 \qquad (5.33)$$

$$\alpha_n = 0 \text{ or } (\underline{q}_{n-1}+\tfrac{1}{2}\underline{K}_F)^2 = K_R^2$$

$$\alpha_{n+j} = 0 \text{ or } q_j^2 = K_B^2,\quad j=1,\ldots,n-1.$$

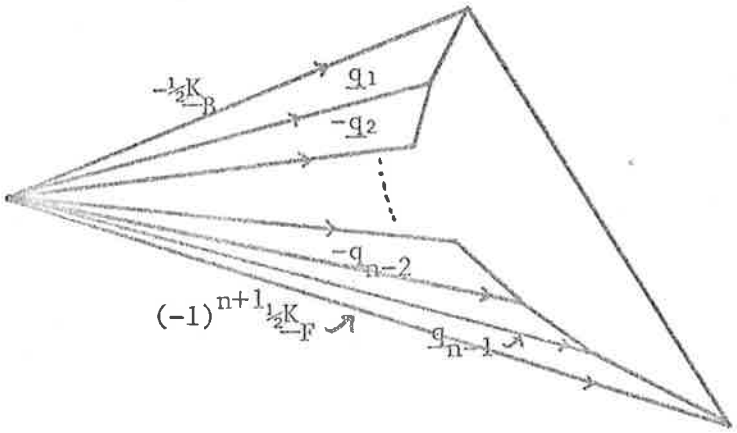

Figure 5.9

Landau diagram of $T_n(W;\underline{k}_B,\underline{k}_F)$ $\alpha_1,\ldots,\alpha_n > 0$.

The argument for eliminating the possibilities is very similar to the one used for the elastic amplitude. In fact all the diagrams with the exception of the one in fig. 5.10 can be eliminated.

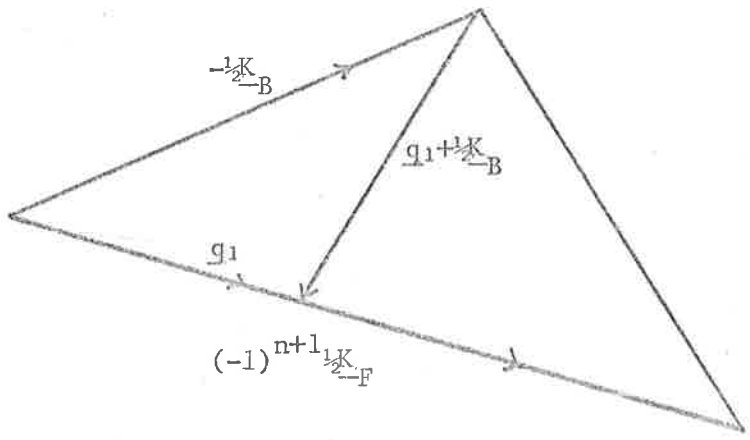

Figure 5.10

This singularity, due to the pinch between the free Greens function and the propagator pole has already been discussed in relation to $T_1(W;\underline{k}_F,\underline{k}_B)$ and its position is given by equation (5.32).

Thus, the breakup amplitude for a system of three identical spinless bosons has at most two types of pinch singularities due to energy denominators. One, the pinch between the free Greens function and propagator pole is present in all the perturbation terms and lies in the region $-\frac{4}{3}B < E < -B$. The other type occurs only in T_1 and corresponds to the pinch between the two Greens function denominators. Its branch point is restricted to energies $E < -\frac{4}{3}B$ and its presence explains why the proof of analyticity for T_1 differed from that of the other terms.

b) Free particle amplitude

The first order term $T_1(W;k_F,k_F')$ has four singularities arising from energy denominator pinches. The Landau diagrams corresponding to the different possibilities may be obtained by the substitution $\underline{K}_B' \to \underline{K}_F$ in fig. 5.8. Diagram (a) corresponds to the rescattering singularity looked at earlier. Its position is independent of the energy, being determined by the magnitude and direction of $\underline{n}_F$ and $\underline{n}_F'$. One sees that diagrams (b) and (d) both give same type of singularity discussed in connection with the breakup amplitude, whose position is given by equation (5.32). We denote this type of singularity by $S_1 = S_1(n_F)$ and remark that if $n_F > n_F' > 1$ then both singularities are on the physical sheet and $S_1(n_F) < S_1(n_F)$. That is $S_1(n_F)$ is further to the left along the negative energy axis.

The diagram (c) of fig. 5.8 representing the simultaneous pinch of all three energy denominators is now also feasible. If, for example n_F, $n_F' > 1$, it is easy to show that this singularity $S_2 = S_2(n_F, n_F', \hat{n}_F \cdot \hat{n}_F')$ must lie on the physical sheet. If $n_F > n_F'$ then the position of this singularity in relation to the type S_1 is $-\frac{4}{3}B < S_2 < S_1(n_F) < S_1(n_F') < -B$. Thus it always lies to the left of the last S_1 type singularity. While it is restricted to this region, for fixed n_F, n_F' one can vary its position by changing the directions of the incoming and outgoing momenta. In fact, it can be shown that as the angle decreases, S_2 moves to the right until some critical value, it coincides with $S_1(n_F)$ and moves off the physical sheet.

It can be demonstrated by arguments similar to those used for the other amplitudes that the higher order terms of the free amplitude perturbation series expansion may each possess the two singularities of type S_1 but no others.

5.4 Concluding Remarks

We have seen that each of the three-body on-shell amplitudes have basically the same analytic structure on the physical sheet in that, with the exception of the Born term of the breakup amplitude all the singularities are on the real axis.

Concerning the pinch singularities from the energy denominators one can see that a pattern is built up as we proceed up the hierachy of three-body amplitudes. The bound-state scattering amplitude has only one energy denominator pinch

singularity, which occurs in T_1 and is due to the pinch of the two energy denominators in the Z's. It lies in the region $E < -4B$ and can be viewed as contributing to the left hand potential cut. The process of determining the singularities of the breakup amplitude merely involve the substitution $\underline{k}_B \rightarrow \underline{k}_F$ which yields less restrictive criteria for the occurrence of singularities. The T_1 term still has a singularity due to the pinch of the two Greens function denominators which is now on the physical sheet only when $(\frac{1}{3})^{\frac{1}{2}} < n_F < (\frac{4}{3})^{\frac{1}{2}}$ and is restricted to $E < -\frac{4}{3}B$. Again it contributes to the potential cut.

Apart from this singularity there is the type $S_1(n_F)$ due to the pinch of the free Greens function denominator with the propagator pole, which occurs in every perturbation term. It is on the physical sheet only when $1 < n_F < (\frac{4}{3})^{\frac{1}{2}}$ and is restricted to $-\frac{4}{3}B < E < -B$. One usually takes the branch cut of this singularity to run in the direction of the unitarity cuts so that there is no overlap of the right hand and left hand cuts. Thus the effect of this singularity is to extend the right hand cut below the two body threshold to an "anomalous" threshold at the point S_1.

When one studies the singularities of the free particle amplitude with $\underline{k}_B, \underline{k}_B'$ replaced by $\underline{k}_F, \underline{k}_F'$ in the Landau conditions one finds that T_1 now may have a further singularity of type S_2 in addition to the two singularities $S_1(n_F)$, $S_1(n_F')$. The pinch singularity of the other diagram which for the other amplitudes gives contribution to the left hand cut now manifests itself as the triangle rescattering singularity whose position is independent of the energy.

To conclude this chapter, we note that the amplitudes of RST should reduce to those in the separable potential model if the Yukawa interaction is replaced by a separable potential. To check this we take a typical first order term for arrangement scattering. In their notation

$$\langle B_3\hat{n}'|V_1|B_1\hat{n}\rangle = \psi_{B_3}(\underline{k}_B+\tfrac{1}{2}\underline{k}_B')\int d\underline{q}\; V_1(\tfrac{1}{2}(-\underline{k}_B-2\underline{k}_B'),\tfrac{1}{2}(2\underline{q}+\tfrac{1}{2}\underline{k}_B)) \times$$

$$\times\, \psi_1(\tfrac{1}{2}(2\underline{q}+\underline{k}_B)).$$

Now when $V_i = -\lambda_i|g_i\rangle\langle g_i|$ so there is a bound state with energy B_i we have

$$\psi_{B_i}(\underline{x}) = (2x^2+B_i)^{-1}g_i(\underline{x}),\quad \lambda_i^{-1} = \langle g_i|G_0(-B_i)|g_i\rangle,$$

and the matrix element reduces to $Z_{31}(W;\underline{k}_B,\underline{k}_B')$. It is easy to verify the higher order terms reduce in an analogous way.

Chapter 6

A STUDY OF THE ON-SHELL N/D METHOD OF SOLUTION FOR S-WAVE ELASTIC n-d SCATTERING IN THE CONTEXT OF THE AMADO MODEL

In recent years it has been suggested that the description of low energy elastic neutron-deuteron scattering by the N/D method may be a viable alternative to the solution of the off-shell Faddeev equations. Indications from calculations reported to date are that the method is only moderately successful. It is however, difficult to assess the reliability of the calculations not only because of the crude nature of the models but also because there is some uncertainty in the experimental results. To elaborate on this point we give some examples.

Barton and Phillips (8) solved the N/D equations for the s-wave quartet and doublet amplitudes using for their driving term the one-nucleon exchange contribution. The breakup channel was neglected. Although the quartet scattering was adequately described below breakup their doublet channel input could not produce the experimentally observed triton bound state. To minimise the effect of short range forces, which they argued were responsible for the bad result in the doublet, they repeated their calculation after introducing a subtraction in the N equation at the two-body threshold. Using the experimental scattering length to fix N at the subtraction point they obtained the rapid variation of $k\cot\delta$ observed experimentally (20) and a triton binding energy of 6 MeV.

A more sophisticated calculation was attempted by Avishai, Ebenhöh and Rinat-Reiner (9), who based their driving terms on the one- and two-nucleon exchange terms of the Amado Model. They treated the effect of the breakup channel in the quartet by calculating an approximate form of the inelasticity, while for the doublet they solved the Frye-Warnock (40) version of N/D equations which required a knowledge of the doublet absorption coefficients. Here again, their results described the quartet amplitude well but were unable to reproduce the doublet channel features. Their best input produced a weakly bound triton at -4.52 MeV and failed to give the required low energy behaviour of the phase shift. Some doubt has been cast on their results for the doublet channel by Sloan (41) who has pointed out the experimental coefficients used in their calculations are almost certainly incorrect.

More recently Bower (10) attempted a pure S-matrix description of low energy n-d scattering in which driving terms were derived from Feynman graphs. He included the following processes : proton exchange, a three nucleon pinch, a two nucleon-pion pinch (included through a pole approximation) and two-pion exchange whose effect was approximated by treating the two pions as a σ-meson resonance. The breakup channel inelasticity was incorporated by a simple step function parameterisation. Although Bower obtains a triton binding energy and doublet scattering length consistent with experiment the results are quite sensitive to the strength of the σ-meson interaction and to the inelasticity. The sensitivity of this calculation to the strength of the most distant singularity is particularly interesting in light of the observation by

Avishai et al that they could improve their doublet results by simply adding a pole contribution from a distant singularity along the left hand cut. We shall comment further on our interpretation of this point in the discussion at the end of the chapter.

Clearly then, there is need to investigate the effect of approximations in the N/D method in a specific model of n-d scattering where the exact amplitudes can be found by the solution of the off-shell equations. Of course, the model we shall utilise in this chapter is the Amado model whose analyticity properties have already been derived in Chapter 4. In section 1 a rigorous dispersion relation for the elastic amplitudes is derived, from which the N/D representation of the amplitudes is constructed. The inelasticity arising from the three-body breakup is included in the N/D equations by means of a modified unitarity relation. In the doublet channel the inelasticity due to breakup and nucleon exchange between the triplet and singlet channels is combined so that one has a single uncoupled dispersion relation to describe the doublet amplitude. In principle, we could use three-particle unitarity but then a system of coupled dispersion relations involving elastic, breakup, and free particle amplitudes must be solved. We should mention that Greben (39) has attempted to describe the doublet scattering by means of a coupled set of dispersion relations in which the singlet virtual state is treated as a weakly bound state. In this model inelasticities describing the effects of the rearrangement couplings may be deduced. However, because we have at our disposal the exact solution of the Amado equations, the exact model inelasticities can be calculated directly from the amplitudes.

Restrictions on the asymptotic inelasticity are derived in the second section which ensure there is no difficulty associated with the solution of the s-wave dispersion relations. In section 3 the driving terms used in the calculations are discussed and conditions for their convergence with increasing order to the exact driving term are suggested. After a few notes on the numerical aspects of the work we proceed to a detailed presentation of results in section 5. Finally, implications of the calculations are discussed and conclusions offered.

6.1 Dispersion Relations for Elastic n-d Scattering and their N/D Representation

It was shown in Chapter 4 that the on-shell n-d amplitudes in the quartet and doublet channels are analytic on the first sheet of the energy plane except for the singularities along the real axis which consist of the right hand unitarity cuts and the left hand potential cuts. In order to construct dispersion relations for the amplitudes (in their partial waves) their asymptotic behaviour at high energies is required. For the n-d amplitudes the perturbation series expansion converges for high energies* and is dominated by the Born term which apart from the spin coefficients Λ^{IS} is the same in the quartet and doublet. The partial wave form of the Born term in the Amado model is

$$Z^{\frac{1}{2}S}_{\ell\,11}(E;k_B,k_B) = \Lambda^{\frac{1}{2}S}_{11}\{ \frac{(-)^\ell}{k_B^2} (\beta_1^2-B)^{-2} Q_\ell(\frac{5}{4} + \frac{\beta_1^2}{k_B^2}) +$$

$$- \frac{(-)^\ell}{k_B^2} (\beta_1^2-B)^{-2} Q_\ell(\frac{5}{4} + \frac{B}{k_B^2}) - \frac{(-)^\ell}{k_B^4} (\beta_1^2-B)^{-1} \frac{dQ_\ell(x)}{dx}]_{x=\frac{5}{4}+}$$

$$+ \frac{\beta_1^2}{k_B^2} \}, \qquad (6.1)$$

---

*see Chapter 7.

from which it can be seen the amplitudes have the asymptotic behaviour

$$X^{\frac{1}{2}S}_{\ell\,11}(E;k_B,k_B) \sim O(E^{-1}) \text{ as } |E| \to \infty. \quad * \tag{6.2}$$

This means that no subtractions are necessary and one can write an unsubtracted dispersion relation for the partial wave n-d amplitudes :

$$X^{\frac{1}{2}S}_{\ell\,11}(z) = \frac{1}{\pi}\int_{s_L} ds\, \frac{\text{Im } X^{\frac{1}{2}S}_{\ell\,11}(s+i0)}{s-z} + \frac{1}{\pi}\int_0^\infty ds\, \frac{\text{Im } X^{\frac{1}{2}S}_{\ell\,11}(s+i0)}{s-z}. \tag{6.3}$$

Here z is related to the complex energy W by

$$z = \frac{4}{3}(W+B). \tag{6.4}$$

For real energies we use the symbol s :

$$s = \frac{4}{3}(E+B).$$

In the usual application of dispersion relations, the driving term,

$$B^{\frac{1}{2}S}_{\ell\,11}(z) = \frac{1}{\pi}\int_{s_L} ds\, \frac{\text{Im } X^{\frac{1}{2}S}_{\ell\,11}(s+i0)}{s-z}, \tag{6.5}$$

is known exactly or can be approximated in some ways. Across the right hand cut the discontinuity below the three-body threshold is given by the elastic unitarity relation

$$\text{Im } X^{\frac{1}{2}S}_{\ell\,11}(s+i0) = -s^{\frac{1}{2}}\left|X^{\frac{1}{2}S}_{\ell\,11}(s+i0)\right|^2, \quad 0 < s < s_{Bu}. \tag{6.6}$$

There is of course no contribution to the doublet unitarity relation from the singlet channel which does not possess a bound state pole on the physical sheet and consequently no rearrangement scattering is possible below three-body breakup.

---

*c.f. the Born term of the Yukawa interaction $V_\ell(k) = \frac{1}{4k^2} Q_\ell(1+\frac{\mu^2}{2k^2})$ has the asymptotic behaviour $V_\ell(k) = O(\frac{\ln E}{E})$ as $E \to \infty$.

For energies above this threshold, elastic unitarity no longer holds; there is coupling with the breakup channel and in the doublet also with the singlet channel. In this case the evaluation of the discontinuity unfortunately involves the half-off shell amplitudes. Avishai, Ebenhöh and Rinat-Reiner (9) have attempted to formulate an approximate method to evaluate the discontinuity. More recently improvements and extensions to this approach have been reported by Greben (39). In our calculation we shall avoid this method of determining the discontinuity in the doublet channel since it introduces the $X^{\frac{1}{2}\,3/2}_{1\,2\;\ell}$ amplitude and thus leads to a coupled set of doublet dispersion relations. Instead we keep to a single channel dispersion relation in the doublet by the introduction of an inelasticity $R^S_\ell(s)$ to take account of the inelastic processes. The modified unitarity relation then reads

$$\text{Im}\, X^{\frac{1}{2}S}_{1\,1\;\ell} = -s^{\frac{1}{2}} R^S_\ell(s) \left| X^{\frac{1}{2}S}_{1\,1\;\ell}(s+i0) \right|^2, \quad s > s_{Bu}. \tag{6.6'}$$

In the work reported in this chapter, the inelasticity is computed directly from the exact amplitude found by solution of the off-shell Amado model equations, or where it is desirable to test the effect of approximations, systematically parameterised in some manner.

With equations (6.5), (6.6') the dispersion relation for the n-d amplitude becomes a nonlinear integral equation*:

$$X_\ell(z) = B_\ell(z) - \frac{1}{\pi} \int_0^\infty \frac{s^{\frac{1}{2}} R_\ell(s) \left| X_\ell(s+i0) \right|^2 ds}{s-z} \tag{6.7}$$

One can solve this type of equation by the N/D method (42) in which the amplitude is expressed in the form

$$X_\ell(z) = \frac{N_\ell(z)}{D_\ell(z)}\, z^\ell. \tag{6.8}$$

---

*From now on we refrain from using superscripts on the amplitudes where they do not alter the argument.

The numerator $N_\ell(z)$ is defined to be an analytic function everywhere except along the negative axis where it has all the left hand singularities of $X_\ell(z)$ (excluding bound state poles), while $D_\ell(z)$ contains the right hand singularities. Any bound states appear as zeros in the D function. The asymptotic behaviour of $X_\ell(z)$as given in equation (6.2) may be satisfied by imposing the following conditions on D and N :

$$D_\ell(z) \sim O(1),$$
$$N_\ell(z) \sim O(z^{-\ell-1}) \text{ as } |z| \to \infty. \tag{6.9}$$

The z^ℓ factor in equation (6.8) has been introduced to ensure the required low energy behaviour for the amplitude. The usefulness of this representation lies in the fact that the nonlinear equation for the amplitude reduces to a linear integral equation for N_ℓ or D_ℓ.

To construct an equation for N_ℓ we note that from their definitions

$$\text{Im } N_\ell(s+i0) = D_\ell(s)s^{-\ell} \text{ Im } B_\ell(s+i0), \quad s < s_L \tag{6.10}$$

and

$$\text{Im } D_\ell(s+i0) = -s^{\ell+\frac{1}{2}}R_\ell(s)N_\ell(s), \quad s > 0. \tag{6.11}$$

Now using the asymptotic behaviour of $D_\ell(z)$ and the fact that $D_\ell(z)$ is analytic everywhere except along the right hand cut one can derive a subtracted dispersion relation for $D_\ell(z)$:

$$D_\ell(z) = 1 - \frac{z-s_0}{\pi}\int_0^\infty \frac{ds\ s^{\ell+\frac{1}{2}}R_\ell(s)N_\ell(s)}{(s-z)(s-s_0)} \ . \tag{6.12}$$

Here the subtraction has been taken at $z = s_0$ and $D_\ell(s_0)$ set equal to 1. Similarly an equation for $N_\ell(z)$ may be derived from the dispersion relation

$$N_\ell(z) - B_\ell(z)z^{-\ell}D_\ell(z) = -\frac{1}{\pi}\int_0^\infty ds\ \frac{B_\ell(s)s^{-\ell}\,\mathrm{Im}\,D_\ell(s+i0)}{(s-z)}$$

which follows from equation (6.10). When equation (6.12) for $D_\ell(z)$ is substituted in, we have

$$N_\ell(z) = B_\ell(z)z^{-\ell} + \frac{1}{\pi}\int_0^\infty ds\ s^{\ell+\frac{1}{2}}R_\ell(s)\left\{\frac{B_\ell(s)s^{-\ell}(s-s_0)-B_\ell(z)z^{-\ell}(z-s_0)}{(s-z)(s-s_0)}\right\}N_\ell(s) \tag{6.13}$$

which is a non-singular linear integral equation for N_ℓ. It appears that D_ℓ and N_ℓ have an implicit dependence on the subtraction point s_0. However, it is well known that N_ℓ/D_ℓ is independent of s_0. A proof of this may be found in the appendix of ref. (43).

6.2 Restrictions on the Asymptotic Inelasticity

For the purpose of solving the integral equation for $N_\ell(s)$ numerically, one usually has to make assumptions about the asymptotic inelasticity. In this section we apply the Fredholm theory of L^2 kernels to determine sufficient conditions for an easy numerical solution of equation (6.13).

We consider the symmetrised form of the integral equation for $N_\ell(s)$ because the symmetrised form of the kernel has the least L^2 norm:

$$\bar{N}_\ell(z) = B_\ell(z)z^{-\ell}(z^{\ell+\frac{1}{2}}R_\ell(z))^{\frac{1}{2}}(z-s_0)^{-\frac{1}{2}}$$
$$+\int_0^\infty ds(s^{\ell+\frac{1}{2}}R_\ell(s))^{\frac{1}{2}}(z^{\ell+\frac{1}{2}}R_\ell(z))^{\frac{1}{2}}\left\{\frac{B_\ell(s)s^{-\ell}(s-s_0)-B_\ell(z)z^{-\ell}(z-s_0)}{(s-z)(s-s_0)^{\frac{1}{2}}(z-s_0)^{\frac{1}{2}}}\right\}\bar{N}_\ell(s), \tag{6.14}$$

where

$$\bar{N}_\ell(z) = N_\ell(z)(z-s_0)^{\frac{1}{2}}(z^{\ell+\frac{1}{2}}R_\ell(z))^{-\frac{1}{2}}.$$

The conditions that $\bar{N}_\ell(z)$ be an L^2 solution require the inhomogeneous term to be an L^2 function, that is

$$\int_0^\infty ds(s-s_0)^{-1}\, B_\ell^2(s)s^{-\ell+\frac{1}{2}}R_\ell(s) < \infty,$$

and the norm of the kernel exist :

$$\int_0^\infty\int_0^\infty ds\, ds' \frac{s^{\ell+\frac{1}{2}}R_\ell(s)s'^{-\ell+\frac{1}{2}}R_\ell(s')}{(s-s_0)(s'-s_0)} \left\{\frac{B_\ell(s)s^{-\ell}(s-s_0)-B_\ell(s')s'^{-\ell}(s'-s_0)}{s'-s}\right\}^2 < \infty. \tag{6.16}$$

Because $B_\ell(s) = 0(s^{-1})$, as $s \to \infty$, the condition of equation (6.15) holds only if

$$\int^\infty ds\, s^{-\ell-5/2}R_\ell(s) < \infty. \tag{6.17}$$

A necessary condition that the norm (6.16) be finite is that each integral exist separately. This gives the restriction

$$\int^\infty ds\, s^{\ell-5/2}R_\ell(s) < \infty. \tag{6.18}$$

To examine the double integral of (6.16) more closely we use the polar coordinates (Γ,θ), where

$$\theta = \operatorname{atan}\frac{s'}{s},\quad 0 \le \theta < 2\pi,$$

$$\Gamma = (s^2+s'^2)^{\frac{1}{2}}.$$

Then because the θ integration is over a finite domain, the norm will exist provided

$$\int^\infty d\Gamma \frac{R_\ell(\Gamma\cos\theta)R_\ell(\Gamma\sin\theta)}{(\Gamma\cos\theta-s_0)(\Gamma\sin\theta-s_0)\Gamma} \times$$
$$\times \left\{\frac{B_\ell(\Gamma\cos\theta)(\Gamma\cos\theta-s_0)(\cos\theta)^{-\ell}-B_\ell(\Gamma\sin\theta)(\Gamma\sin\theta-s_0)(\sin\theta)^{-\ell}}{(\cos\theta-\sin\theta)}\right\}^2 < \infty. \tag{6.19}$$

When $\tan\theta \neq 1$ this reduces to the requirement

$$\int^\infty d\Gamma\, R_\ell(\Gamma\cos\theta)R_\ell(\Gamma\sin\theta)\Gamma^{-3} < \infty. \tag{6.20}$$

For the case $\tan\theta=1$ on application of l'Hôpital's rule one obtains

$$\int^\infty d\Gamma\, R_\ell^2(\Gamma)\Gamma^{-3} < \infty. \tag{6.21}$$

As a result of the constraints of equations (6.17), (6.18), (6.20) and (6.21) it follows that N_ℓ will have an L^2 Fredholm solution subject to the following restrictions on the asymptotic behaviour of R_ℓ:

$$\int^{\infty} ds\ R_\ell^2(s) s^{-3} < \infty, \tag{6.22}$$

and

$$\int^{\infty} ds\ R_\ell(s) s^{\ell-5/2} < \infty.$$

The second bound severely limits the high energy behaviour of R_ℓ for $\ell > 0$ and must be viewed as a consequence of the fact that we have only investigated the existence of solutions using the L^2 theory. Perhaps weaker bounds may be obtained by using a less restrictive class of norms in some Banach space. However, we are concerned only with the solution of the N/D equations in the s-wave, where provided*

$$R_0(s) = o(s),\ s \to \infty \tag{6.23}$$

the equations are Fredholm and therefore readily soluble numerically. In particular, this means it is not necessary to introduce high energy cut-offs or similar artifices to solve the s-wave equations.

6.3 Driving Terms

To solve the quartet and doublet dispersion relation a method for making systematic approximations to the exact driving term (equation (6.5)) is needed. In two body potential scattering a convenient approximation is one based on the multiple scattering series obtained by iteration of the Lippmann-Schwinger equation. Employing this approach to the n-d equations we define a sequence of approximate inputs B_n by

$$B_n(z) = \frac{1}{\pi} \int_{s_L} ds\ \Sigma_{i=0}^{n-1} \frac{\text{Im } T_i(s+i0)}{s-z} \tag{6.24}$$

where for the quartet channel

$$T_n = (Z_{11}^{\frac{1}{2}\,3/2}\ \tau_1)^n\ Z_{11}^{\frac{1}{2}\,3/2} \tag{6.25}$$

---

*By $R_\ell(s) = o(s),\ s \to \infty$ we mean $R_\ell(s)/s \to 0$ as $s \to \infty$.

while in the doublet

$$T_0 = Z^{\frac{1}{2}\frac{1}{2}}_{11}$$

$$T_n = \left(Z^{\frac{1}{2}\frac{1}{2}}_{11}\tau_1 \;\; Z^{\frac{1}{2}\frac{1}{2}}_{12}\tau_2\right) \begin{bmatrix} Z^{\frac{1}{2}\frac{1}{2}}_{11}\tau_1 & Z^{\frac{1}{2}\frac{1}{2}}_{12}\tau_2 \\ Z^{\frac{1}{2}\frac{1}{2}}_{21}\tau_1 & Z^{\frac{1}{2}\frac{1}{2}}_{22}\tau_2 \end{bmatrix}^{n-1} \begin{bmatrix} Z^{\frac{1}{2}\frac{1}{2}}_{21} \\ Z^{\frac{1}{2}\frac{1}{2}}_{11} \end{bmatrix}. \qquad (6.26)$$

With this definition the n^{th} order inputs include contributions from the first to the n^{th} order nucleon exchanges. In the quartet there are only proton exchanges from the triplet channel whereas intermediate nucleon exchanges in the doublet can occur in both the triplet and singlet channels.

Implicit in this definition of the order of input, is the assumption that inclusion of higher order contributions gives a successively better approximation to the exact input. Such intuitive reasoning is justified to some extent by the observation that the leading singularity of each term in the multiparticle scattering series of the two-body Lippmann-Schwinger equation for Yukawa or exponential interactions lies further to the left away from the physical region with increasing order of input. Hence, if the discontinuity across the left hand cut is known for the first few orders of terms, the integral of these discontinuities should give increasingly better approximations to the exact input. Of course, the rate of convergence depends on several factors; the strength of the two body interactions, the range of the forces and the coupling between channels. Investigations of the N/D method by Bjorken and Goldberg (44) and Luming (45) indicate that when the strength of the interaction is small, inputs derived from the Born term and first order term yield good results which become progressively worse as the strength is increased. We shall give results for the Amado model which indicate that using this method of approximation results in a sequence which appears to converge as the order of input is increased.

To calculate the inputs B_n, rather than using the form (6.24) which requires explicit knowledge of the position of the singularities and their discontinuities we used the alternative form

$$B_n(s) = \Sigma_{i=0}^{n-1}\{\mathrm{Re}T_i(s+i0) - P\int_0^\infty ds' \frac{\mathrm{Im}\, T_i(s'+i0)}{s'-s}\}\ , \qquad (6.27)$$

because the discontinuities of the Born series terms across the right hand cuts are readily available from the solution of the off-shell Amado model equations.

6.4 Some Notes on Numerical Methods

Basically there were three types of calculations carried out in the course of this work, the solution of the off-shell integral equations, the computation of the driving terms and the solution of the N/D equations. This required numerical evaluation of integrals over the interval $[0,\infty)$ which were treated by mapping into the finite interval $[-1,1]$ with a conformal transformation and using a quadrature rule described in appendix D. We give an outline of the salient features of the various calculations:

a) Solution of the off-shell equations

The solution of the n-d scattering equations was obtained by means of the rotation of contours method described in section 4 of Chapter 3. In the numerical work the following values of the parameters were chosen:

$\beta_1 = 1.40979 \times 10^{13}\ \mathrm{cm}^{-1}$,

$\beta_2 = 1.1771 \times 10^{13}\ \mathrm{cm}^{-1}$,

$\lambda_1 = 15.9677 \times 10^{13}\ \mathrm{cm}^{3}$,

$\lambda_2 = 6.4001 \times 10^{13}\ \mathrm{cm}^{3}$,

$\frac{m}{\hbar^2} = 2.40926 \times 10^{24}\ \mathrm{MeV}^{-1}\ \mathrm{cm}^{-2}$.

The partial wave amplitudes were calculated as follows:

1) Quartet

$$X^{\frac{1}{2}\,3/2}_{\ell\ 1\,1}(E+i0;k_B,k_B) = Z^{\frac{1}{2}\,3/2}_{\ell\ 1\,1}(E;k_B,k_B)$$

$$+ \int_0^\infty dp p^2 e^{3i\theta} Z^{\frac{1}{2}\,3/2}_{\ell\ 1\,1}(E;k_B,pe^{i\theta})\tau_1(E-\tfrac{3}{4}p^2e^{2i\theta})Z^{\frac{1}{2}\,3/2}_{\ell\ 1\,1}(E;pe^{i\theta},k_B)$$

$$+ \int_0^\infty\int_0^\infty dp\ dp' p^2 p'^2 e^{3i\theta} Z^{\frac{1}{2}\,3/2}_{\ell\ 1\,1}(E;k_B,pe^{i\theta})\tau_1(E-\tfrac{3}{4}p^2e^{2i\theta}) \times$$

$$\times R^{\frac{1}{2}\,3/2}_{\theta\ \ell\ 1\,1}(E;p,p')Z^{\frac{1}{2}\,3/2}_{\ell\ 1\,1}(E;p'e^{i\theta},k_B) \qquad (6.28)$$

2) Doublet

$$X^{\frac{1}{2}\frac{1}{2}\,\frac{1}{2}}_{\ell\ 1\,1}(E+i0;k_B,k_B) = Z^{\frac{1}{2}\frac{1}{2}\,\frac{1}{2}}_{\ell\ 1\,1}(E;k_B,k_B) +$$

$$+ \Sigma_{j=1}^2 \int_0^\infty dp p^2 e^{3i\theta} Z^{\frac{1}{2}\frac{1}{2}\,\frac{1}{2}}_{\ell\ j\,1}(E;k_B,pe^{i\theta})\tau_j(E-\tfrac{3}{4}p^2e^{2i\theta}) \times$$

$$\times Z^{\frac{1}{2}\frac{1}{2}\,\frac{1}{2}}_{\ell\ 1\,j}(E;pe^{i\theta},k_B) + \Sigma_{i,j=1}^2 \int_0^\infty\int_0^\infty dp dp' p^2 p'^2 e^{3i\theta} Z^{\frac{1}{2}\frac{1}{2}\,\frac{1}{2}}_{\ell\ j\,1}(E;k_B,pe^{i\theta}) \times$$

$$\times \tau_j(E-\tfrac{3}{4}p^2e^{2i\theta})R^{\frac{1}{2}\frac{1}{2}\,\frac{1}{2}}_{\theta\ \ell\ ij}(E;p,p')Z^{\frac{1}{2}\frac{1}{2}\,\frac{1}{2}}_{\ell\ i\,1}(E;p'e^{i\theta},k_B). \qquad (6.29)$$

The $R_{ij\theta}$ are obtained from equation (4.31) by replacing K_D by $K_{D\theta}$, the doublet kernel on the rotated contour. The integrals were calculated numerically using the quadrature rule given in the appendix. The restriction on the maximum angle of rotation, $\theta < \text{atan}\,(\frac{3B}{E+B})^{\frac{1}{2}}$ made it necessary to use an increasing number of quadrature points to obtain convergence and the method becomes impractical for energies greater than 80 MeV (COM) where $\theta_m = .277^c$. The most suitable choice for θ was found to be midway in the allowable range, although rotating the integration contours only a small way from the singularities could be compensated for by increasing the number of quadrature points. In the calculations reported here, for energies up to about 50 MeV little difference between

48 and 32 point quadrature rules was detected. For higher energies up to 70 MeV, 48 point quadratures were used. The main difficulty in extending the order of the quadrature proved to be the rapidly increasing computer time required to construct the kernels on the rotated contours, even after all possible symmetries had been taken into account.

b) Calculation of Inputs

To find the various orders of input via equation (6.27) it was necessary to compute the perturbation series terms for physical energies. The integrals for the $T_n(s+i0)$ were evaluated using the rotation of contours for approximately fifty different energies up to 80 MeV. All other values were deduced by interpolation. As an example of the typical behaviour of T_n we have shown T_3 for the s-wave of the quartet equation in fig. 6.1. The real and the imaginary parts vary most rapidly below the breakup threshold becoming quite smooth at higher energies. Care was taken when computing the principle value integral in equation (6.27) to ensure the numerical integration routine took account of this low energy behaviour.

Another problem arose from the divergence of the perturbation series of the s-wave equations in both the quartet and doublet channels for low energies. In table (6.1) we have calculated the first ten partial sums of the T_n for the quartet at three different energies. One sees that the series diverges strongly at -2 MeV, oscillating in sign and increasing in absolute magnitude. At 10 MeV although convergence is not yet apparent* the sequence of partial sums

---

*It is shown in Chapter 7 (fig. 7.3) that the perturbation expansion does converge at 10 MeV.

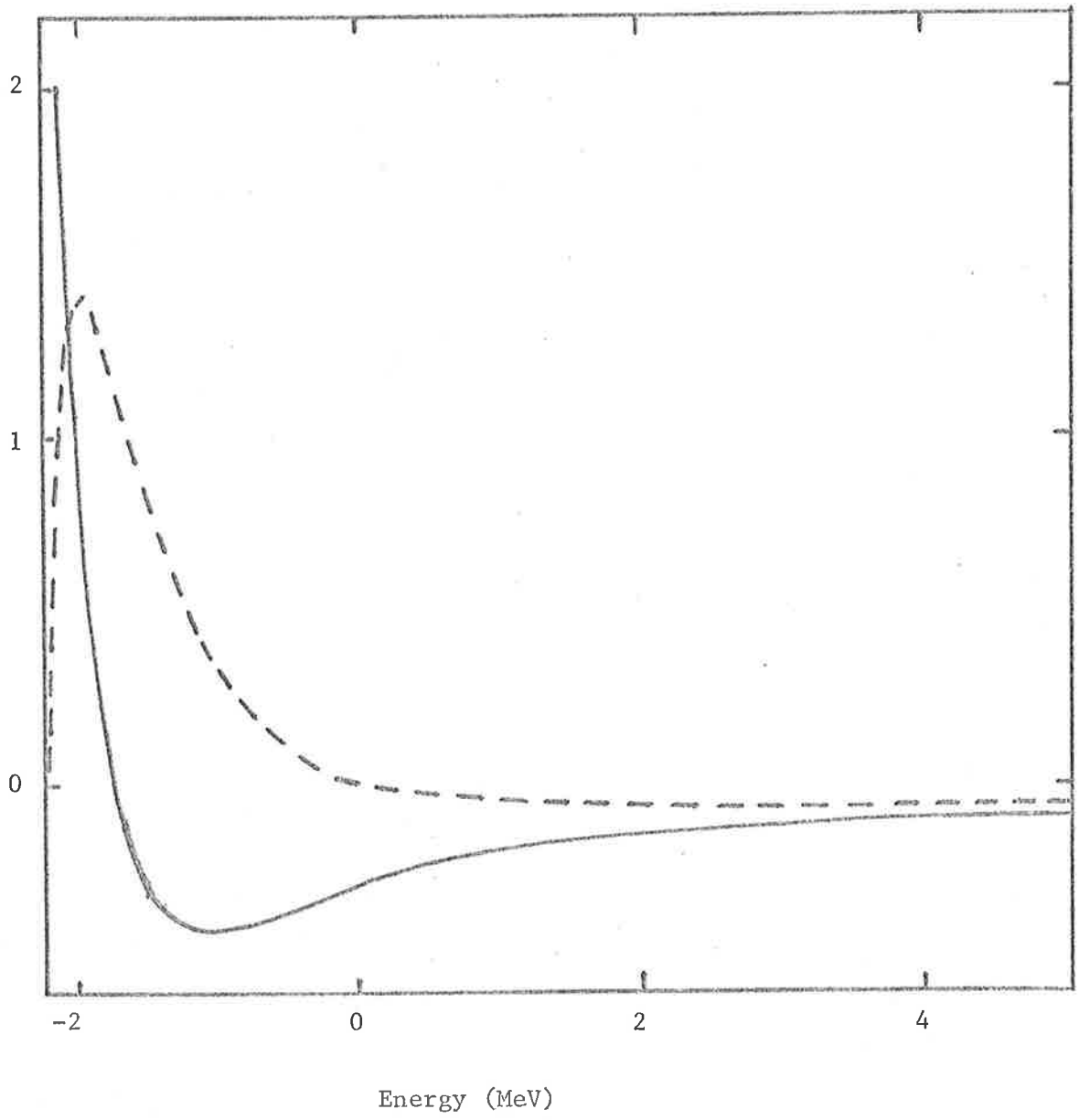

Figure 6.1

T_3 for s-wave of quartet channel

—— Re T_3

--- Im T_3

is not increasing noticably in magnitude while at 70 MeV convergence is clearly evident. Thus as the order increases, the peak in Im T_n below the breakup becomes more and more pronounced in comparison with the higher energies.

E(MeV)	-2		10		70	
	$Re\Sigma T_n$	$Im\Sigma T_n$	$Re\Sigma T_n$	$Im\Sigma T_n$	$Re\Sigma T_n$	$Im\Sigma T_n$
n						
1	+4.023 E-06	0	+4.245 E-07	0	+3.468 E-08	0
2	-3.318 E-06	-5.265 E-06	+1.989 E-07	-7.608 E-07	-1.138 E-08	-4.994 E-08
3	+6.352 E-06	+1.393 E-05	-5.609 E-07	-4.709 E-07	-5.624 E-08	-3.782 E-08
4	+5.627 E-06	-3.784 E-05	-9.877 E-08	+2.941 E-08	-5.203 E-08	-1.705 E-08
5	-4.664 E-05	+7.573 E-05	+1.116 E-07	-5.216 E-07	-4.310 E-08	-1.876 E-08
6	+1.851 E-04	-1.179 E-04	-4.018 E-07	-4.669 E-07	-4.396 E-08	-2.313 E-08
7	-5.212 E-04	+6.478 E-05	-1.538 E-07	-8.760 E-08	-4.597 E-08	-2.269 E-08
8	+1.209 E-03	+3.970 E-04	+4.333 E-08	-4.332 E-07	-4.578 E-08	-2.177 E-08
9	-2.224 E-03	-2.119 E-03	-3.058 E-07	-4.489 E-07	-4.532 E-08	-2.188 E-08
10	+2.666 E-03	+6.926 E-03	-1.782 E-07	-1.697 E-07	-4.538 E-08	-2.207 E-08

Table 6.1

Sum of the first n terms in the s-wave perturbation series of the quartet channel, for three COM energies (arbitrary units).

Consequently, accurate evaluation of the principal value integral becomes increasingly difficult. At the same time, the contribution from the integral in equation (6.27) tends to cancel with ReT_n to give values for B_n which are several orders smaller than ReT_n or $Im\ T_n$, and hence introduces an additional source of error. For this reason the calculation of inputs was limited to the first four orders.

c) Solution of the N/D equations

The integral equation for N is nonsingular and is easily solved by reduction to a matrix equation using numerical quadratures. To save computing time the input and the inelasticity were determined exactly for a set of given points up to 70 MeV and the other values found by interpolation.

Above this energy the inputs B_n were matched to functions of the form $\frac{a_n}{b_n+E}$, the coefficients being determined by the requirement of continuity of B_n and its derivative at 70 MeV. Similarly the asymptotic inelasticity was parameterised by a monotonically increasing function. It was found that the solution of the N/D equations up to 70 MeV was quite insensitive to whether the inelasticity approached a constant value or increased linearly with energy.

To find the D function in the physical energy region from equation (6.12) one has to compute an integral involving N. The quickest way to obtain the values at the quadrature points proved to be by the interpolation of the points of the numerical solution of the N equation.

6.5 Results

The first four orders of driving term for the quartet are given in fig. 6.2. On comparison with the exact input calculated from the Amado model it is clear that the sequence of inputs is converging well. The doublet channel inputs shown in fig. 6.3 appear to be converging albeit slowly. Here the driving terms do not converge to the exact input as computed from equation (6.27). The reason for this is that the on-shell amplitude from which the input is derived includes a contribution from the triton pole which is not present in the multiple scattering series expansion. Nevertheless, the exact input satisfies the N/D representation of the amplitude; in this case the triton occurs as a pole in the N function rather than as a zero of D. The dashed curve b in fig. 6.3 represents the exact input with the contribution from the triton pole subtracted.

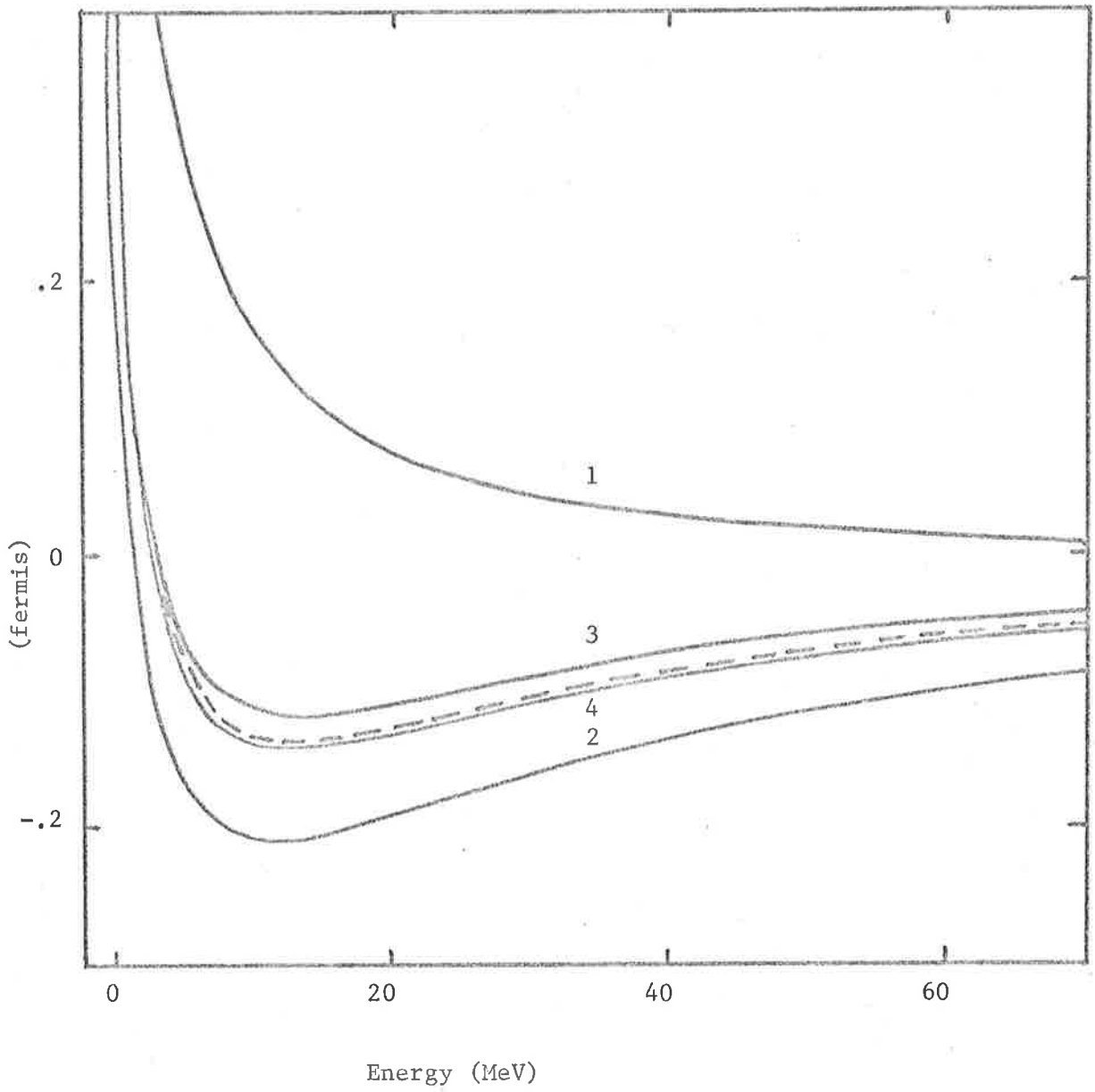

Figure 6.2

Curves 1-4 are the s-wave quartet channel inputs B_1 to B_4. The exact input from the Faddeev equations is represented by the dashed curve.

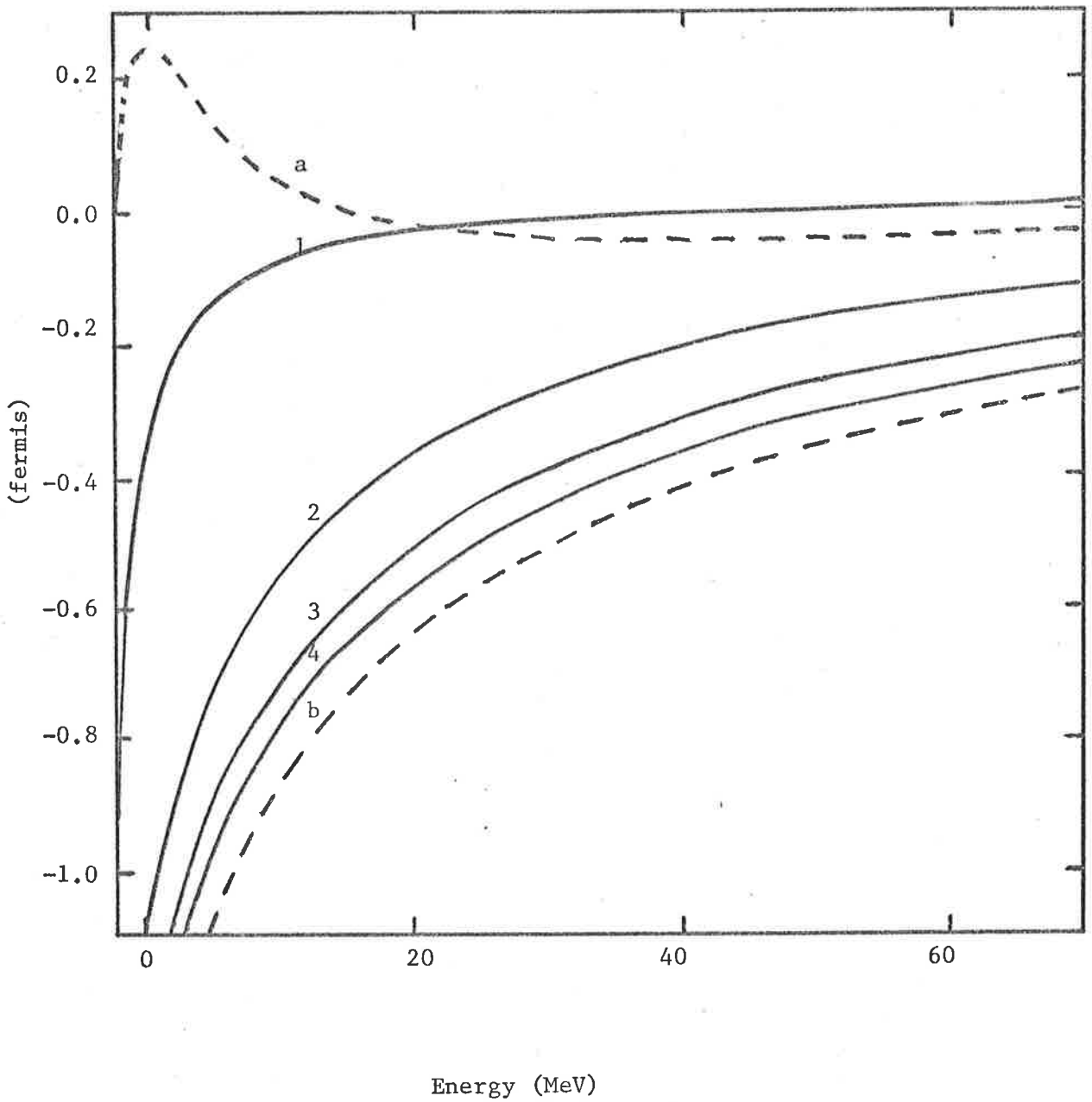

Figure 6.3

Curves 1-4 are the s-wave doublet channel inputs B_1 to B_4. The exact input from the Faddeev equations is represented by the dashed curve a. Curve b is the exact input with a contribution from the triton pole subtracted.

In order to test the dispersion relation approach, in particular the effectiveness of standard approximations, the equations were solved in several ways. First, we tested how well the on-shell amplitudes, computed with the various orders of input, compared with the exact amplitudes. So that the results were independent of any approximation to the inelasticities, we used the exact inelasticities derived from the Amado model amplitudes. As a check of the numerical accuracy of the calculation, the phase shifts were found from the exact inputs and compared with the exact model values. For low energies agreement was within $.2^{o}$ and at the upper limit of 70 MeV within 1^{o}. The inelasticities for the s-wave amplitudes are shown in fig. 6.4. In the quartet channel, the inelasticity increases slowly near the breakup threshold and is very nearly linear at higher energies. In the doublet channel, the coupling between the neutron and singlet antibound state has an important influence; there is an abrupt rise in the inelasticity near the threshold but at higher energies the inelasticity again increases linearly. The rates of increase of the inelasticities in the linear region appear to be very nearly the same in both channels.

The results for the solution of the quartet N equation for all the inputs are listed in table 6.2. The solutions although widely differing for the first and second inputs appear to be converging to the solution with the exact input. The quartet phase shifts and absorption coefficients are given in table 6.3.

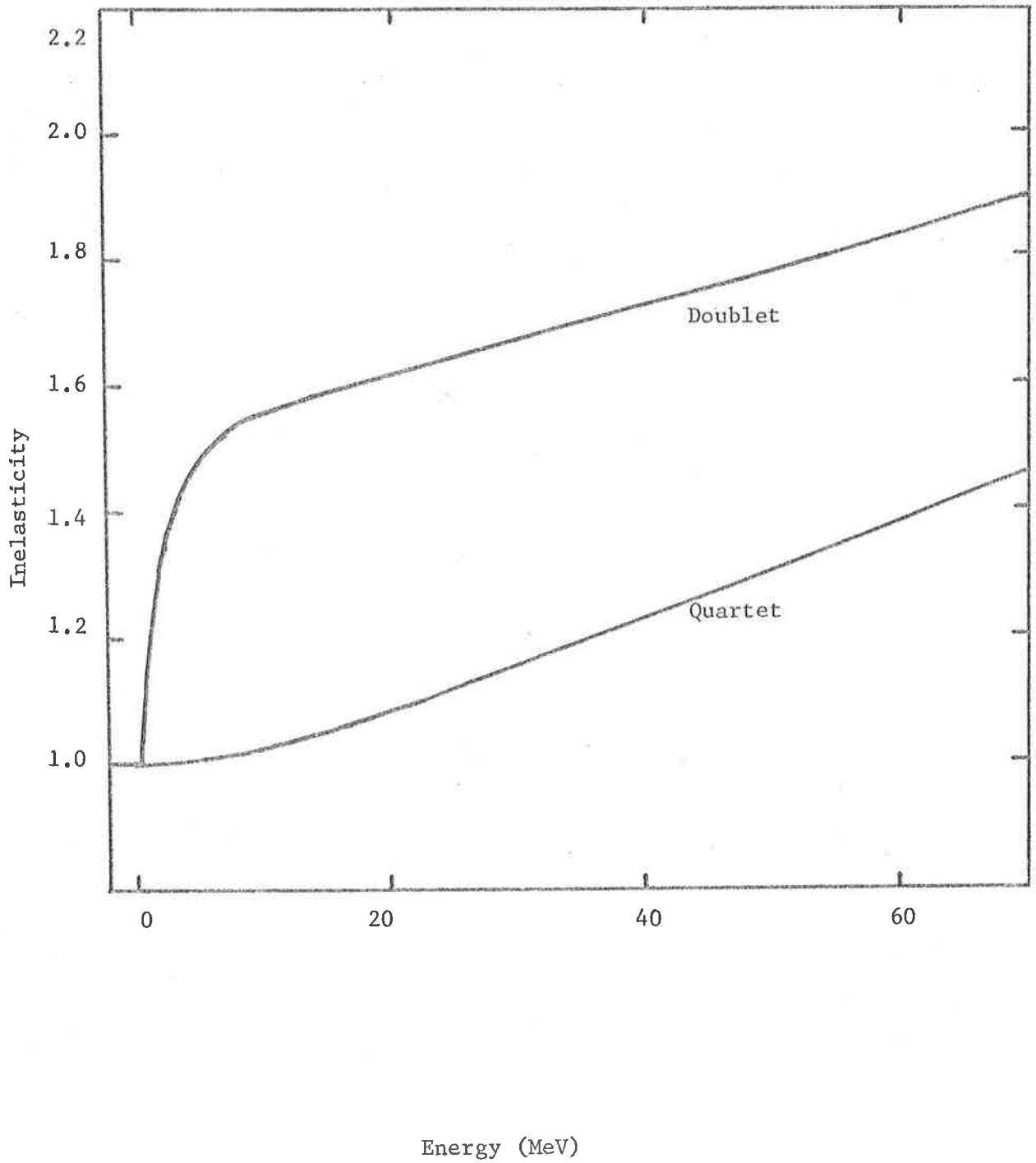

Figure 6.4

Inelasticities for the s-wave quartet and doublet channels.

QUARTET

E(MeV)	1	2	3	4	EXACT
-2.0	+2.286	-265.710	-55.991	-9.358	-10.773
-1.0	+1.413	-155.310	-26.827	-5.462	-6.151
0.	+1.048	-108.621	-18.746	-3.726	-4.216
5.	+0.484	-39.575	-6.690	-1.220	-1.389
10.	+0.331	-22.215	-3.640	-0.613	-0.714
20.	+0.207	-10.050	-1.611	-0.235	-0.282
30.	+0.155	-5.850	-0.897	-0.115	-0.142
40.	+0.124	-3.731	-0.571	-0.064	-0.082
50.	+0.104	-2.570	-0.387	-0.039	-0.052
60.	+0.089	-1.831	-0.277	-0.025	-0.035
70.	+0.078	-1.340	-0.204	-0.016	-0.024

DOUBLET

-2.0	.4627	.3299	.1540	.0459	-.0135
-1.0	.2867	.3680	.2736	.2191	.1768
0.	.2072	.3653	.3087	.2642	.2451
2.	.1303	.3364	.3174	.2995	.2905
5.	.0789	.2835	.2948	.3052	.2964
10.	.0417	.2227	.2451	.2589	.2653
20.	.0165	.1386	.1753	.1943	.2082
30.	.0075	.0878	.1236	.1527	.1642
40.	.0033	.0573	.0933	.1188	.1305
50.	.0011	.0364	.0691	.0941	.1052
60.	-.0002	.0224	.0513	.0741	.0854
70.	-.0009	.0096	.0365	.0575	.0688

Table 6.2

Solution of N equations (arbitrary units) for inputs B_1 to B_4 and also the exact input. The subtraction point has been chosen at $s_0 = -50$.

QUARTET

	1		2		3		4		EXACT	
E(MeV)	δ_R	η	δ_R	η	δ_R	η	δ_R	η	δ_R	η
-2.225	180.0	1.00	180.0	1.00	180.0	1.00	180.0	1.00	180.0	1.00
-2.	151.0	1.00	150.9	1.00	150.5	1.00	151.2	1.00	150.7	1.00
0.	109.3	1.00	107.7	1.00	107.6	1.00	107.5	1.00	107.7	1.00
5.	83.5	.992	79.6	.992	78.6	.992	78.6	.992	78.7	.992
10.	73.2	.957	68.1	.961	64.9	.961	64.9	.961	65.2	.962
15.	66.7	.914	55.8	.930	55.7	.930	55.6	.930	55.9	.930
20.	61.4	.876	48.6	.907	48.5	.908	48.4	.908	48.7	.908
25.	58.1	.836	43.0	.893	42.6	.894	42.5	.895	42.9	.893
30.	54.2	.811	38.0	.886	37.6	.888	37.6	.888	38.1	.886
40.	48.5	.766	30.0	.889	30.4	.886	29.9	.889	30.7	.884
50.	43.8	.735	24.4	.898	24.8	.895	24.4	.898	25.2	.892
60.	39.7	.717	19.9	.913	20.7	.906	20.1	.911	21.1	.903
70.	36.2	.706	16.3	.928	17.4	.918	16.7	.925	17.9	.914
Ghost	-12.0		-51.0		-62.2		None		None	

DOUBLET

-2.225	0.	1.000	180.0	1.000	180.0	1.000	180.0	1.000	180.0	1.000
-2.	65.6	1.000	162.7	1.000	173.0	1.000	178.0	1.000	181.0	1.000
0.	39.8	1.000	130.8	1.000	146.9	1.000	154.6	1.000	159.0	1.000
5.	19.2	.898	89.8	.344	118.0	.431	128.3	.515	135.8	.595
10.	12.0	.953	53.9	.442	84.7	.294	103.7	.310	115.0	.358
15.	8.4	.975	40.3	.577	59.0	.369	77.5	.278	91.5	.263
20.	6.2	.986	31.8	.688	46.3	.473	56.4	.364	70.6	.276
25.	4.6	.992	25.5	.774	37.7	.576	47.2	.437	57.0	.333
30.	3.4	.995	21.5	.826	33.0	.637	40.8	.506	48.7	.396
40.	1.7	.999	15.2	.902	25.9	.736	32.2	.622	38.2	.516
50.	0.6	1.000	10.5	.948	20.5	.811	26.2	.706	31.8	.591
60.	-0.1	1.000	6.9	.976	16.1	.872	21.4	.780	21.3	.668
70.	-0.7	1.000	3.2	.994	12.6	.934	17.6	.835	23.9	.707
Triton Binding Energy	No bound state		-5.1		-7.7		-9.4		-11.0	

Table 6.3

Real parts of phase shifts and absorption coefficients ($\eta=\exp(-2\delta_I)$). The first four sets are from the solution of the N/D equations with the approximate driving terms. The exact set is obtained by solution of the off-shell equations.

The agreement of the results obtained with the second, third and fourth order driving terms compared with the exact phase is striking. Considering how much the solution of the N equation varies with the different inputs it is curious how constant the N/D ratio is.

The approximate nature of the inputs is reflected more clearly in the behaviour of the D function at negative energies. With the first three orders of input the D function has a zero at negative energies. From table 6.3 we see the first input gives rise to a zero at -12 MeV and that with the increasing order of input it moves further to the left occuring at -51 and -62 MeV respectively for the second and third inputs. It is not present at all when the fourth order driving term or the exact input is used. Since the effective interaction in the quartet is repulsive, this zero cannot correspond to a three-body bound state. The occurrence of such states is well known in field theory (46) and they are called ghosts. Their presence indicates the approximate nature of the lower order inputs. It is interesting to note that Bower (10) is his quartet channel calculation with S-matrix inputs predicted a ghost by constructing a sum rule, but was unable to remove it by varying the driving terms in his model.

In the more complex doublet channel the results of calculations are less satisfactory. The exact n-d amplitude found by direct solution of the Amado model equations has a zero just about the two body threshold. As a result, the doublet phase shift (see table 6.3), normalised to 180° at the scattering threshold increases to 181° at -2 MeV and then decreases steadily to 24° at 70 MeV. The approximate inputs were unable to reproduce this behaviour. The phase shifts

from these inputs decrease monotonically near the threshold and too quickly at higher energies. However, the phases appear to be approaching the exact phase although much more slowly than in the case of the quartet channel. There is an interesting comparison in this regard between the solutions of the quartet and doublet N equations. Unlike the solutions of the quartet N equation one can see from table 6.2 that the solutions for the doublet are all of approximately the same magnitude. The major effect of increasing the order of the input is to alter the solution below three-body breakup.

The absorption coefficients reproduce the dip of the exact coefficient but generally produce a dip which is too sharply peaked. They do however, approach the exact values with increasing order of input. A similar pattern is observed with the binding energy of the triton. Although the zero of the D functions appraches the exact model value of -11.01 MeV with the higher order inputs it still falls short of it by 1.6 MeV in the fourth order approximation.

In the usual application of the N/D method the exact form of the inelasticity is unknown. We therefore also carried out calculations designed to test the sensitivity of the N/D solutions to variations in the inelasticity. In the quartet channel where the inelasticity increases slowly it appeared reasonable to neglect inelasticity all together. The phase shifts which result under this appoximation are shown in fig. 6.5. For the first three inputs neglecting the effect of the breakup channel has had little effect on the quartet phase shifts. Comparison with the results of table 6.3 indicates the effect of omitting inelastic effects increases the phase shifts by about 5° at higher energies. There is, of course, no basis for

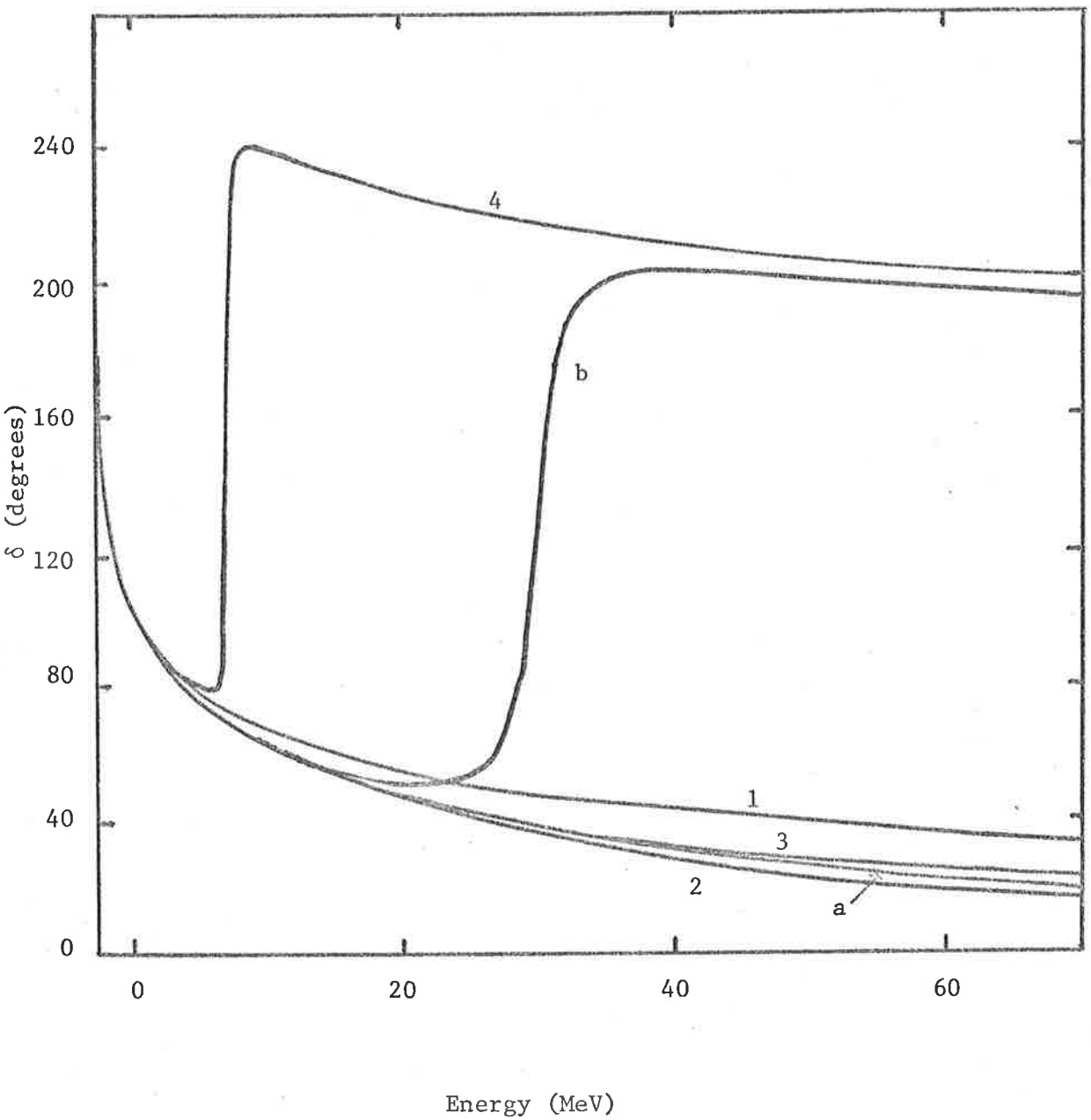

Figure 6.5

The curves labelled 1 to 4 are the quartet phase shifts in the absence of inelasticity using the inputs B_1 to B_4. Curve a is the real part of the exact quartet phase shift. Curve b is the phase shift obtained by using the exact input but neglecting inelasticity.

comparison with the absorption coefficients which are equal to unity at all energies. However, the phase shift resulting from the fourth input is quite different; although matching the other phases well near the breakup threshold it increases rapidly in the vicinity of 7 MeV, rising to 240°, then falls off slowly and approaches an asymptotic value of 180°. A similar behaviour occurs when the exact input is used. The rapid variation of phase now appears near 25 MeV.

This somewhat puzzling behaviour may be explained by noting that a ghost appears with the first three inputs on solving the N/D equations with the exact inelasticity. Recalculating the D function in the absence of inelasticity one now finds a ghost at -13.5, -40 and -254 MeV for the first three inputs. Again, no ghost is present with the fourth order input or the exact driving term. Because the phase shifts have been derived in the absence of inelasticity the usual form of Levinson's theorem is valid. That is, the difference in phase

$$\delta(-2.225) - \delta(\infty) = n\pi$$

where n is the number of zeros in the D function, irrespective whether they correspond to bound states or ghosts. On this basis we predict $\delta(-2.225) - \delta(\infty) = \pi$ for the first three inputs and $\delta(-2.225) - \delta(\infty) = 0$ for the fourth order and exact inputs, which is consistent with the results obtained.

It may be noted that for the exact quartet channel phase (Final column table 6.3), $\delta(-2.225) - \delta(\infty) = \pi$, in the absence of a zero in D. However, in this case the inelasticity has to be taken into account and Levinson's theorem is no longer applicable. Sloan (47) has suggested that this phase difference of π may be explained in terms of a modified form of Levinson's theorem conjectured by Swan (48) for a system of composite particles.

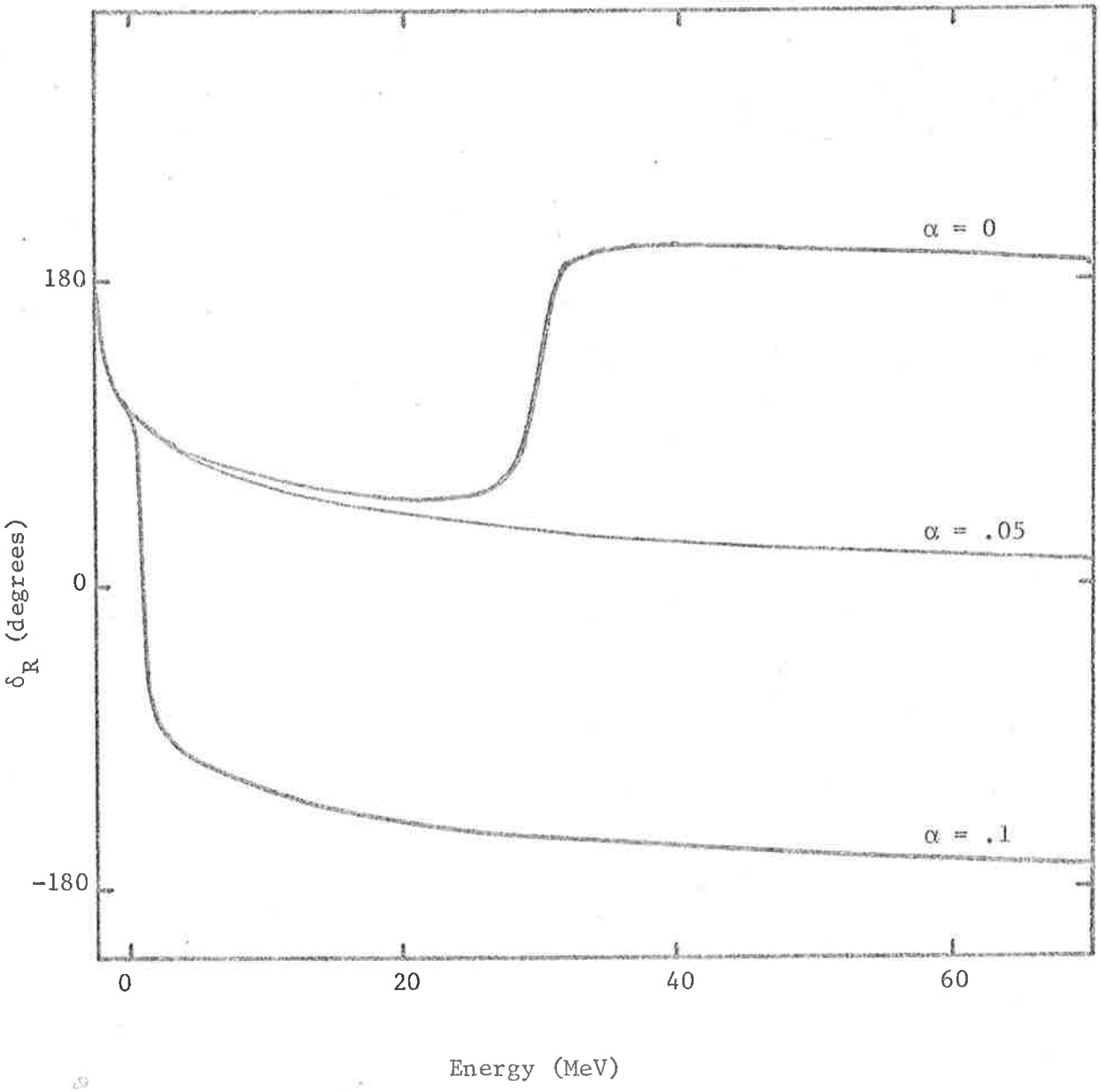

Figure 6.6

Real parts of phase shifts for various model inelasticities defined in (6.30), using the exact quartet driving term.

Finally the simple step function parameterisation of inelastic effects was also tested in the quartet. That is, the inelasticity is defined by

$$R(S) = 1, \quad E < 0$$
$$= 1+\alpha, \quad E > 0 \qquad (6.30)$$

The equations were solved for several values of α using the exact input. The resultant phases shown in fig. 6.6 indicate the asymptotic phase shift is quite sensitive to small changes in α and that the difference $\delta(-2.225) - \delta(\infty)$ increases with increasing α.

The doublet N/D solutions using the exact double driving term are also sensitive to the inelasticity. In fig. 6.7 we have shown the phase shifts resulting from the model inelasticity of equation (6.30) for $\alpha = .4, .6, .8$. With $\alpha = .6$ the doublet phase shift is comparable with the exact model phase, which one might anticipate since the exact doublet inelasticity (see fig. 6.4) increases very quickly to 1.6 above the breakup threshold.

6.6 Discussion and Conclusions

In the light of the results presented it is clear that the N/D method of solution for the quartet amplitude works very well with all orders of driving term once the exact inelasticity is known. With the last three orders of input the agreement with the exact amplitude is outstanding over the entire energy range. Referring to fig. 6.3, we see that this excellent agreement has been obtained despite the fact that there is some difference between the second, third and fourth order inputs for higher energies. Thus it appears even though the singularities in the higher order multiparticle scattering series give a non-negligible contribution to the quartet input in the form of a uniform background at higher

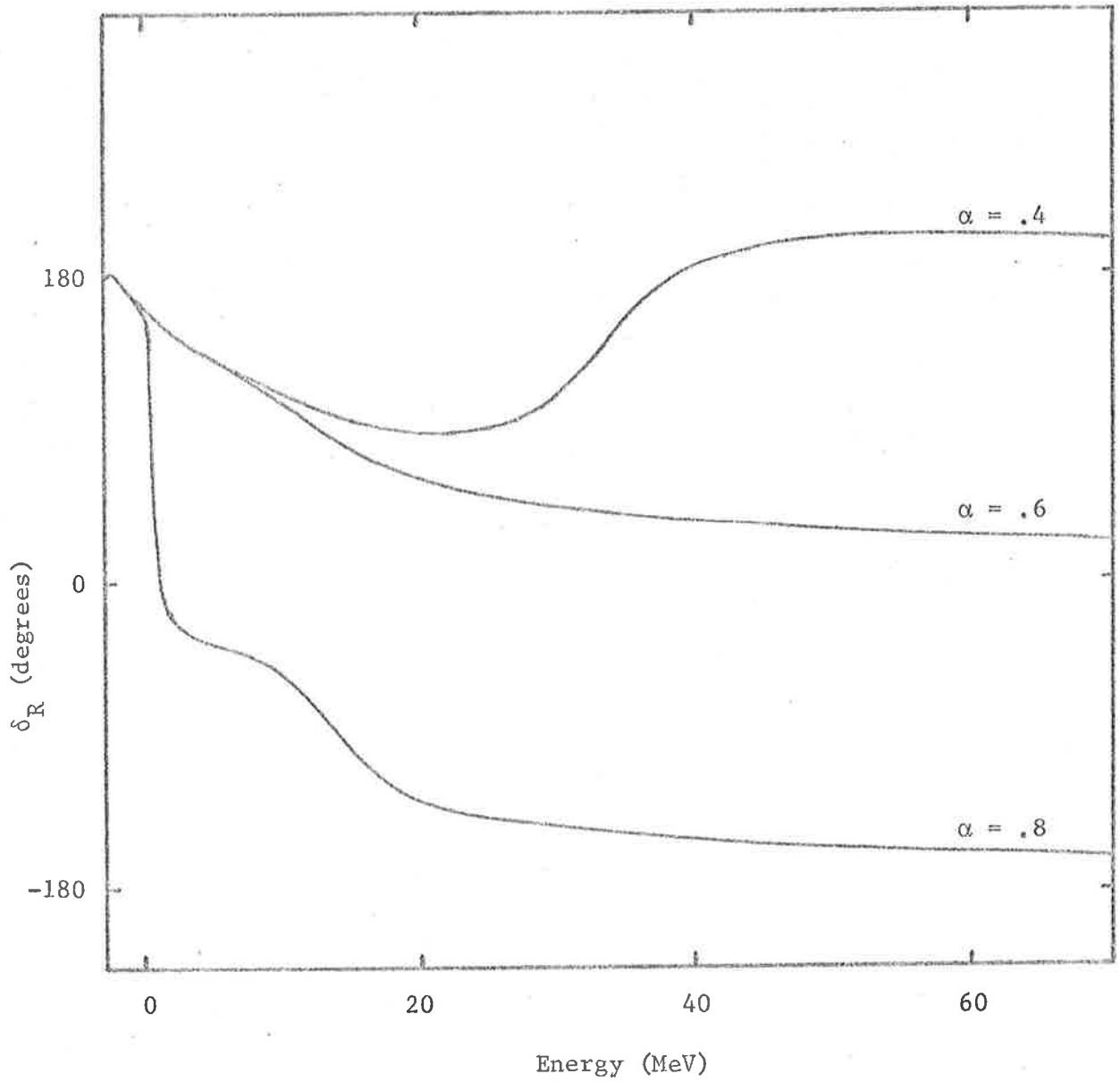

Figure 6.7

Real parts of phase shifts for various model inelasticities defined in (6.30) using the exact doublet driving term.

energies its effect on the phase and absorption coefficients is minimal. However, the approximate nature of the various driving terms is clearly mirrored in the position of the zero in the D function at negative energies. There the first order driving term causes a strong ghost to appear at -12.0 MeV and as the order of the input is increased the position of the ghost moves further to the left eventually disappearing in the fourth order and exact inputs.

The results in the doublet are not so promising. The driving terms appear to converge with increasing order but the corresponding phases, absorption coefficients and triton binding energy approach the exact model values slowly. To explain this slow convergence one must take into account the more complicated nature of the doublet driving terms arising from the coupling between the singlet and ~~doublet~~ triplet channels. For example, the fourth order driving term contains contributions from eight third order terms alone, and fifteen terms in all, from the multiple scattering series expansion of the doublet amplitude. The couplings are of different signs and strengths, which cause interference and cancelation between the terms. There is an indication in the doublet N function (table 6.2) that the major change in the form of the solution with the increasing order of driving terms occurs for energies below breakup. Here the N function values become significantly smaller at -2 MeV. What is happening is that the N/D solution is trying to reproduce the zero in the exact doublet amplitude which occurs just above the two-body threshold in the Amado model. Because the position of this zero depends quite critically on the inputs in this region, even the small contributions from higher order terms are important and may be a reason for the slow convergence of the solutions. As with the quartet amplitude, we

are inclined to believe that the differences between the driving terms at higher energies are not so important. Further support for this interpretation is afforded by the exact doublet input with a triton pole contribution subtracted (curve (b) of fig. 6.3). In this form the low energy behaviour is hidden but on inclusion of the triton pole contribution (curve (a)) it is clearly evident.

The above conclusions are consistent with the physical argument originally advanced by Barton and Phillips (8). They argued that, because the interaction in the quartet channel is repulsive, the neutron cannot get too close to the deuteron and so only the longest range forces which correspond to the nearest singularities (present in the Born term) should dominate; while in the doublet channel the effective interaction is attractive, enabling the neutron and deuteron to come sufficiently close for the short range forces to have an effect. That is the more distant singularities in the higher order terms should be important in determining the detailed structure of the doublet amplitude. A further point which deserves comment is the role played by the leading singularities of the Born and first order multi-particle scattering series terms. We showed in Chapter 4 that the leading singularity in the first order terms, the result of a pinch between the energy denominators, was close to the physical region because of the small deuteron binding energy, and that no pinch singularities from energy denominators were present in the higher order terms. In the limit of constant vertex functions the second order driving term should therefore be the exact input. One might expect that even in the case of

the Yamaguchi vertex function, as the singularities in the remaining terms are of the order of the inverse range parameter and far away from the physical region that the second order driving term would be a good approximation to the exact one. In the quartet this reasoning is partially justified because the second order input has the correct shape and gives excellent results. Even in the doublet where the small contributions of higher order terms are significant the second order input is approaching the general shape of the higher order ones.

Having investigated the N/D approach for on-shell amplitudes in the Amado model one must ask to what degree the results can be extrapolated to better models of the on-shell amplitudes. Basically this involves using more realistic two-body potentials, inclusion of tensor forces and short range repulsion. We are inclined to believe the same difficulties with convergence would still occur in the s-wave doublet channel. Although the Amado model is very simple it gives a triton binding which is less than 3 MeV from the exact value and similarly reproduces the zero in the on-shell amplitude just above the scattering threshold, in fair agreement with experimental results which indicate it occurs just below. Thus the improvements due to more realistic potentials are in the nature of perturbations and should have little effect on the convergence of the doublet driving terms.

Let us now expand on a remark made at the beginning of the Chapter concerning the n-d calculation by Bower. Avishai et al found they could obtain good doublet results once a pole term was added to their input and the strength adjusted accordingly.

On the basis of our calculations with better inputs it appears that there is no justification for such a term. It merely turns out to be a convenient way to combine the effects of the short range forces at the expense of introducing extra parameters. Although it is not possible to compare the present work with Bower's results directly because of the different nature of the models, it is fair to say his good results for the triton binding energy are due in part to the pole approximation introduced to describe the two-pion exchange. The triton binding energy and the phase shift are noticably dependent on the strength of the residue of this pole term and in this sense his results are similar to those of Avishai et al. It is thus not at all certain whether this parameterisation of the two-pion exchange is not masking other more distant particle exchange effects.

With regard to the importance of having an accurate description of the inelasticity it was demonstrated that quite a varied behaviour of the amplitudes could be achieved by neglecting it entirely or crudely approximating it. If better approximations are developed,as has been reported by Greben, it appears that the behaviour is more realistic. The spectacular behaviour of the quartet phase under the neglect of inelastic effects does however indicate the type of problems one might face in the application of N/D techniques to describe systems of four or more particles. For example, the quartet amplitude resulting from the third order driving term in the absence of inelasticity gives a phase almost identical with that of the exact amplitude, whereas with the slightly better fourth order input the asymptotic behaviour is quite different.

That is the N/D solutions are in certain circumstances sensitive to small changes in input and an improved input may not give better phases unless the inelastic effects are at the same time described accurately.

In summary it can be said that the N/D method applied to s-wave n-d scattering is only partly successful. The quartet channel is well described. In the doublet channel the features are described qualitatively but the N/D method cannot compete with the accurate numerical solution of the Faddeev equations. Furthermore, to describe the doublet channel even qualitatively it has been necessary to use driving terms of up to fourth order, whose construction becomes more difficult with increasing order. We have found that the calculation of the fourth order order input and subsequent solution of the N/D equations with it involves as much work as the direct solution of the off-shell Amado equations. There would appear therefore to be no advantage in using N/D techniques in preference to the Faddeev equations for s-wave doublet scattering. Perhaps a more promising avenue for the N/D method is in the generalisation to few-particle nuclear reactions where although off-shell equations have been formulated, their numerical solution is not yet practicable (49,50). Even here however, in the situation that the scattering system gives rise to bound states, one should expect that use of first or second order driving terms may be insufficient to predict even qualitative features of the scattering to any degree.

Chapter 7

EIGENVALUE SPECTRA OF THE n-d KERNELS

There is an intrinsic interest in the eigenvalues of the kernels because they determine the number of bound states and the convergence of the perturbation series expansions of the scattering equations. In this chapter we are concerned mainly with the eigenvalues for physical scattering energies, where a corollary of the Fredholm methods discussed in Chapter 3 enables the eigenvalue spectra to be determined numerically.

The results of calculations for the s-wave eigenvalue trajectories in the quartet and doublet channels are presented in section 2; their threshold behaviour is discussed is section 3. In section 4 we make use of the relation between the eigenvalues and the on-shell amplitude to investigate quantitatively the rapid variation of $k_B \cot\delta$ near threshold in the s-wave doublet channel. Finally, a possible application of the method used to calculate the eigenvalues for physical energies to four-body scattering problems is suggested.

7.1 General Properties

Fewer properties can be inferred for the eigenvalues of the three-body kernels than for the two-body Lippmann-Schwinger kernels*. Basically, this is because the properties of the two-body eigenvalues which rely on the simple relationship between the integral equation and the Schrödinger equation are no longer valid for the three-body eigenvalues where there is a more complicated relationship between the Faddeev equations and the three-body Schrödinger equation.

---

*For a list of two-body eigenvalue properties see refs. (23, 51).

For simplicity we shall consider the kernel of the system of identical spinless bosons, the eigenvalue equation for which is

$$\int d\underline{p}' Z(W;\underline{p},\underline{p}')\tau(W-\tfrac{3}{4}p'^2)\phi_i(W;\underline{p}') = \eta_i(W)\phi_i(W;\underline{p}). \tag{7.1}$$

Because the kernel is a function of p,p' and $\hat{p}\cdot\hat{p}'$ only, the eigenvalues η_{ℓ_i} of the partial wave kernel,

$$\int_0^\infty dp\ p^2 Z_\ell(W;p,p')\tau(W-\tfrac{3}{4}p'^2)\phi_{\ell_i}(W;p) = \eta_{\ell_i}(W)\phi_{\ell_i}(W;p) \tag{7.1'}$$

where

$$Z_\ell(W;p,p') = \frac{1}{2\ell+1}\int_{-1}^{1} du\ P_\ell(u) Z(W;\underline{p},\underline{p}'),\ \cos u = \hat{p}\cdot\hat{p}' \tag{7.2}$$

are eigenvalues of equation (7.1) as well. Unless it is necessary to exhibit the partial wave dependence explicitly we shall use the eigenvalue equation (7.1).

First let us note some characteristics of the eigenvalues for real energies below the scattering thresholds. In this region the eigenvalues are real. This is a consequence of the fact that $\tau(W-\frac{3}{4}p^2)$ is a real negative function when $E < -B$ and $Z(E;\underline{p},\underline{p}')$ is a real symmetric kernel. Thus multiplying equation (7.1) by $|\tau|^{\frac{1}{2}}$, η_i is an eigenvalue of the equation

$$\overline{K}(E)\ \overline{\phi}_i(E) = \eta_i(E)\overline{\phi}_i(E), \tag{7.3}$$

where

$$\overline{K}(E) = -|\tau|^{\frac{1}{2}} Z(E) |\tau|^{\frac{1}{2}}$$

is a Hermitian operator and hence is real.

As a result of the theory of Hermitian kernels there follow the sum rules

$$||\overline{K}(E)||^n = \Sigma_{i=0}^{\infty} \eta_i^n(E), \qquad n=2,3,\ldots,\ E < -B, \tag{7.4}$$

whenever $||\overline{K}(E)||$ exists. It was shown in Chapter 3 that $||K(E)||$ (and hence $||\overline{K}(E)||$) is finite in the bound state region $E < -B$.

For each eigenvalue passing through unity, the homogeneous AL equation has a solution corresponding to a three-body bound state at that energy. Hence by the sum rules (7.4) there can be only a finite number of bound states.

However, it should be mentioned that there is one exceptional case in the limit that the two-body binding energy $-B = 0$, for which $\lim_{E\to 0}||\overline{K}(E)||$ does not exist. The existence of this divergent norm gives rise to a series of very weakly bound three-body states when $B \sim 0$, a fact first noticed by Efimov (52,53). Amado and Noble (54,55) by an elegant argument were able to show that the reason the norm diverges in the limit $E,B \to 0$ is that the infinite sequence of eigenvalues η_i has an accumulation point greater than unity*. Thus for a two-body bound state with zero binding energy, as the energy approaches the scattering threshold from the bound state region, the number of eigenvalues exceeding unity increases beyond limit and from (7.4) the norm $||\overline{K}(0)||$ diverges. The properties of the Efimov states in the Amado model have been investigated numerically by Dodd and Stelbovics (56).

There are several additional properties of the eigenvalues in the bound-state region which follow if one can show the AL kernel is a positive definite operator. However, in the case of the Amado model of three identical spinless bosons where a numerical calculation of the s-wave spectrum indicates the partial wave kernel is positive definite, we are unable to prove this rigorously because of the complicated nature of the kernel.

Turning to complex energies one can ask under what conditions the eigenvalues are analytic functions of energy. To answer this question it is sufficient to find out where $\frac{d\eta_i}{dW}$ is finite.

---

*There is in fact a different accumulation point in each partial wave subset. Only the s-wave accumulation point exceeds unity.

Calculation of $\frac{d\eta_i}{dW}$ from the equation

$$(\phi_i^*, \tau Z \tau \phi_i) = \eta_i(\phi_i^*, \tau\phi_i) \tag{7.5}$$

yields

$$\frac{d\eta_i}{dW} = \frac{(\phi_i^*, \tau \frac{dZ}{dW} \tau \phi_i)}{(\phi_i^*, \tau\phi_i)} \, . \tag{7.6}$$

Since the numerator will always be finite for complex energies the η_i are analytic unless $(\phi_i^*, \tau\phi_i)$ vanishes. One can show (51) that this may only occur if two eigenvalue trajectories coincide at a particular energy. We will see such an exceptional event does not take place for the eigenvalues in the Amado model of n-d scattering. Excluding this possibility the η_i are real analytic functions everywhere except for the righthand cuts running along the real axis. Using the sum rules (7.4), η_i may be represented by the dispersion relation

$$\eta_i(W) = \int_{-B}^{\infty} dE \, \frac{\text{Im } \eta_i(E+i0)}{E-W} \, . \tag{7.7}$$

The eigenvalues $\eta_i(E+i0)$ in the physical region are of prime importance with regard to convergence of the perturbation series expansions of the n-d scattering equations. However, one has the difficulty that the eigenvalue equation (7.1') for physical energies cannot be readily solved because of the singularities in $Z_\ell(E+i0,p,p')$ and $\tau(E+i0-\frac{3}{4}p^2)$. The problem is not so much the singularity in the propagator, whose position is fixed at each energy, but the logarithmic singularity in Z_ℓ which depends both on the energy and the other momentum variable that makes it impractical to use numerical quadratures on this kernel.

We shall now show how to circumvent this difficulty by using the phase transformation introduced in Chapter 3 to reformulate the eigenvalue problem. First, let us define a modified Fredholm determinant $D(\lambda;W)$ for the kernel $K(W) = Z(W)\tau(W)$ by

$$D(\lambda;W) = \Sigma_n \lambda^n D_n(W), \tag{7.8}$$

where the $D_n(W)$ are defined in equation (3.15). Suppose λ_i, $i=1,2,\ldots$ are the roots of the equation

$$D(\lambda;W) = 0.$$

Then Smithies (22) has shown that each eigenvalue of K is given by $\eta_i = \lambda_i^{-1}$.

Now, from equations (7.8) and (3.38) one has the identity

$$\Sigma_n \lambda^n D_n(E+i0) = \Sigma_n \lambda^n D_{\theta n}(E), \quad -\pi/2 < \theta < 0. \tag{7.9}$$

But $\Sigma_n \lambda^n D_{\theta n}(E)$ is the modified Fredholm determinant obtained from $K_\theta(E)$ (equation (3.35)) and so it follows that $K(E+i0)$ and $K_\theta(E)$, $-\pi/2 < \theta < 0$, have the same eigenvalue spectrum.

Therefore, to determine the eigenvalues one needs only to solve

$$\int_0^\infty dp' p'^2 e^{3i\theta} K_\ell(E;pe^{i\theta},p'e^{i\theta})\phi_{\theta i}(E;p') = \eta_i(E+i0)\phi_{\theta i}(E;p), \quad -\pi/2 < \theta < 0, \tag{7.10}$$

where the troublesome singularities are rotated well away from the integration contour by choosing θ near $\pi/4$, and their numerical calculation becomes an easy matter.

7.2 Numerical calculation of Eigenvalues

We now present the results of calculations for the eigenvalue spectra of the s-wave quartet and doublet channel equations.

In the numerical solution of (7.10) θ was set at either $.8^c$ or $.6^c$ giving a negligible difference in the results.

For real energies in the bound state region, there are no singularities on the integration contour and in this region we set $\theta = 0$. The s-wave eigenvalues in the bound state region are shown in figs. (7.1) and (7.2). In the quartet channel the eigenvalues all appear to be negative, indicating the kernel is negative definite. As the energy increases, the eigenvalues decrease monotonically and only the leading eigenvalue exceeds unity. Because $K^{\frac{1}{2}}_{11}{}^{3/2} = -\frac{1}{2}K$, the eigenvalue trajectories for the spinless boson system are known as well. Thus the spinless system has two bound states, a ground state at -25 MeV and a weakly bound excited state at -2.37 MeV. The doublet channel supports both negative and positive eigenvalues. In Fig. 7.2 the leading two positive and negative ones are shown. There is only one eigenvalue which exceeds unity. The bound state which it gives rise to at -11.01 MeV is the triton. The second positive eigenvalue falls well short of a bound state reaching a maximum of .63 at threshold. The leading negative eigenvalue finishes with a value of -.93, just failing to pass through the unit circle.

The eigenvalues for physical energies are shown in Figs. 7.3 and 7.4. In the quartet, the two leading eigenvalues have been plotted in the complex plane. They emerge from the origin at $E = -\infty$ and as the energy is increased move along the real axis until the two-body threshold is reached, at which point they rise vertically up into the complex plane. The rapid nature of this increase is indicated on the trajectories. As the energy increases up to the three-body threshold, the energy dependence decreases while the trajectories "turn over" rather noticeably

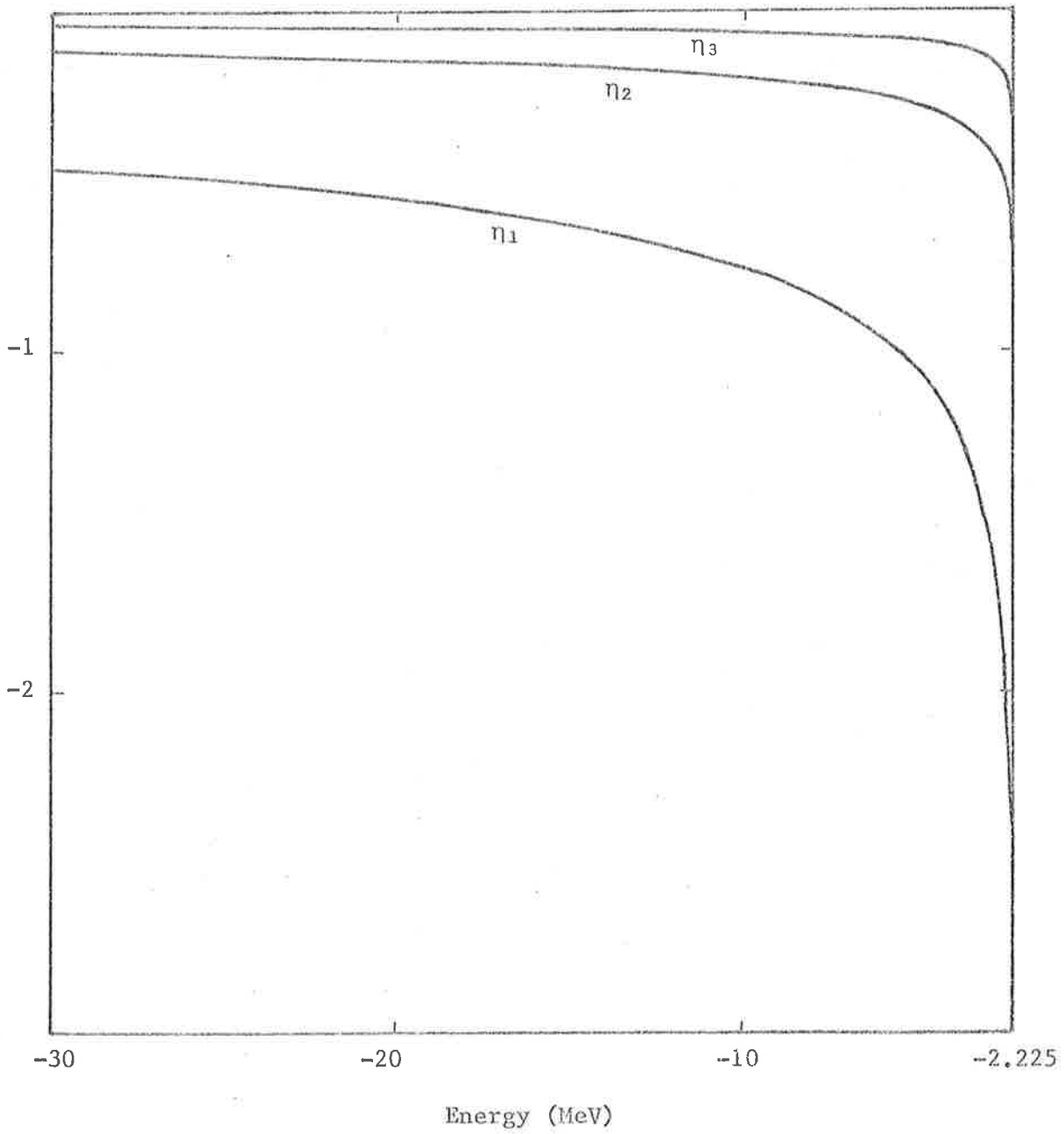

Figure 7.1

Leading three s-wave quartet channel eigenvalue trajectories in the bound state region.

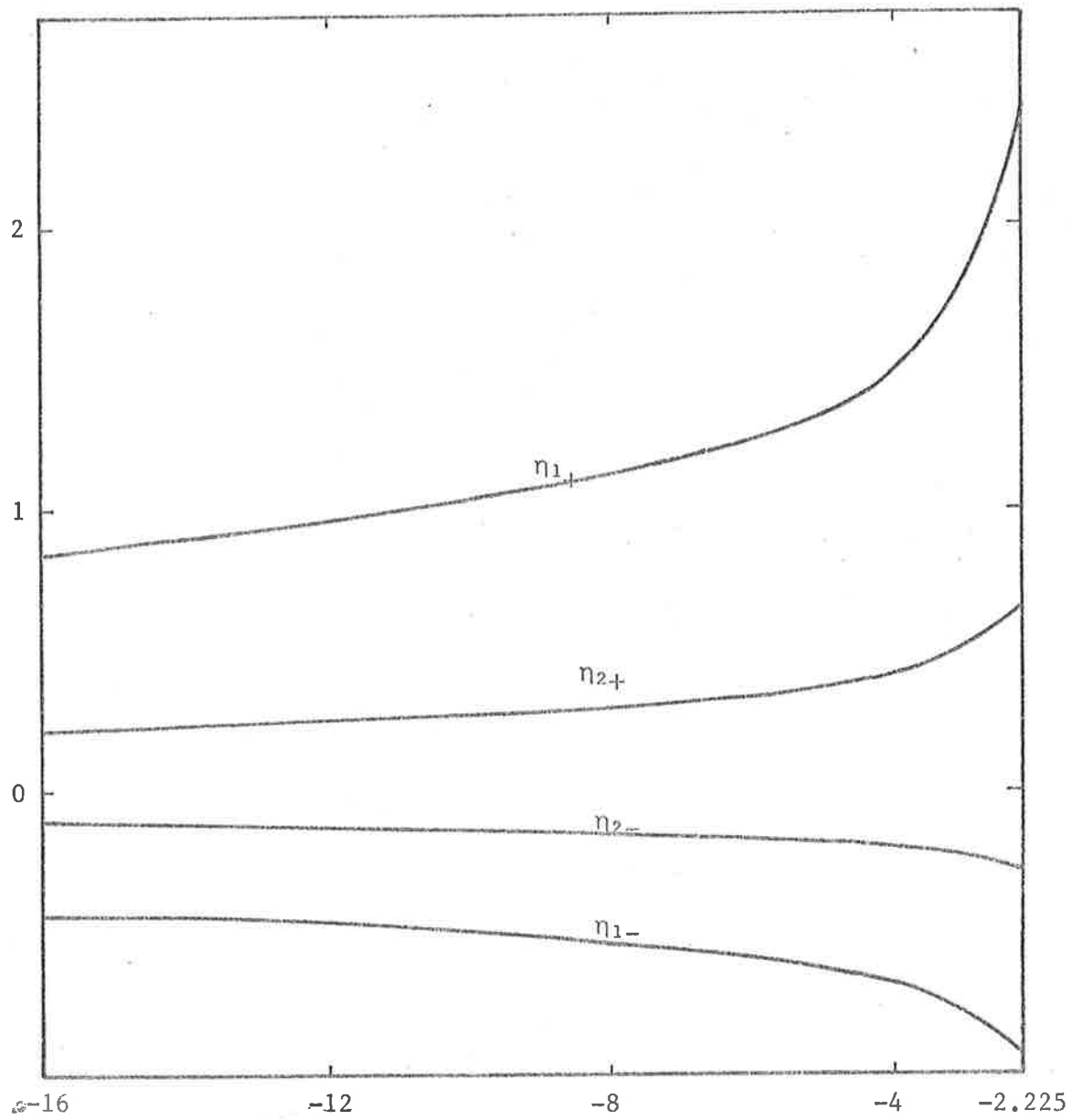

Figure 7.2

Leading eigenvalue trajectories in the s-wave doublet channel for energies in the bound state region.

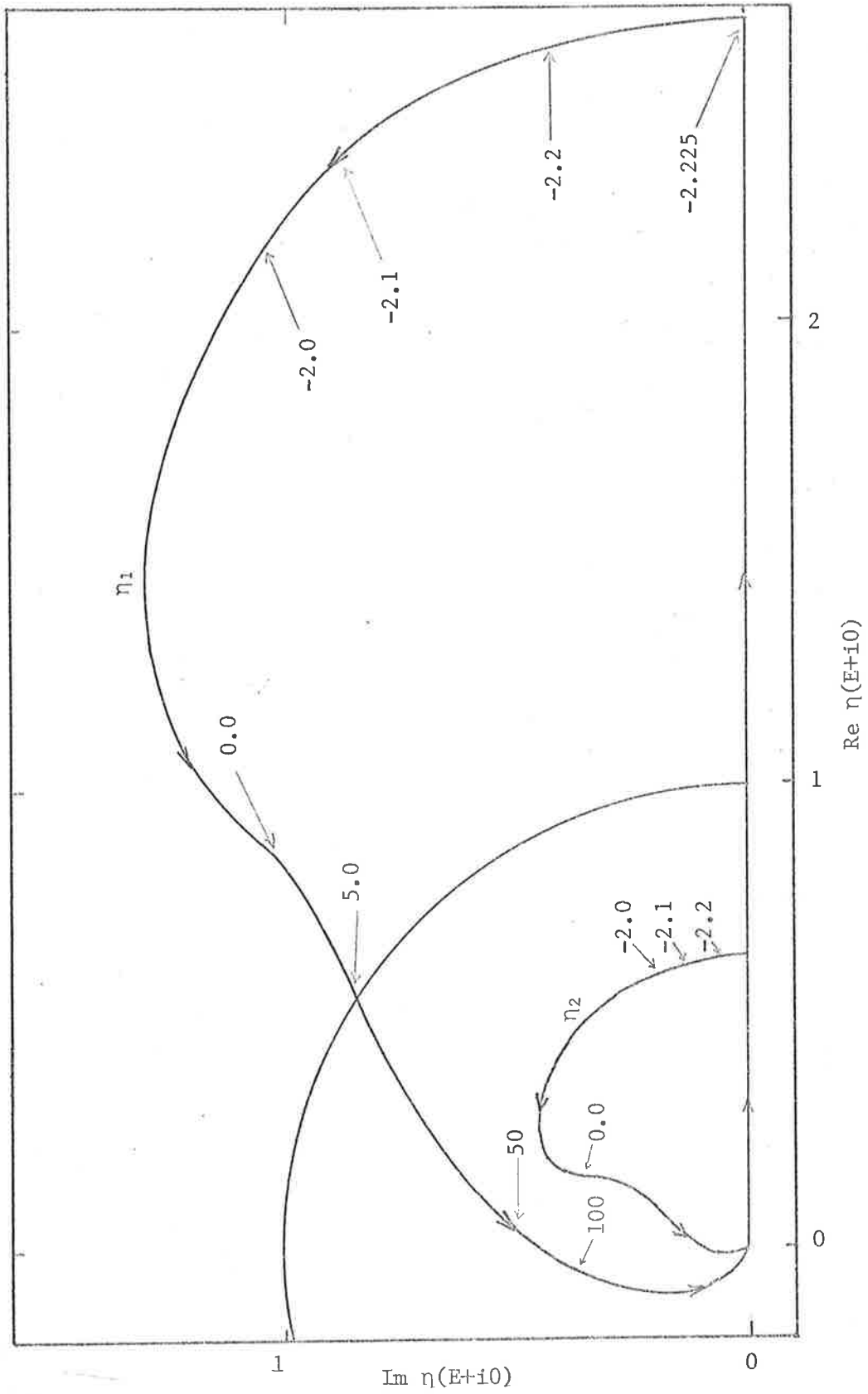

Figure 7.3

Leading two s-wave eigenvalue trajectories in the quartet channel for physical energies. The positions of the eigenvalues are given for several energies to illustrate their energy dependence.

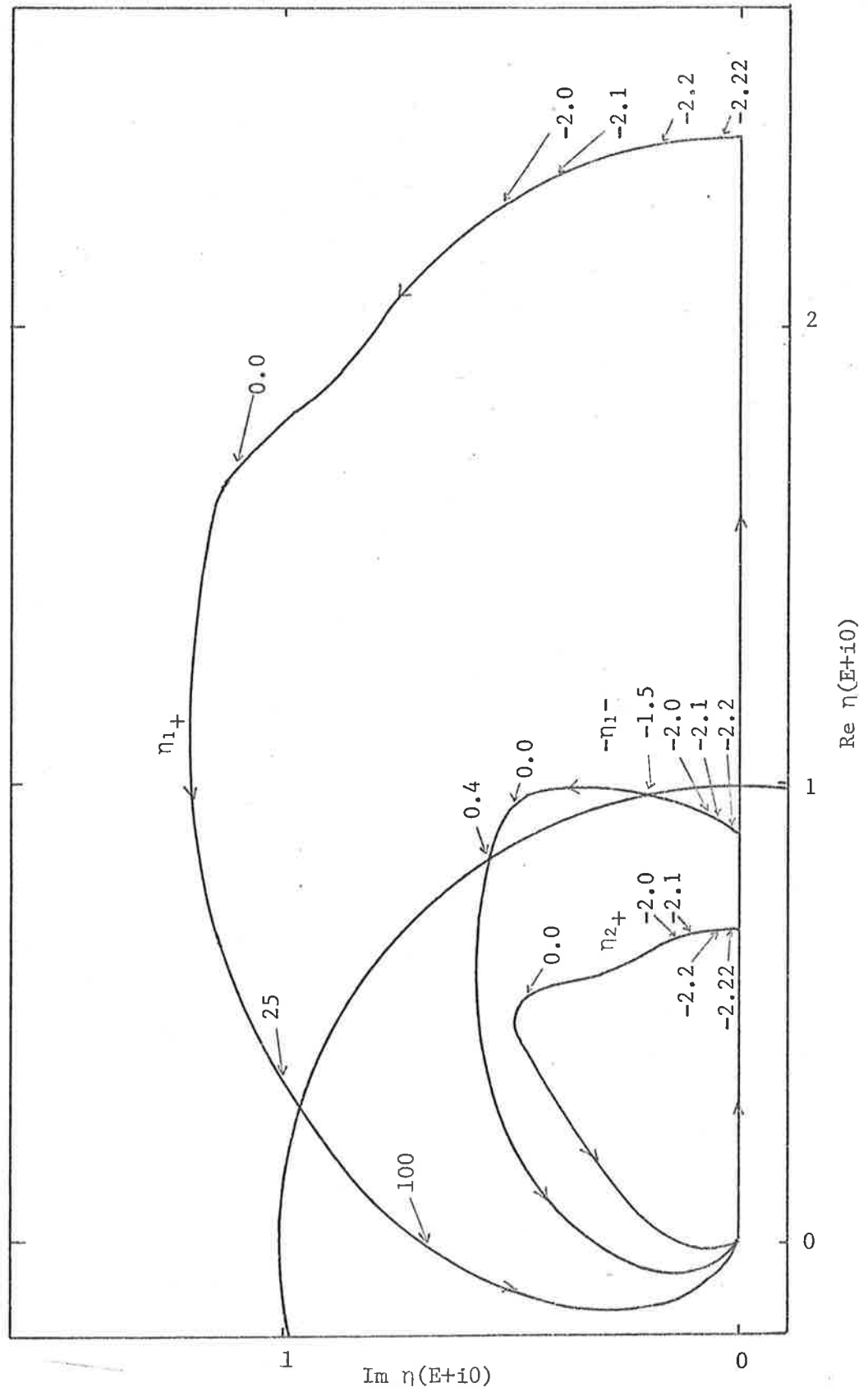

Figure 7.4

Leading three s-wave eigenvalue trajectories in the doublet channel for physical energies. The positions of the eigenvalues are given for several energies to illustrate their energy dependence.

near E = 0, but then flatten out for positive energies. The higher energy behaviour is relatively featureless. The leading eigenvalue enters the unit circle between 5 and 7 MeV and then the eigenvalues tend uniformly to zero from the adjacent quadrant after crossing the imaginary axis. While the solution of the scattering equation by the perturbation expansion is justified for E > 7 MeV, the leading eigenvalue decreases only slowly, and one would not expect the expansion to converge well below 30 MeV.

The doublet channel s-wave trajectories for the three eigenvalues of greatest magnitude are shown in fig. 7.4. η_{1+}, η_{2+} are the trajectories of the two leading positive eigenvalues in the bound state region. They display the same type of behaviour at the two-body threshold as do the quartet eigenvalues. Also, there is again an indentation of the trajectories similar to the quartet trajectories. Thereafter they tend uniformly to zero. η_{1+} enters the unit circle at E = 30 MeV. The eigenvalue trajectory associated with the leading negative trajectory has a distinctly different behaviour and shape. At the scattering threshold it appears to move initially, vertically into the complex plane, but then the real part increases noticeably and causes the trajectory to cross the unit circle. Initially the energy dependence of η_{1-} compared with η_{1+}, η_{2+} is very slight but becomes more marked once it passes through the unit circle at -1.5 MeV. The trajectory turns over and re-enters it at .4 MeV, and tends to zero as $E \to \infty$. It does not have the dip near E = 0 characteristic of η_{1+}, η_{2+}. Several of the other negative eigenvalues trajectories have a similar shape.

7.3 Low Energy Behaviour of the Eigenvalues

As we have seen most of the eigenvalues have the characteristic that they rise vertically into the complex plane when they first become complex. The mechanism for this behaviour can be found by an argument similar to that used by Weinberg (23) for two-body eigenvalue trajectories. We determine the behaviour of Im $\eta_i(E+i0)$ in the limit $E \to -B$ by writing equation (7.1) in the form

$$\eta_i Z\psi_i = Z\tau Z\psi_i, \tag{7.11}$$

where

$$\psi_i(E+i0;p) = \tau(E+i0-\tfrac{3}{4}p^2)\phi_i(E+i0;p).$$

Then

$$\eta_i(E+i0) = \frac{(Z\psi_i, \tau Z\psi_i)}{(\psi_i, Z\psi_i)} \tag{7.12}$$

when $-B < E < 0$, because in this region $Z(E+i0) \equiv Z(E)$ and is real. By equations (2.8), (2.9), (2.10)

$$\text{Im } \tau(E+i0-\tfrac{3}{4}p^2) = -\pi\delta(E+B-\tfrac{3}{4}p^2), \quad -B < E < 0, \tag{7.13}$$

so that for each partial wave the imaginary part of η_{ℓ_i} is given by

$$\text{Im } \eta_{\ell_i}(E+i0) = \frac{-\frac{2\pi}{3}k_B\int_0^\infty dpp^2 \left| Z_\ell(E;k_B,p)\psi_{\ell_i}(E+i0;p)\right|^2}{\int_0^\infty\int_0^\infty dpdp'p^2p'^2\psi_{\ell_i}^*(E+i0,p')Z_\ell(E;p,p')\psi_{\ell_i}(E+i0,p)}. \tag{7.14}$$

In the limit $k_B \to 0$ by explicit calculation of $Z_\ell(E;k_B,p)$ it is easy to deduce that

$$Z_\ell(E;k_B,p) \to k_B^\ell f(p)$$

and hence

$$\text{Im } \eta_{\ell_i}(E+i0) \to k_B^\ell C_{\ell_i} \quad \text{as } E \to -B. \tag{7.15}$$

The behaviour of $\mathrm{Re}\eta_{\ell_i}(E+i0)$ can be found from equation (7.7). We have

$$\mathrm{Re}\eta_{\ell_i}(E+i0) = P\int_{-B}^{\infty} \frac{dE'\ \mathrm{Im}\eta_i(E'+i0)}{E'-E},$$

and in the limit $E \to -B$ the threshold behaviour of $\mathrm{Im}\eta_{\ell_i}$ implies

$$\mathrm{Re}\eta_{\ell_i}(E+i0) = C_{0\ell_i} + C_{1\ell_i}(E+B).$$

Thus the s-wave eigenvalues have the threshold behaviour

$$\eta_j(E+i0) - \eta_j(-B) = A_j(E+B) + iB_j(E+B)^{\frac{1}{2}} \tag{7.16}$$

and the increase is pure imaginary in agreement with the calculations. The same argument can be carried through in the doublet channel coupled equations, where the eigenvalue equation is (writing the eigenvector as a two component vector)

$$\eta_\ell \begin{bmatrix} \phi_1 \\ \phi_2 \end{bmatrix} = \begin{bmatrix} Z_{11} & Z_{12} \\ Z_{21} & Z_{22} \end{bmatrix} \begin{bmatrix} \tau_1 & 0 \\ 0 & \tau_2 \end{bmatrix} \begin{bmatrix} \phi_1 \\ \phi_2 \end{bmatrix}. \tag{7.17}$$

Then defining

$$\begin{bmatrix} \psi_1 \\ \psi_2 \end{bmatrix} = \begin{bmatrix} \tau_1 & 0 \\ 0 & \tau_2 \end{bmatrix} \begin{bmatrix} \phi_1 \\ \phi_2 \end{bmatrix}, \tag{7.18}$$

and noting that since there is no bound state in the singlet channel, $\mathrm{Im}\tau_2 = 0$, one obtains

$$\mathrm{Im}\eta_\ell(E+i0) = \frac{-\frac{2}{3}\pi k_B \Sigma_{i,j=1}^{2} \int_0^\infty dp\, p^2 Z_{1i}(E;k_B,p) Z_{2j}(E;k_B,p)}{\Sigma_{i,j=1}^{2}(\psi_i, Z_{ij}\psi_j)} \times$$

$$\times\ \psi_i^*(E+i0;p)\psi_j(E+i0;p) \tag{7.19}$$

In the limit $E \to -B$ each $Z_{ij} \to k_B^{\ell} f_{ij}(p)$ and we have $\mathrm{Im}\eta_{\ell}(E+i0) \to (E+B)^{\ell+\frac{1}{2}}$. Thus the doublet eigenvalues also have the threshold behaviour of equation (7.16). The different shape and low energy behaviour of the greatest negative eigenvalue η_{1-} may also be explained in terms of equation (7.16) if one supposes that A_{1-}, B_{1-} are small in magnitude and in addition $B_{1-} < A_{1-}$.

7.4 Application to Low Energy S-wave n-d Scattering

There is a well known relationship between the Fredholm determinant and the on-shell amplitude in the two-body scattering theory with local potentials which can be extended to the n-d equations below three-body breakup through the derivation by Sugar and Blankenbeclar (25). We note their proof may be directly applied by making the replacements $V \to Z(E)$, $G(E+i0) \to \tau(E+i0)$. Since $\mathrm{Im}\tau(E+i0)$ is a δ function and $\mathrm{Im}Z(E+i0) = 0$ when $-B < E < 0$ we have

$$X_{\ell}(E+i0;k_B,k_B) = \frac{D_{\ell}(E+i0)-D_{\ell}^{*}(E+i0)}{2ik_B D_{\ell}(E+i0)}, \quad \text{where } D_{\ell} \text{ is the Fredholm determinant of } Z_{\ell}\tau. \tag{7.20}$$

For positive energies where $Z_{\ell}(E+i0)$ is complex the relation (7.20) no longer holds. Thus below breakup the phase shift δ_{ℓ} is simply the negative of the argument of $D_{\ell}(E+i0)$. Now expressing the Fredholm determinant in the form

$$D_{\ell}(E+i0) = \Pi_i(1-\eta_{\ell}(E+i0))$$

the phase shift may be written in terms of the eigenvalues as

$$\delta_{\ell} = \Sigma_i \delta_{\ell_i}$$

where

$$\delta_{\ell_i} = -\arg(1-\eta_{\ell_i}(E+i0)). \tag{7.21}$$

Eigenvalues with positive imaginary parts give contributions to the phase shift with $0 < \delta_{\ell_i} \leq \pi$ while those with negative imaginary parts have eigenphases restricted to $-\pi \leq \delta_{\ell_i} < 0$. We shall now apply this formalism to describe the low energy scattering in the s-wave doublet.

The interesting feature of the doublet channel scattering is the rapid variation of $k_B \cot\delta$ just above the scattering threshold. In fig.7.5 we show $k_B \cot\delta$ as calculated from the simple Amado model, and there is a pole near -1.9 MeV. Although the experimental results place its position just below threshold the main features are reproduced in this model.

The qualitative explanation (e.g. ref. (3)) of this pole is based on the observation that in the identical spinless boson system (see section 7.2) there is a weakly bound excited state as well as the ground state. This means the on-shell amplitude (continued below the scattering threshold) must have a zero between the bound states, since there is at each, a pole with positive residue. Because the singlet interaction is only slightly weaker than the triplet, one might expect the pole to remain even though the excited state has moved off the physical sheet.

To test the importance of the leading two positive eigenvalues which the intuitive argument suggests, we have calculated the phase shifts showing the relative effect of the various eigenvalues. The total phase shift has been plotted against k_B in curve (a) of fig. 7.6. It increases initially to a maximum of 182.0° and then decreases monotonically up to the breakup threshold. The contribution of the phase shifts from the triton eigenvalue trajectory η_{1+} and the excited state η_{2+} are shown in (b). The phase shift at the two-body threshold starts off at 180° because

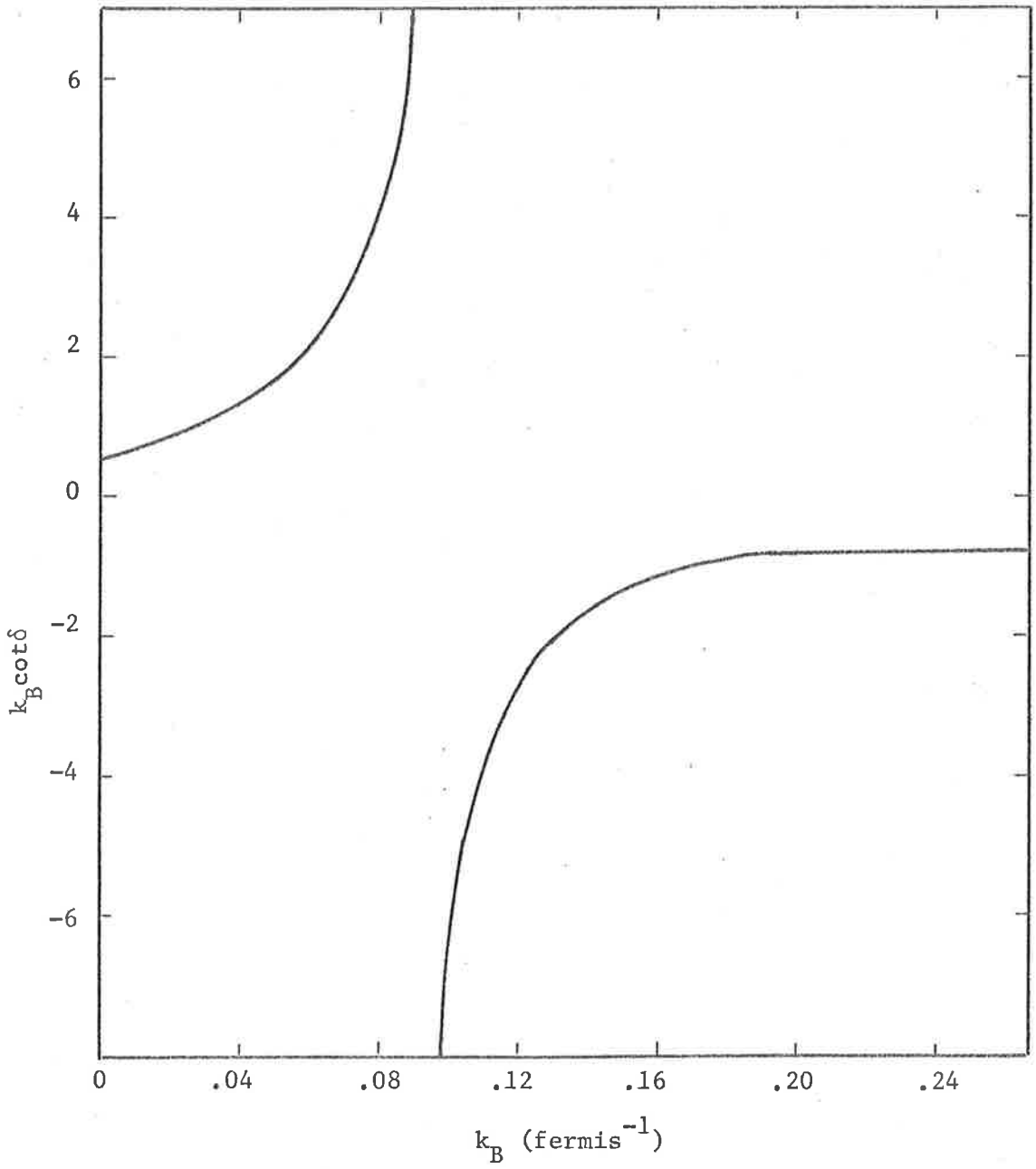

Figure 7.5

$k_B \cot\delta$ in the s-wave doublet below three-body breakup.

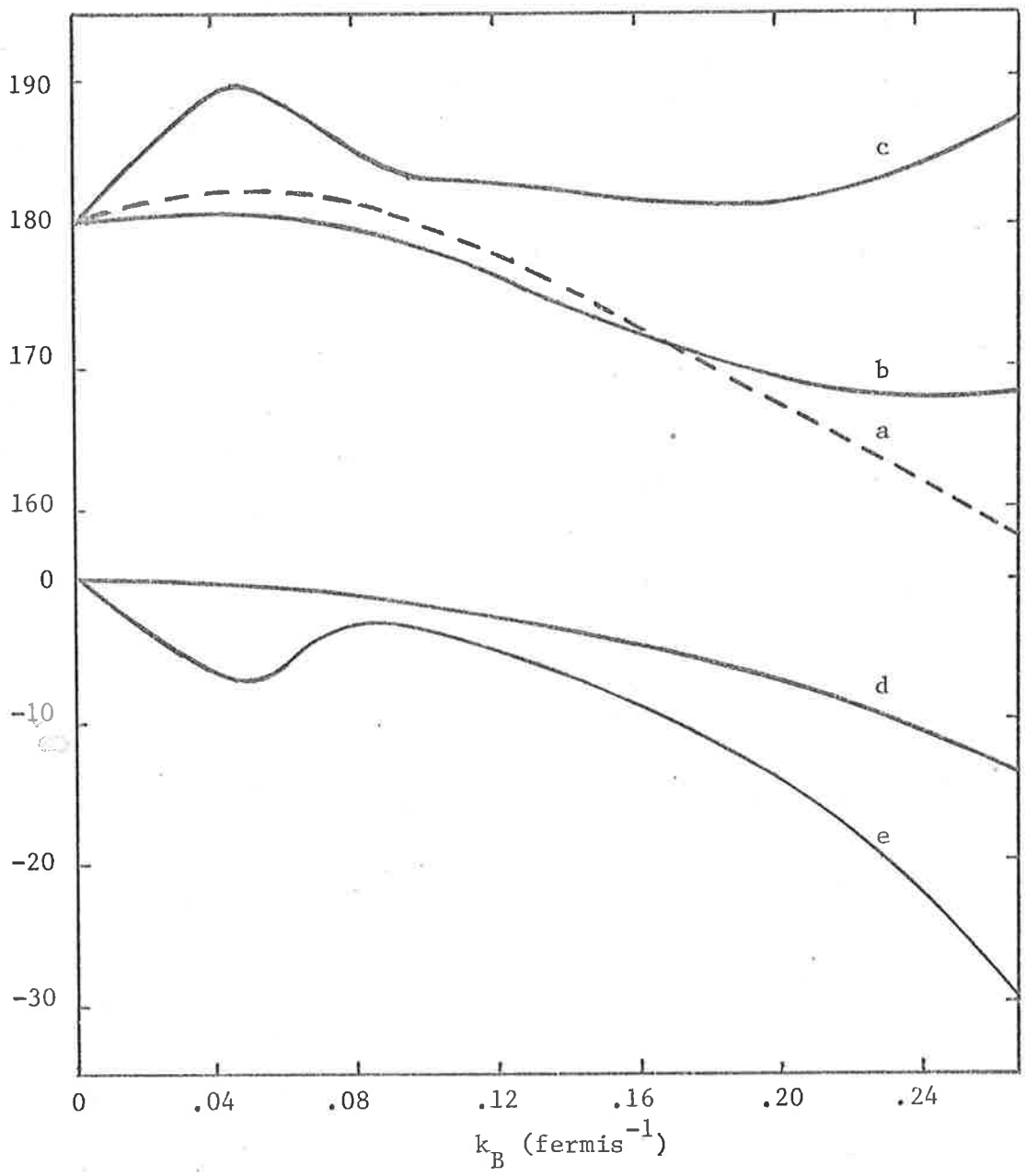

Figure 7.6

Phase shifts below three-body breakup in the s-wave doublet channel. The dashed curve a is the exact model phase. Curve b represents the sum of the eigenphases of η_{1+}, η_{2+} and c is the sum of the eigenphases of all positive eigenvalues. Curve d is the eigenphase of η_{1-}, the leading negative eigenvalue while the phase resulting from the sum of all the negative eigenphases is given by e.

$\mathrm{Re}\eta_{1+}(-2.225) > 1$. Near the threshold the sum of these eigenphases is within 2° of the phase shift and the agreement is quite good up to -.5 MeV. Thereafter the phase decreases too slowly. The sum of all the positive eigenphases is indicated in (c). The smaller positive eigenphases (there are non negligible contributions from about 5) give a significant contribution near E = -2.225 MeV. The phase rises quickly to a maximum of 189°, then decreases to 182° at which point it remains constant, increasing again as the three-body threshold is neared. The sum of the negative phases mirrors the quick increase near threshold to produce the smoothly varying total phase. The eigenphase of η_{1-}, the leading negative trajectory (curve (e)) shows clearly the effect of the small $\mathrm{Im}\eta_{1-}$ near threshold. It has little effect in the variation of $k_B\cot\delta$ near -2.225 MeV but does contribute a substantial portion of the negative phase near E=0.

In summary it appears that the qualitative explanation of the rapid variation in $k_B\cot^2\delta$ is correct. However, the excellent agreement with sum of the eigenphases of the triton trajectory and the next positive trajectory is somewhat fortuitous. The contributions from the remaining eigenvalues are not small but cancel each other out to a large extent.

7.5 Discussion

In conclusion we take the opportunity to indicate a further possible application of the methods used to compute the eigenvalues for physical scattering energies to numerical calculations in the four-body problem. There the equations require the off-shell three-body amplitudes as part of the input (see for example ref.(49)).

In an attempt to reduce the equations to manageable proportions it is natural to approximate the three-body amplitude by a separable expansion in the same way as the two-body amplitude is approximated by a separable sum to reduce the complexity of the Faddeev equations.

One way of obtaining a separable expansion is to use the Sturmian expansion, in which case the three-body amplitude is expressed in the form

$$X(W) = \Sigma_i \frac{|\phi_i><\phi_i|Z(W)}{1-\eta_i(W)} \tag{7.22}$$

where $|\phi_i>$ and η_i are defined in equation (7.1). A four-body calculation using a truncated expansion of this type has been attempted (57) for energies in the bound state region. We believe one can extend this approach to the scattering region in the following manner. First we define the amplitude $X_{\theta\theta}$ by

$$X_{\theta\theta}(E;\underline{p},\underline{p}') = Z(E;\underline{p}e^{i\theta},\underline{p}'e^{i\theta}) + \int d\underline{p}''\, K(E;\underline{p}e^{i\theta},\underline{p}''e^{i\theta}) \times$$

$$\times X_{\theta\theta}(E;\underline{p}'',\underline{p}') \tag{7.23}$$

and then use equation (7.10) to write $X_{\theta\theta}$ in the Sturmian expansion as

$$X_{\theta\theta}(E) = \Sigma_i \frac{|\phi_{\theta i}><\phi_{\theta i}|e^{-3i\theta}}{1-\eta_i(E+i0)} Z_\theta(E), \quad -\pi/2 < \theta < 0. \tag{7.24}$$

One can deduce by arguing as in section 4 of chapter 3 that

$$X_{\theta\theta}(E;\underline{p},\underline{p}') \equiv X(E+i0;\underline{p}e^{i\theta},\underline{p}'e^{i\theta}).$$

A similar expansion may be derived for half off-shell amplitudes. The fact that the expansions are not known for real momenta is not a disadvantage because a rotation of contours in the four-body equations which is necessary to avoid the energy dependent singularities requires a knowledge of the $X_{\theta\theta}$ amplitude anyway.

APPENDICES

A. The Landau Rules

We give a brief summary of the Landau rules. Consider a function $F(z)$ defined by the integral

$$F(z) = \int_{R_n} dx_1 \ldots dx_n \frac{f(z,x_i)}{s_1(z,x_i)\ldots s_m(z,x_i)}, \tag{A.1}$$

where $f(z,x_i)$ is regular and the s_i may vanish for some values of z. In order to determine the analytic structure of $F(z)$ we use Feynmans identity to rewrite (A.1) as

$$F(z) = (m-1)! \int_{R_n} dx_1 \ldots dx_n \int_0^1 d\alpha_1 \ldots d\alpha_m \times \times \frac{\delta(\Sigma_i \alpha_i - 1) f(z,x_i)}{(\Sigma_i \alpha_i s_i)^m}. \tag{A.2}$$

The integrand now contains the singularity surface $D = \Sigma_i \alpha_i s_i = 0$ in the space of $n+m$ variables. The necessary conditions for a singularity are

$$D = 0, \tag{A.3}$$

$$\frac{\partial D}{\partial \alpha_i} = 0, \quad i=1,\ldots,m, \tag{A.4}$$

$$\frac{\partial D}{\partial x_j} = 0, \quad j=1,\ldots,m. \tag{A.5}$$

The condition (A.4) is equivalent to

$$\alpha_i = 0 \text{ or } s_i = 0. \tag{A.4'}$$

Equations (A.3) to (A.5) are known as the Landau rules.

B. Notes on Some Denominators

In this appendix we indicate how one may determine a region in the k plane where a particular denominator does not vanish for some of the denominators encountered in Chapter 5.

The denominators (5.3) to (5.6) are each of the form

$$N^2e^{-2i\theta} + (\underline{x} + M\underline{k}_F e^{-i\theta})^2. \tag{B.1}$$

We know from equations (4.21), (4.22), (4.23) that this denominator cannot vanish if

$$0 < \mathrm{Im} ke^{-i\theta} < \frac{N\cos\theta}{Mn_F}.$$

Since $n_F^2 < \frac{4}{3}$ it follows the denominators (5.3) to (5.6) cannot vanish in the region

$$0 < \mathrm{Im} ke^{-i\theta} < (\tfrac{4}{3})^{\frac{1}{2}}\beta. \tag{B.2}$$

To find where denominator (5.7) vanishes we take real and imaginary parts of the equation which gives the equations

$$(1-\frac{n_F^2}{4}(1-x)^2)\{R + \frac{\frac{1}{2}(1-x)\underline{y}.\underline{n}_F}{(1-\frac{n_F^2}{4}(1-x)^2)}\}^2 - I^2) - Z^2 - y^2 - \frac{(1-x)^2}{4} \times$$

$$\times \frac{(\underline{y}.\underline{n}_F)^2}{(1-\frac{n_F^2}{4}(1-x)^2)} = 0, \tag{B.3}$$

and

$$2I\{R + \frac{\frac{1}{2}(1-x)\underline{y}.\underline{n}_F}{(1-\frac{n_F^2}{4}(1-x)^2)}\} = 0. \tag{B.4}$$

Here $z^2 = \frac{3}{4}q_2^2$, $\underline{y} = \underline{q}_1 + \frac{1}{2}\underline{q}_2$ and $ke^{-i\theta} = R+iI$. Because $n_F^2 < \frac{4}{3}$ and $x\in[0,1]$ the solutions are confined to the line $\mathrm{Im} ke^{-i\theta} = 0$.

Turning to the denominators (5.12) which are present in $T_{1\theta}(W;\underline{k}_B,\underline{k}_F)$, we note they are all of the type

$$N^2e^{-2i\theta} + (x^2 + \ell\underline{k}_B e^{-i\theta} + M\underline{k}_F e^{-i\theta})^2. \tag{B.5}$$

Because this denominator vanishes only when

$$(\ell\hat{n}\ \mathrm{Im}k_B e^{-i\theta} + M\underline{n}_F \mathrm{Im}ke^{-i\theta})^2 > N^2\cos^2\theta,$$

it follows that (B.5) must also be non-vanishing when

$$0 < |\ell|\,|\mathrm{Im}k_B e^{-i\theta}| + |M|n_F|\mathrm{Im}ke^{-i\theta}| < N\cos\theta$$

and in particular when

$$0 < |\ell|\mathrm{Im}k_B e^{-i\theta} + |M|n_F\mathrm{Im}ke^{-i\theta} < N\cos\theta,\ \mathrm{Im}k_B e^{-i\theta} > 0,$$

$$\mathrm{Im}ke^{-i\theta} > 0.$$

As a result, the denominators in equation (5.12) are non-vanishing when

$$0 < \mathrm{Im}k_B e^{-i\theta} + (\tfrac{4}{3})^{\frac{1}{2}}\mathrm{Im}ke^{-i\theta} < 2B^{\frac{1}{2}}\cos\theta,$$

$$\mathrm{Im}ke^{-i\theta},\ \mathrm{Im}k_B e^{-i\theta} > 0. \qquad \text{(B.6)}$$

To investigate the region where denominator (5.18) may vanish we require that the solutions satisfy the following equations for real and imaginary parts:

$$(1-\tfrac{3}{16}n_F^2)(\{R+\frac{\frac{3}{8}\underline{n}_F\cdot\underline{q}_1}{1-\frac{3}{16}n_F^2}\}^2 - I^2) - \frac{(\frac{3}{8}\underline{n}_F\cdot\underline{q}_1)^2}{1-\frac{3}{16}n_F^2} - \tfrac{3}{4}q_1^2 + B\cos 2\theta = 0, \qquad \text{(B.7)}$$

$$2I\{R(1-\tfrac{3}{16}n_F^2) + \tfrac{3}{8}\underline{n}_F\cdot\underline{q}_1\} = B\sin 2\theta. \qquad \text{(B.8)}$$

Substituting (B.8) into (B.7) one finds that for a solution to exist it is necessary that

$$I^2 \le \frac{B\cos^2\theta}{(1-\frac{3}{16}n_F^2)}$$

$$\le \tfrac{4}{3}B\cos^2\theta.$$

Thus denominator (5.18) has no solutions in the region

$$\mathrm{Im}ke^{-i\theta} > (\tfrac{4}{3}B)^{\frac{1}{2}}\cos\theta.$$

To discuss the denominators (5.20) contained in $T_{2\theta}(W;\underline{k}_F,\underline{k}_F')$ we note that the first two are of type (B.1). There are no singularities due to the vanishing of these denominators if

$$0 < \mathrm{Im} k e^{-i\theta} \frac{|\underline{n}_F' + \tfrac{1}{2}\underline{n}_F|}{2} < \beta\cos\theta$$

In particular, they cannot vanish in the region

$$0 < \mathrm{Im} k e^{-i\theta} < (\tfrac{4}{3})^{\frac{1}{2}}\beta\cos\theta.$$

Finally to determine when the energy denominator in (5.20) vanishes one can take real and imaginary parts of the equation

$$W - (\underline{q}_1 e^{i\theta} - \tfrac{1}{2}\underline{k}_F')^2 - (\underline{q}_2 e^{i\theta} - \tfrac{1}{2}\underline{k}_F)^2 - (\underline{q}_1 e^{i\theta} - \tfrac{1}{2}\underline{k}_F') \cdot (\underline{q}_2 e^{i\theta} - \tfrac{1}{2}\underline{k}_F) = 0.$$

Setting $\underline{n}_c = \tfrac{1}{2}\underline{n}_F' + \underline{n}_F$, $\underline{x} = \underline{q}_2 + \tfrac{1}{2}\underline{q}_1$ we obtain

$$(1 - \tfrac{3}{16}n_F'^2 - \tfrac{1}{4}n_c^2)\left(\left\{R + \frac{\frac{3}{4}\underline{q}_1 \cdot \underline{n}_F' + \underline{x} \cdot \underline{n}_c}{2(1 - \frac{3}{16}n_F'^2 - \frac{1}{4}n_c^2)}\right\}^2 - I^2\right) - \frac{(\frac{3}{4}\underline{q}_1 \cdot \underline{n}_F' + \underline{x} \cdot \underline{n}_c)^2}{4(1 - \frac{3}{16}n_F'^2 - \frac{1}{4}n_c^2)} -$$

$$- \tfrac{3}{4}q_1^2 - x^2 = 0, \qquad \text{(B.9)}$$

$$I\left\{R + \frac{\frac{3}{4}\underline{q}_1 \cdot \underline{n}_F' + \underline{x} \cdot \underline{n}_c}{2(1 - \frac{3}{16}n_F'^2 - \frac{1}{4}n_c^2)}\right\} = 0. \qquad \text{(B.10)}$$

But since $(1 - \frac{3}{16}n_F'^2 - \frac{1}{4}n_c^2) > 0$ for all n_F, $n_F' < (\frac{4}{3})^{\frac{1}{2}}$ there are no solutions to these equations if $\mathrm{Im} k e^{-i\theta} \neq 0$.

C. Properties of a Mapping encountered in Chapter 5

To study the mapping of the region

$$0 < \mathrm{Im} k_B e^{-i\theta} + (\tfrac{4}{3})^{\frac{1}{2}} \mathrm{Im} k e^{-i\theta} < 2B^{\frac{1}{2}} \cos\theta, \qquad \text{(C.1)}$$

$$\mathrm{Im} k_B e^{-i\theta} > 0, \quad \mathrm{Im} k e^{-i\theta} > 0,$$

to the k plane, we consider the equation

$$k_B e^{-i\theta} + (\tfrac{4}{3})^{\frac{1}{2}} k e^{-i\theta} = X + iY. \qquad \text{(C.2)}$$

With $Y = 2B^{\frac{1}{2}}\cos\theta$ it has the solution

$$k e^{-i\theta} = (\tfrac{3}{16})^{\frac{1}{2}}\left(X + i2B^{\frac{1}{2}}\cos\theta - \frac{4}{3}\frac{Be^{-2i\theta}}{X + i2B^{\frac{1}{2}}\cos\theta}\right). \qquad \text{(C.3)}$$

As $\mathrm{Re} k e^{-i\theta} \to \pm\infty$, $\mathrm{Im} k e^{-i\theta} \to (\frac{3}{4}B)^{\frac{1}{2}}\cos\theta$. It is not hard to show $\mathrm{Im} k e^{-i\theta}$ takes its maximum value of $(\frac{4}{3}B)^{\frac{1}{2}}\cos\theta$ when $\mathrm{Re} k e^{-i\theta} = \dfrac{(\frac{4}{3}B)^{\frac{1}{2}}}{\sin\theta}$.

Its minimum value is $(\frac{4}{3}B)^{\frac{1}{2}}\cos\theta(1 - \frac{1}{3}\tan^2\theta)$ when $\mathrm{Re} k e^{-i\theta} = \dfrac{-B^{\frac{1}{2}}\cos\theta}{\tan\theta}$.

Thus provided $|\theta| < \pi/3$ the locus of (C.3) lies entirely in the upper half $ke^{-i\theta}$ plane. By taking $0 < Y < 2B^{\frac{1}{2}}$ one can verify that the region (C.1) is mapped into the k plane between the boundaries given by (C.3) and $\mathrm{Im}ke^{-i\theta} = 0$ and this region is simply connected if $|\theta| < \pi/3$.

D. A Note on the Numerical Integration of $\int_0^\infty f(x)dx$

While the Gaussian quadrature of order n has an error term whose numerical coefficient decreases rapidly with n, the error is also proportional to the $2n^{th}$ order derivative of f. Now when the integration contour is nearby to a singularity of the integrand, it may happen that the approximation to the exact integral is not improved by simply increasing the order of the quadrature. In these circumstances it is better to split the integration into subintervals and evaluate each integral by using a Gaussian quadrature of moderate order. In this manner one may increase the accuracy of the composite quadrature by increasing the number of subintervals without increasing the order or derivative in the error term. In our calculations we transformed the interval of integration from $[0,\infty)$ to $[-1,1]$ by means of the mapping $x = P[\frac{1+y}{1-y}]$ which gives

$$\int_0^\infty f(x)dx = \int_{-1}^{1} f(P[\frac{1+y}{1-y}])\frac{2p}{(1-y)^2}\,dy.$$

The interval $[-1,1]$ was then split up into 8 subintervals and up to 8 point Gaussian quadrature rules were used in each subinterval. P is a parameter which may be adjusted in order to further improve convergence.

REFERENCES

1. L.D. Faddeev, *Mathematical Aspects of the Three-Body Problem in the Quantum Scattering Theory* (Israel Program for Scientific Translations, Jerusalem 1965).
2. I. Duck in *Advances in Nuclear Physics, 1* (1968).
3. L.M. Delves and A.C. Phillips, Rev. Mod. Phys. *41*, 497 (1969).
4. R.D. Amado, Ann. Rev. Nucl. Science *19*, (1969).
5. R. Aaron, R.D. Amado, and Y.Y. Yam, Phys. Rev. *140*, B 1291 (1965).
6. J.H. Hetherington and L.H. Schick, Phys. Rev. *137*, B 935 (1965).
7. R. Aaron and R.D. Amado, Phys. Rev. *150*, 857 (1966).
8. G. Barton and A.C. Phillips, Nucl. Phys. *A132*, 97 (1969).
9. Y. Avishai, W. Ebenhöh, and A.S. Rinat-Reiner, Ann. Phys. *55*, 341 (1969).
10. R.H.J. Bower, Ann. Phys. *73*, 372 (1972).
11. A.T. Stelbovics and L.R. Dodd, Phys. Lett. *48B* No.1, 13 (1974).
12. A.S. Rinat and M. Stingl, Ann. Phys. *65*, 141 (1971).
13. R.D. Amado, Phys. Rev. *132*, 485 (1963).
14. C.B. Lovelace, Phys. Rev. *135B*, 1225 (1964).
15. R.D. Amado, Phys. Lett. *33*, 333 (1974).
16. L.R. Dodd, Phys. Rev. D, *3*, No.10, 2536 (1971).
17. M. Rubin, R. Sugar and G. Tiktopoulos, Phys. Rev. *146*, 1130 (1966).
18. M. Rubin, R. Sugar and G. Tiktopoulos, Phys. Rev. *159*, 1348 (1967).
19. M. Rubin, R. Sugar and G. Tiktopoulos, Phys. Rev. *162*, 1555 (1967).
20. W.T.H. van Oers and J.D. Seagrave, Phys. Lett. *24B*, 562 (1967).
21. M.L. Goldberger and K.M. Watson, *Collision Theory* (John Wiley and Sons, New York 1964).
22. F. Smithies, *Integral Equations* (Cambridge University Press 1958).
23. S. Weinberg, Phys. Rev. *131*, No. 1, 440 (1963).
24. N.N. Khuri, Phys. Rev. *107*, No. 4, 1149 (1957).

25. R. Sugar and R. Blankenbecler, Phys. Rev. *136*, No. 2B, 472 (1964).

26. K. Meetz, J. Math. Phys. *3*, No. 4, 690 (1961).

27. F. Coester, Phys. Rev. *133*, B 1516 (1964).

28. M. Scadron, S. Weinberg and J. Wright, Phys. Rev. *135*. B 202 (1964).

29. L. Brown, D. Fivel, B.W. Lee and R. Sawyer, Ann. Phys. (N.Y.) *23*, 167 (1963).

30. C.B. Lovelace, in *Strong interactions and High Energy Physics* (edited by R.G. Moorhouse, Oliver and Boyd, London, 1964).

31. T. Kato, Trans. Amer. Math. Soc., *70*, No. 2, 195 (1951).

32. D.D. Brayshaw, Phys. Rev., *176*, 1855 (1968).

33. G. Skorniakov and K. Ter-Martirosian, Sov. Phys. - JETP, *31*, 775 (1956).

34. R.J. Eden, P.V. Landshoff, D.I. Olive and J.D. Polkinghorne, *The Analytic S-matrix* (Cambridge University Press, 1966).

35. L.D. Faddeev, Sov. Phys. - JETP, *12*, 1014 (1961).

36. G. Flamand, in *Application of Mathematics to Problems in Theoretical Physics - Corgese Lectures in Theoretical Physics* (edited by F. Lurcat, Gordon and Breach, N.Y., 1965).

37. L.R. Dodd, J. Math. Phys. *11*, 207 (1970).

38. P.R. Graves-Morris, Ann. Phys. N.Y. *41*, 477 (1967).

39. J.M. Gregen, *Unitarity and Analyticity in Nuclear Reaction Theory* (Ph.D. Thesis, Groningen 1974).

40. G. Frye and R.L. Warnock, Phys. Rev. *130*, No. 1, 478 (1963).

41. I.H. Sloan, Nucl. Phys. *A168*, 211 (1971).

42. G.F. Chew, *The Analytic S-matrix* (W.A. Benjamin Inc., N.Y. 1966), pp 66-72.

43. A.W. Martin, Phys. Rev., *135* No. 4B, 967 (1964).

44. J.D. Bjorken and A. Goldberg, Nuovo Cimento, *16*, 539 (1960).

45. M. Luming, Phys. Rev., *B136*, 1120 (1964).

46. S.C. Frautschi, *Regge Poles and S-Matrix Theory* (W.A. Benjamin Inc., N.Y. 1963), pp 13-17.

47. I.H. Sloan, Phys. Lett. *34B*, No.4, 243 (1971).

48. P. Swan, Proc. Roy. Soc. (London), *A228*, 10 (1955).

49. S. Weinberg, Phys. Rev. *133*, B232 (1964).

50. L. Rosenberg, Phys. Rev. *140*, B219 (1965).

51. R.G. Newton, *Scattering Theory of Waves and Particles* (McGraw-Hill Book Co., N.Y., 1966), pp 235-243.

52. V. Efimov, Phys. Lett., *33B*, 563 (1970).

53. V. Efimov, Sov. J. Nucl. Phys. *12*, 589 (1971).

54. R.D. Amado and J.V. Noble, Phys. Lett. *35B*, 25 (1971).

55. R.D. Amado and J.V. Noble, Phys. Rev. *D5*, 1992 (1972).

56. A.T. Stelbovics and L.R. Dodd, Phys. Lett., *39B*, 450 (1972).

57. I.M. Narodetsky, E.S. Galpern and V.N. Lyakhovitsky, Phys. Lett., *46B*, 51 (1973).

THREE-BODY BOUND STATES IN AMADO'S MODEL

A. T. STELBOVICS and L. R. DODD
Mathematical Physics Department, University of Adelaide, Adelaide, South Australia 5001

Received 10 March 1972

We have calculated the eigenvalue trajectories of the scattering kernel for a system of three, identical particles with Yamaguchi interactions, for both spin half and spin zero particles. For potential strengths corresponding to large values of the two-body scattering length, we find several, weakly-bound, three-body excited states of the type proposed by Efimov, and calculate their binding energies.

Recently Amado and Noble [1], following a conjecture by Efimov [2], have proved that the number of $J = 0^+$ bound states in a system of three, identical bosons increases without limit as the strength of the pair interaction approaches a critical value which corresponds to zero binding energy of the ground state of the two-body system. In fact the number of bound states in the three-body system is estimated as

$$N \approx (1/\pi) \log |a|, \qquad (1)$$

where a is the two-particle scattering length in units of the potential range. Amado and Noble explain this remarkable effect in terms of the non-compactness of the kernel of the integral equations of three-particle scattering theory when the first rearrangement threshold coincides with the three-body breakup threshold.

Since previous numerical calculations based on the Faddeev equations have not reported the existence of such bound states, we have carried out a systematic search in the context of Amado's original model [3, 4], i.e. three spinless bosons with separable Yamaguchi interactions.

The eigenstates ϕ_i and associated eigenvalues λ_i of the scattering kernel for this problem are determined by

$$\int Z(\boldsymbol{k}, \boldsymbol{k}'; \epsilon)\tau(\epsilon - \tfrac{3}{4}k'^2)\phi_i(\boldsymbol{k}')\mathrm{d}^3k' = \lambda_i \phi_i(\boldsymbol{k}) \qquad (2)$$

where

$$Z(\boldsymbol{k}, \boldsymbol{k}'; \epsilon) = \pi^{-2}[(1 + k^2 + \tfrac{1}{4}k'^2 + \boldsymbol{k}\cdot\boldsymbol{k}')\times (1 + k'^2 + \tfrac{1}{4}k^2 + \boldsymbol{k}\cdot\boldsymbol{k}')(\epsilon + k^2 + k'^2 + \boldsymbol{k}\cdot\boldsymbol{k}')]^{-1}$$

and

$$\tau^{-1}(\epsilon - \tfrac{3}{4}k'^2) = \mu^{-1} - ((\epsilon + \tfrac{3}{4}k'^2)^{1/2} + 1)^{-1}.$$

The eigenvalues λ_i are functions of the two dimensionless parameters μ and ϵ, where $\mu = \pi^2 mg/\hbar^2\beta^3$, g and β being the usual strength and range parameters of the Yamaguchi potential and m the particle mass, and $-\epsilon$ is the energy of the three-body system in units of $\hbar^2\beta^2/m$. For fixed μ the eigenvalues describe trajectories in the complex λ plane as the energy ϵ is varied [5]. The trajectories $\lambda_i(\epsilon)$ are real for real energies $-\epsilon$ below the threshold for scattering i.e. when $\epsilon > \epsilon_2$, where $\epsilon_2 = (\mu^{1/2} - 1)^2$ if the two particle system is bound ($\mu > 1$) and $\epsilon_2 = 0$ otherwise ($\mu < 1$). If a trajectory λ_i passes through unity in this energy region, there exists a three-particle bound state with energy ϵ_0 determined by $\lambda_i(\epsilon_0, \mu) = 1$ and binding energy $\epsilon_3 = \epsilon_0 - \epsilon_2$. The number of bound states for a particular strength μ is given by the number of eigenvalues λ_i which exceed unity at the scattering threshold $\epsilon = \epsilon_2$.

It is well known that there are two $J = 0^+$ states when $\mu > 1$, the ground state and a weakly bound excited state [4] which are associated with the two largest eigenvalues of eq. (2). States of the type predicted by Efimov are expected in the neighbourhood of $\mu = 1$ and for small ϵ, where the factor $(\epsilon + k^2 + k'^2 + \boldsymbol{k}\cdot\boldsymbol{k}')^{-1}$ in the kernel of eq. (2) becomes divergent. The results of our calculations of the leading eigenvalues for values of $\mu \approx 1$ are listed in table 1. The associated scattering length (in units of β^{-1}) is $a = 2\mu/(\mu - 1)$. The accuracy of our numerical methods limit the values of a considered to $\ln|a| \lesssim 13$, but we see that for this value of the strength four excited states have appeared.

In figs. 1 and 2 the energies of the bound states are shown as functions of $\ln|a|$. The arrows indicate the movement of the binding energy as the strength parameter μ is increased.

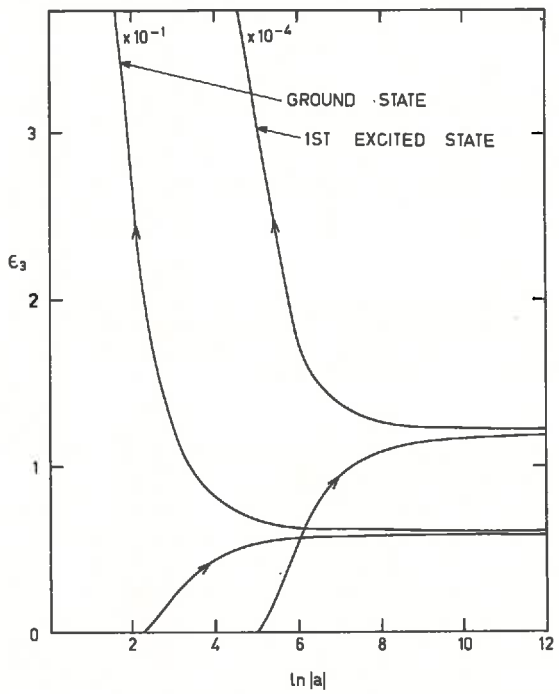

Fig.1. Binding energies for the ground and first excited $J = 0^+$ states.

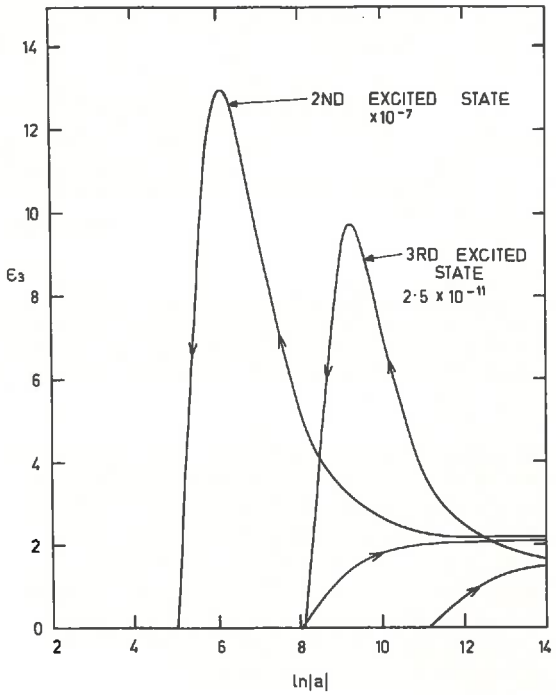

Fig.2. Binding energies for the second and third excited $J = 0^+$ states.

Table 1
Eigenvalues for $J = 0^+$ states.

$\mu - 1$	$\ln\|a\|$	λ_1	λ_2	λ_3	λ_4	λ_5
1.42×10^{-2}	4.962	3.7848	1.9219	0.999	0.5275	0.2930
5.94×10^{-4}	8.122	3.6753	2.2088	1.5493	1.0001	0.6433
2.65×10^{-5}	11.23	3.6685	2.3108	1.8783	1.3926	1.0004
-4.52×10^{-6}	13.00	2.3314	2.0057	1.595	1.1942	0.8516
-3.00×10^{-5}	11.107	2.2944	1.8470	1.3746	0.9998	0.7208
-6.58×10^{-4}	8.019	2.1952	1.5242	1.0000	0.6632	0.4508
-1.35×10^{-2}	4.985	1.8555	1.0002	0.5676	0.3438	0.2177
-1.88×10^{-1}	2.157	1.0000	0.4139	0.2112	0.1180	0.0699

The ground state appears at $\ln|a| = 2.16$ or $\mu = 0.812$. The horizontal asymptote at ϵ=0.0606 gives the binding energy when $\mu = 1$. As μ increases the binding energy increases rapidly. The first excited state exhibits similar behaviour.* In contrast the second and third excited states have the characteristics predicted by Efimov; they become less tightly bound as the strength $\mu > 1$ increases, eventually disappearing. For example the second excited state is only bound for values of the strength between $\mu = 0.999\,342$ and $\mu = 1.0142$.

The eigenvalues of the kernel of the coupled equations for spin half particles are functions of four dimensionless parameters, the triplet strength $\mu_t = \pi^2 m g_t/\hbar^2 \beta_t^3$, the singlet strength $\mu_s = \pi^2 m g_s/\hbar^2 \beta_s^3$, the ratio of the range parameters $\gamma = \beta_s/\beta_t$ and the energy $-\epsilon$. In our calculations, we set $\mu_t \geq \mu_s$ and $\gamma = 1$ (with the choice $\gamma = 1$ the kernel of the coupled equations reduces to that of the spinless case when $\mu_t = \mu_s$). In table 2 the leading eigenvalues for the $J = \frac{1}{2}^+$ states are shown for various values

*The present calculations indicate that as the potential strength is increased, the first excited state of the three-body system appears at μ=0.9965. slightly before the formation of a two-body bound state becomes possible at $\mu = 1$.

Table 2
Eigenvalues for $J = \frac{1}{2}^+$ states

$\mu_t - 1$	$\mu_s - 1$	λ_1	λ_2	λ_3	λ_4
5.95×10^{-4}	5.94×10^{-4}	3.6753	2.2088	1.5493	1.0001
1.42×10^{-2}	5.94×10^{-4}	2.4681	1.5202	0.7868	0.4229
1.00×10^{-1}	5.94×10^{-4}	2.4866	1.0482	0.4392	0.2044
3.00×10^{-1}	5.94×10^{-4}	2.5618	0.7782	0.2873	0.1195
1.00×10^{-1}	1.00×10^{-1}	4.2638	1.5358	0.6131	0.2785
1.00×10^{-1}	1.42×10^{-2}	2.5590	1.0722	0.4480	0.2080
1.00×10^{-1}	1.00×10^{-2}	2.5357	1.0645	0.4452	0.2071
1.00×10^{-1}	1.00×10^{-3}	2.4886	1.0489	0.4394	0.2045
1.00×10^{-1}	5.94×10^{-4}	2.4866	1.0482	0.4392	0.2049

of μ_t and μ_s. These results appear to confirm Efimov's statement that the number of excited states is determined by the smaller of the scattering lengths; for fixed μ_s, all the excited states can be made to vanish by increasing μ_t sufficiently**, while on the other hand the leading eigenvalues are sensitive to changes in μ_s for fixed μ_t only when μ_s is of the order of μ_t.

** In the usual application of this model to the triton, μ_t is sufficiently large so that there are no excited states.

References

[1] R. D. Amado and J. V. Noble, Phys. Letters 35B (1971) 25.
[2] V. Efimov, Phys. Letters 33B (1970) 563.
[3] R. D. Amado, Phys. Rev. 132 (1963) 485.
[4] R. Aaron, R. D. Amado and Y. Y. Yam, Phys. Rev. 136 (1964) 650.
[5] S. Weinberg, Phys. Rev. 131 (1963) 1440.
[6] R. Aaron, R. D. Amado and Y. Y. Yam, Phys. Rev. 140 (1965) 1271.

* * * * *

DISPERSION RELATIONS FOR ELASTIC n-d SCATTERING IN THE AMADO MODEL

A.T. STELBOVICS and L.R. DODD
Department of Mathematical Physics, University of Adelaide, Adelaide, S. Australia 5001

Received 15 November 1973

The formulation of rigorous, dispersion relations for on-shell three-body amplitudes in a separable model is reported. The results of approximate N/D calculations of s-wave n-d elastic scattering are compared with exact, numerical solutions of the Faddeev equations.

While calculations of elastic n-d scattering based on on-shell dispersion relations [1, 2] have met with some success, it is difficult to assess their reliability because of the number of theoretical approximations and experimental uncertainties involved. The work reported in this letter was undertaken in order to test the on-shell approach to the calculation of three-body scattering amplitudes within the context of a well-known separable-potential model [3] where comparison with accurate numerical solutions of the Faddeev equations is possible.

Rigorous dispersion relations for three-particle scattering amplitudes have been derived by Rubin, Sugar and Tiktopoulos [4] for a system of three particles interacting via local two-body Yukawa forces. It can be shown [5] that their results are essentially unchanged if the Yukawa potential is replaced by a sum of separable interactions in such a way that the two-body t-matrices have the same bound state poles. Except for the possibility of simple poles in the first order terms, all the singularities of the on-shell three-particle amplitudes lie on the real axis of the complex energy plane and consist of the right hand unitarity cuts, the left hand potential cuts and under certain conditions associated with two particle bound states, anomalous singularities. It follows that the on-shell amplitudes of the Amado model [3] of n-d scattering, in which the two-body interactions are separable, non-local Yamaguchi potentials, satisfy dispersion relations of the type formulated in ref. [4]*.

Because accurate solution of the Faddeev equations with separable potentials is straightforward by the method of rotation of contours [6], the Amado model provides a means of testing the three-body dispersion relations and investigating the utility of various approximations in their solutions. In this note, we present the results of a direct comparison of solutions of the on-shell N/D equations for s-wave elastic n-d scattering with exact solutions of the off-shell Faddeev equations for the Amado model.

The N/D equations in the form in which N is determined by a non-singular integral equation involving only the inelasticity and an input function $B(E)$, have been used to represent the analytic structure of the quartet and doublet amplitudes. The inelasticity which was regarded as part of the input information**, was found directly from the solutions of the Faddeev equations. The input function $B(E)$, which is defined by an integral over the discontinuity of the amplitude $T(E)$ on the left hand cut, was calculated from the following formula,

$$B(E) = \mathrm{Re}\, T(E+\mathrm{i}\epsilon) - \frac{1}{\pi} \mathrm{P} \int_{E_\mathrm{R}} \mathrm{Im} \frac{T(E'+\mathrm{i}\epsilon)}{E'-E}\, \mathrm{d}E' \qquad (1)$$

which only requires a knowledge of the amplitude for energies on the right hand cut.

In order to check the dispersion-relations, the exact input was computed from the accurate, numerical solutions of the Faddeev equations. On solving the N/D equations with this input, the exact amplitude was reproduced both in the quartet and doublet cases.

* It is shown in ref. [5] that the elastic n-d amplitudes have no anomalous singularities.

** If three-particle unitarity is used then a system of coupled dispersion relations involving elastic, breakup and free particle amplitudes must be solved.

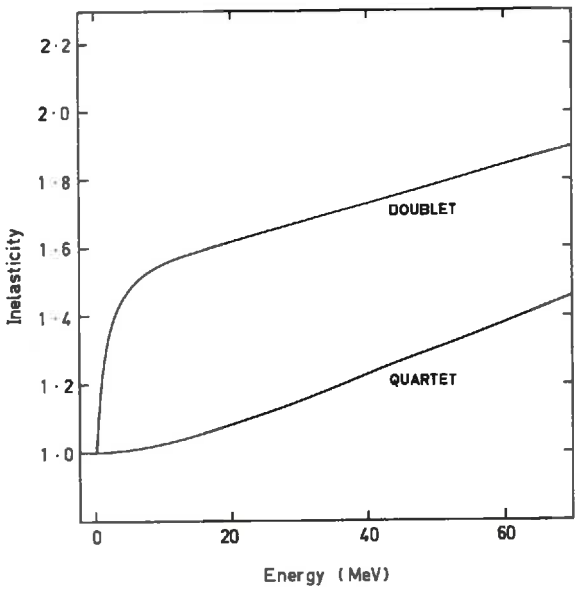

Fig. 1. Inelasticities for the quartet and doublet channels are shown as a function of centre of mass energy in the Amado model (Inelasticity $\rho = (1/k|T|^2)\,\mathrm{Im}\,T$.

In the usual applications of the N/D method, the exact input is not known but must be approximated. In two-body potential scattering the most convenient approximation is based on the multiple scattering series obtained by iteration of the Lippamnn–Schwinger equation. Following this approach we have solved the doublet and quartet dispersion relations using input functions calculated from the first to the fourth order terms of the iterative solution of the Faddeev equations.

In fig. 1 the inelasticities for the quartet and doublet channels in the Amado model are shown. In the quartet channel the inelasticity increases slowly at energies just above the threshold for breakup and is approximately linear at higher energies. In the doublet channel, the coupling between the neutron and the singlet antibound state has an important influence; there is an abrupt rise in the inelasticity near threshold but at higher energies the inelasticity is again almost linear. In fig. 2 the approximate input functions calculated from the multiple scattering series are compared with the exact input functions, eq. (1). In the doublet case we note that the approxi-

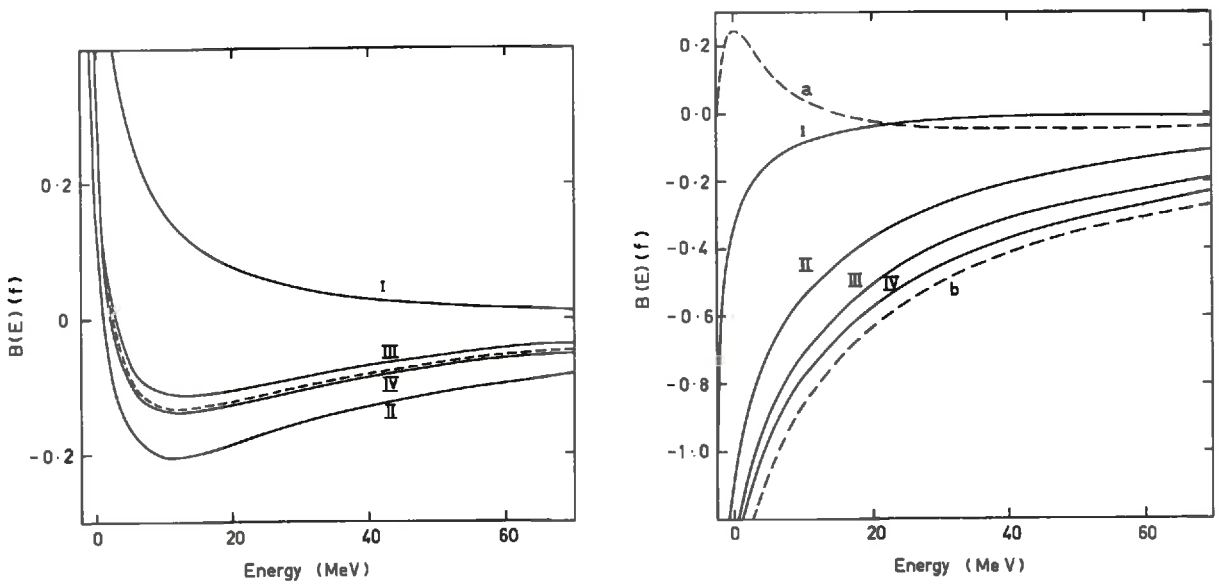

Fig. 2. Inputs labelled I–IV are derived from the first four orders of the multiple scattering series. (a) Quartet channel. The exact input from the Faddeev equations is represented by the dashed curve. (b) Doublet channel. The dashed curve labelled a is the exact input calculated from the Faddeev equations. The dashed curve b represents the exact input with a contribution from the triton pole substracted.

Table 1

Real parts of phase shifts and absorption coefficients ($\eta = \exp(-2\delta_I)$) for varying centre of mass energies. The first four sets are from the solution of the N/D equations with the approximate inputs. The exact set has been obtained by solution of the Faddeev equations. For the doublet channel the triton binding energy is shown for all the input.

	1		2		3		4		exact	
E(MeV)	δ_R	η	δ_R	η	δ_R	η	δ_R	η	δ_R	η
QUARTET										
−2.225	180.0	1.000	180.0	1.000	180.0	1.000	180.0	1.000	180.0	1.000
−2	151.0	1.000	150.9	1.000	150.5	1.000	151.2	1.000	150.7	1.000
0	109.3	1.000	107.7	1.000	107.8	1.000	107.4	1.000	107.7	1.000
5	83.5	0.992	97.6	0.992	78.7	0.992	78.6	0.992	78.7	0.992
10	73.2	0.957	65.1	0.961	65.0	0.961	64.8	0.961	65.2	0.962
12	66.7	0.914	55.8	0.930	55.8	0.930	55.5	0.930	55.9	0.930
20	61.4	0.876	48.6	0.907	48.7	0.907	48.3	0.908	48.7	0.908
25	58.1	0.838	43.0	0.893	42.8	0.893	42.4	0.895	42.9	0.893
30	54.3	0.810	38.0	0.886	37.8	0.887	37.5	0.889	38.1	0.886
40	48.5	0.766	30.0	0.888	30.7	0.885	29.8	0.890	30.7	0.884
50	43.8	0.735	24.4	0.898	25.1	0.893	24.2	0.899	25.2	0.892
60	39.8	0.716	19.8	0.913	21.0	0.904	19.8	0.913	21.1	0.903
70	36.2	0.707	16.3	0.928	17.8	0.915	16.3	0.921	17.9	0.914
DOUBLET										
−2.225	0.0	1.000	180.0	1.000	180.0	1.000	180.0	1.000	180.0	1.000
−2	65.6	1.000	162.7	1.000	173.0	1.000	178.0	1.000	181.0	1.000
0	39.8	1.000	130.8	1.000	146.9	1.000	154.6	1.000	159.0	1.000
5	19.2	0.898	89.8	0.344	118.0	0.431	128.3	0.515	135.8	0.595
10	12.0	0.953	53.9	0.442	84.7	0.294	103.7	0.310	115.0	0.358
15	8.4	0.975	40.3	0.577	59.0	0.369	77.5	0.278	91.5	0.263
20	6.2	0.986	31.8	0.688	46.3	0.473	56.4	0.364	70.6	0.276
25	4.6	0.992	25.5	0.774	37.7	0.576	47.2	0.437	57.0	0.333
30	3.4	0.995	21.5	0.826	33.0	0.637	40.8	0.506	48.7	0.396
40	1.7	0.999	15.2	0.902	25.9	0.736	32.2	0.622	38.2	0.516
50	0.6	1.000	10.5	0.948	20.5	0.811	26.2	0.706	31.8	0.591
60	−0.1	1.000	6.9	0.976	16.1	0.872	21.4	0.780	27.3	0.668
70	−0.7	1.000	3.2	0.994	12.6	0.934	17.6	0.835	23.9	0.707
Triton binding energy	No bound state		−5.1		−7.7		−9.4		−11.0	

mate inputs do not converge to the exact input. The reason for this behaviour is that the method used to compute the exact input from the Faddeev equations includes a contribution from the triton pole which is not present in the multiple scattering series. Both forms of input satisfy the N/D representation of the amplitude; in the case of the exact input the triton occurs as a pole of the N function rather than as a zero of the D function. In fig. 2b the dashed curve b represents the exact input with the contribution from the triton pole subtracted.

In table 1 our results for the phase shifts and absorption coefficients are listed. In the quartet channel, the agreement of the second, third and fourth order approximations with the exact values is remarkably good. In the more complex doublet channel, the results are less satisfactory. The phase shifts in all orders decrease too quickly as the energy increases, although their values improve with increasing order of the input function. Similarly the absorption coefficients reproduce the dip of the exact coefficient but are too large at low energies and too small at

higher energies. The results do, however, appear to be converging slowly to the exact values. The binding energy of the triton, which is determined by the position of the zero of the Fredholm denominator, although also approaching the exact model value, falls short of it by 1.6 MeV in the fourth order approximation. It is clear from the details of the calculations that while the solution of the quartet channel N/D equation is relatively insensitive to the input the doublet channel is quite sensitive to small changes in the input.

We conclude that the N/D method is a practical way of unitarizing the multiple scattering series and is capable of reproducing the features of the exact amplitudes in the Amado model with reasonable accuracy. Although not competing in accuracy with complete solutions of the off-shell Faddeev equations, the on-shell dispersion relations would appear to provide a useful tool in the phenomenological analysis of n-d scattering.

References

[1] G. Barton and A.C. Phillips, Nucl. Phys. A132 (1969) 97.
[2] Y. Avishai, W. Ebenhöh and A.S. Rinat-Reiner, Annals of Physics 55 (1969) 341.
[3] R.D. Amado, Phys. Rev. 131 (1963) 485;
R. Aaron, R.D. Amado and Y.Y. Yam, Phys. Rev. 140 (1965) B1291;
R. Aaron and R.D. Amado, Phys. Rev. 150 (1966) 857.
[4] M. Rubin, R. Sugar and G. Tiktopoulos, Phys. Rev. 146 (1966) 1130; 159 (1967) 1348; 162 (1967) 1555.
[5] A. Stelbovics, Ph. D. thesis, University of Adelaide (unpublished).
[6] J.H. Hertheringtom and L.H. Schick, Phys. Rev. 137 (1965) B935.